Delft University of Technology

4D Printing for Biomedical Applications

Yarali, Ebrahim; Mirzaali, Mohammad J.; Ghalayaniesfahani, Ava; Accardo, Angelo; Diaz-Payno, Pedro J.; Zadpoor, Amir A.

Important note
To cite this publication, please use the final published version (if applicable).
Please check the document version above.

4D Printing for Biomedical Applications

Ebrahim Yarali, Mohammad J. Mirzaali,* Ava Ghalayaniesfahani, Angelo Accardo, Pedro J. Diaz-Payno, and Amir A. Zadpoor

4D (bio-)printing endows 3D printed (bio-)materials with multiple functionalities and dynamic properties. 4D printed materials have been recently used in biomedical engineering for the design and fabrication of biomedical devices, such as stents, occluders, microneedles, smart 3D-cell engineered microenvironments, drug delivery systems, wound closures, and implantable medical devices. However, the success of 4D printing relies on the rational design of 4D printed objects, the selection of smart materials, and the availability of appropriate types of external (multi-)stimuli. Here, this work first highlights the different types of smart materials, external stimuli, and design strategies used in 4D (bio-)printing. Then, it presents a critical review of the biomedical applications of 4D printing and discusses the future directions of biomedical research in this exciting area, including in vivo tissue regeneration studies, the implementation of multiple materials with reversible shape memory behaviors, the creation of fast shape-transformation responses, the ability to operate at the microscale, untethered activation and control, and the application of (machine learning-based) modeling approaches to predict the structure–property and design–shape transformation relationships of 4D (bio)printed constructs.

E. Yarali, M. J. Mirzaali, A. Ghalayaniesfahani, P. J. Diaz-Payno,
A. A. Zadpoor
Department of Biomechanical Engineering
Faculty of Mechanical Engineering
Delft University of Technology (TU Delft)
Mekelweg 2, Delft 2628 CD, The Netherlands
E-mail: m.j.mirzaali@tudelft.nl

E. Yarali, A. Accardo
Department of Precision and Microsystems Engineering
Faculty of Mechanical Engineering
Delft University of Technology (TU Delft)
Mekelweg 2, Delft 2628 CD, The Netherlands

A. Ghalayaniesfahani
Department of Chemistry
Materials and Chemical Engineering
Giulio Natta
Politecnico di Milano
Piazza Leonardo da Vinci, 32, Milano 20133, Italy

P. J. Diaz-Payno
Department of Orthopedics and Sports Medicine
Erasmus MC University Medical Center
Rotterdam 3015 CN, The Netherlands

The ORCID identification number(s) for the author(s) of this article can be found under https://doi.org/10.1002/adma.202402301

1. Introduction

Additive manufacturing (AM) processes, also known as 3D printing techniques, enable the fabrication of 3D objects with complex geometries and tailored mechanical properties.[1–5] This technology, however, has hitherto been largely constrained to the creation of static objects that exhibit constant properties over time.[6,7] This limitation has been mitigated by the advent of 4D printing, a disruptive technology that introduces a temporal component to the traditionally static 3D printed constructs, thereby enabling the fabrication of dynamic structures that respond to external stimuli.

The implications of 4D printing are profound. These dynamic structures can undergo controlled transformation between multiple states, thereby exhibiting advanced functionalities, such as shape adaptation and environmental responsiveness.[8] Unlike 3D printing objects, which feature static applications, 4D printed constructs have found applications in a variety of fields including, but not limited to, self-assembly,[9] self-healing,[10,11] shape-morphing (e.g., self-folding),[12,13] and multifunctionality.[14] This range of applications extends from wearable and medical devices to robotic systems, sensors, and actuators.[7]

In regenerative medicine, 4D (bio-)printing has the potential to revolutionize tissue engineering by enabling the creation of functional tissues and organs.[15] Moreover, the technology's scalability across various length scales (i.e., from micro to macro)[16,17] opens the door for the production of miniaturized soft robots and sensors[16,17] as well as microscaffolds for in vitro cell studies.[18,19]

The cornerstone of 4D printing is the rational selection of stimuli-responsive materials, such as shape memory polymers (SMPs), hydrogels, and liquid crystal polymers (LCPs), among others.[16] The successful integration of these materials is dependent on a well-designed interaction mechanism, a compatible 3D printing technique, and the precise application of external stimuli. Particularly in biomedical applications, the materials selected must also meet biocompatibility criteria to be considered for in vivo use.

Various 3D printing technologies serve as the foundational methods for 4D printing processes. These include direct ink writing (DIW),[15] fused deposition modeling (FDM),[20] vat photopolymerization[21] (e.g., stereolithography (SLA) or digital

**ADVANCED
SCIENCE NEWS**

www.advancedsciencenews.com

**ADVANCED
MATERIALS**

www.advmat.de

light projection (DLP)[22]), direct laser writing (DLW) (e.g., two-photon polymerization (2PP)[23,24]), selective laser sintering (SLS),[25] and selective laser melting (SLM)[26]). Moreover, hybrid techniques that combine 3D printing with conventional manufacturing processes have also been developed, including molding-integrated[27] and electroless metallic plating-integrated 4D printing.[28] The choice of a specific 4D printing process depends on various factors, including the intended application, the length scale, the mechanical and biological properties of the relevant materials, as well as the production method (e.g., batch or mass productions).[6]

Design strategies, often inspired by origami/kirigami-based principles[29–32]), are integrated into 4D printing processes to create multifunctional structures that challenge the boundaries of conventional manufacturing techniques. These strategies operate at various length and time scales, potentially transforming how materials and devices are conceptualized and fabricated.

Given the growing interest in personalized healthcare solutions, 4D printing has attracted considerable attention for its role in pioneering advanced biomedical devices, including stents, occlusion devices, microneedles (MNs), implants, and scaffolds, among others.[33] Nevertheless, the practical implementation of 4D printed biomedical devices requires a comprehensive understanding of the underlying principles and mechanisms that govern the 4D (bio-)printing process. This review, therefore, aims to elucidate these principles by offering a detailed explanation of the 4D printing process, an overview of the range of smart (bio-)materials, and a comprehensive analysis of relevant applications in biomedicine.

2. 4D Printing Process

The dynamism inherent in 4D printed constructs stems from their ability to undergo temporal transformations between multiple states (i.e., commonly a shift from a temporary to a permanent configuration) upon exposure to external stimuli.[19,34] This introduces an additional layer of complexity to the design process, necessitating careful consideration of three fundamental parameters: i) the selection of stimuli-responsive materials, ii) the types of external stimuli to be employed, and iii) the rational design of the geometry and/or topology of the 4D printed construct.[35]

Among stimuli-responsive materials, SMPs and hydrogels have received a great deal of attention, owing to their wide applicability and responsiveness to a diverse range of stimuli (e.g., physical, chemical, or biological stimuli[36,37]). For example, SMPs can return to a predetermined shape upon thermal activation, while hydrogels may swell or contract in response to changes in pH or temperature. This broad array of activation mechanisms provides designers with a range of possibilities for engineering tailored responses in 4D printed constructs.

Moreover, the mechanics of design cannot be underestimated as it plays a pivotal role in the predictability and controllability of self-morphing behaviors. Devising a suitable geometry is essential for conveying the intrinsic material properties and stimuli-responsiveness into the desired mechanical performance. As such, there is a growing emphasis on the necessity to develop complex algorithms and computational tools for the geometrical and topological optimization of 4D printed constructs.

The stimulus itself, acting as a trigger for the dynamic change, requires careful selection and calibration. Stimuli can range from light, heat, and humidity to more specialized triggers, such as electric or magnetic fields, and even biological molecules, such as enzymes. The type of stimulus chosen has direct implications for the application at hand. For instance, in the biomedical context, the use of bio-responsive stimuli is a key to the development of smart drug delivery systems or tissue scaffolds that adapt to the physiological environment.

To elucidate, consider the application of 4D printing in drug delivery systems. In such a scenario, the geometric design should facilitate controlled substance release, while material selection should ensure biocompatibility and responsiveness to physiological stimuli (e.g., pH changes in the digestive tract). Furthermore, the external stimulus (e.g., a bio-responsive element) should be carefully aligned with the specific medical requirements, whether they relate to time-release mechanisms or targeted drug delivery.

This section, therefore, aims to provide a comprehensive review of the critical elements underpinning the 4D printing process, including an analysis of the most promising stimulus-responsive materials, a classification and evaluation of applicable external stimuli, and a discussion on the advancements in design methodologies for 4D constructs.

2.1. Materials

The smart materials used in 4D printing for biomedical applications must meet a triad of crucial criteria: i) biocompatibility, to ensure physiological safety, ii) functional responsiveness under physiological conditions, such as body temperature or pH level, and iii) mechanical robustness during and after shape transformation.[38,39] For example, temperature-responsive 4D printed biomedical constructs should not only be biocompatible but also operational at body-compatible temperatures (≈37 °C). As another example, the magnetic fields actuating magnetoresponsive 4D printed biomedical devices must exhibit noncytotoxic properties to ensure cellular safety.[40]

Stimuli-responsive or "smart" materials manifest characteristics, such as shape transformation or shape memory effect (SME), upon exposure to specific external stimuli.[16,41] While shape transformation entails an immediate shift from a temporary to a permanent state, SME materials possess the ability to "memorize" and revert to their original shape upon re-exposure to an activating stimulus. The kinetics of these transformations—specifically, the rate of shape change—is an aspect of paramount significance in specific sectors, such as soft robotics.[42] Despite significant progress in the creation of fast-response 4D printed objects, the field remains in its early stages and requires further studies.

In the ever-evolving landscape of 4D printing research, the continuous exploration and integration of novel materials and design methodologies serve as catalysts for advancements in biomedical applications. A number of smart materials, such as SMPs, hydrogels, LCPs, shape memory alloys (SMAs), dielectric elastomers (DEs), piezoelectric materials, magnetoactive materials, and bioactive particles or fillers, meet the aforementioned criteria. Notably, SMPs and hydrogels emerge as the

**ADVANCED
SCIENCE NEWS**

www.advancedsciencenews.com

**ADVANCED
MATERIALS**

www.advmat.de

forerunners in the domain of 4D (bio-)printing, owing to their superior printability, biocompatibility, and capacity for complex shape transformation.[36,43–45]

2.1.1. Types of 4D-Printing Materials

SMPs: SMPs are smart polymers that are renowned for their stimuli-responsive properties. Upon exposure to specific external stimuli, such as temperature, light, or pH, these polymers can transition between their temporary and permanent shapes.[41,46] Such morphological changes can range from simple bending to more complex forms, such as helixing or topographical modifications, depending on the mechanical properties of the SMPs.[47] In the domain of biomedicine, the versatile properties of SMPs (i.e., biocompatibility, mechanical robustness, tunability (i.e., tailored stiffness), and processability[48]) have facilitated their deployment in various applications, such as bone repair tools,[49] drug delivery systems,[50,51] occlusion devices,[52,53] scaffolds,[54,55] and embolization devices.[56]

Two distinct methodologies can be employed for programming the SME in SMPs: manual and AM-based processes.[57] The latter, albeit more challenging, is often more effective in achieving complex shape transformations but requires a comprehensive understanding of printing parameters and geometrical complexities for effective shape morphing. In contrast, the manual method provides less precise and sophisticated but more straightforward programming options.

SMPs may be characterized as being one-way, two-way, or multiway SMEs, depending on their cyclic behavior and the number of stored shapes, which can be chemically manipulated.[58,59] To quantify the SME in SMPs, such parameters as the strain recovery ratio (R_r) and the strain fixity ratio (R_f), are widely used[60] (**Figure 1ai**). These parameters quantify the capability of SMPs to recover to their original shape and to maintain a temporary shape, respectively.[60] Ideally, both R_r and R_f should approach 100% for an SMP to be considered highly effective.

To schematically illustrate the programming and recovery steps in SMPs, Figure 1ai shows a 3D thermomechanical cycle of SMPs under controlled mechanical loading at the macroscale. The cycle includes four steps: i) loading (path AB), ii) cooling (path BC), iii) unloading (path CD), and iv) heating or recovery (path DA or DE). The first three steps are collectively referred to as the "programming" process. During the loading stage, one (or multiple) temporary shape(s) are formed. The cooling stage stabilizes the temporary shapes, which result from the solidification phenomenon. External loads are removed during the unloading stage. The permanent shape is retrieved in the heating stage. The heating stage comprises two recovery processes: stress-free-strain-recovery and fixed-strain-stress-recovery processes. In the stress-free-strain-recovery process, shape or strain is recovered under stress-controlled conditions (the green hashed line or blue solid line in Figure 1ai). In the fixed-strain-stress-recovery process, force is retrieved under strain-controlled conditions (the red dashed line in Figure 1ai). It is worth noting that the loading stage does not necessarily require temperatures higher than T_{trans} (known as cold programming).[61]

SMPs can be made from either natural polymers, such as polypeptides, and polysaccharides, or synthetic ones, such as polylactic acid (PLA) and polycaprolactone (PCL).[62,63] While synthetic polymers usually offer superior mechanical strength as compared to natural ones, they might pose toxicity risks.[64] Biodegradable SMPs can be synthesized using synthetic monomers, such as ϵ-caprolactone and p-dioxanone.[65]

Temperature-responsive SMPs are commonly used due to their broad range of glass transition temperatures, which can vary from −70 to 150 °C.[66] SMPs with higher glass transition temperatures are preferred for extreme conditions. For instance, a high-temperature-responsive SMP based on polyamide/diacrylate has been 4D printed using a light-assisted AM technique called liquid crystal display (LCD) 3D printing[67] (Figure 1aii). The glass transition temperatures of SMPs can be adjusted to achieve body-friendly temperatures by modifying the involved chemical reagents or manufacturing processes. In the first method, the composition of the base SMP is altered through copolymerization and adjusting the concentration of cross-linkers.[68,69] In the second method, the glass transition temperature is controlled by creating composite SMPs through multimaterial 4D printing[57,59,70] or by adding nano-/microparticles to SMPs.[71] In addition, 3D printing parameters, such as printing speed, can influence the glass transition temperature.

Hydrogels: Hydrogels constitute a fascinating subset of smart soft polymers due to their unique hydrophilic characteristics and versatile mechanical properties. Composed of a 3D network that encompasses both swelling and nonswelling polymeric components,[72] hydrogels can absorb substantial amounts of water, leading to transitions between distinct states: sol–gel, gel–gel, and gel–sol–gel.[45] These transitions are dependent on environmental parameters, such as water content, temperature, pH levels, and ionic concentrations.[45]

Molecularly, hydrogels can be stabilized through either chemical bonding (i.e., irreversible, covalent bonds) or physical bonding (i.e., reversible, hydrogen, and van der Waals' bonds).[73] Striking a balance between swelling ratio and mechanical strength represents a central challenge in hydrogel research. This trade-off becomes particularly pivotal in the domain of 3D printing, where sufficient stiffness is necessary for the construction of freestanding structures. The cross-linking density is a crucial factor in this regard, as a higher cross-linking density leads to increased stiffness of the hydrogel.[74]

Owing to their inherent biocompatibility and bioprintability, hydrogels have been intensively researched for their applicability in 4D printing in biomedical engineering. They have demonstrated the capability for complex and controllable deformations, even in the presence of living cells.[15] Various 3D printing techniques, such as extrusion-based printing,[75,76] laser-assisted bioprinting,[77,78] and the drop-on-demand (DOD) technique,[79] have been employed to fabricate hydrogel-based structures. Each method comes with its unique set of challenges, including the quest for high resolutions in 4D printed structures. DOD, for example, is a promising technique that addresses this challenge by accurately controlling the deposition of hydrogel droplets and the timing between them to achieve the required resolution.[80]

In the rapidly expanding field of 4D printing, hydrogels have been deployed as shape-morphing agents in many applications, such as sensors, soft actuators,[81] controlled drug delivery systems,[44] and in vitro studies on cellular differentiation.[18] For example, temperature-responsive hydrogels offer exciting
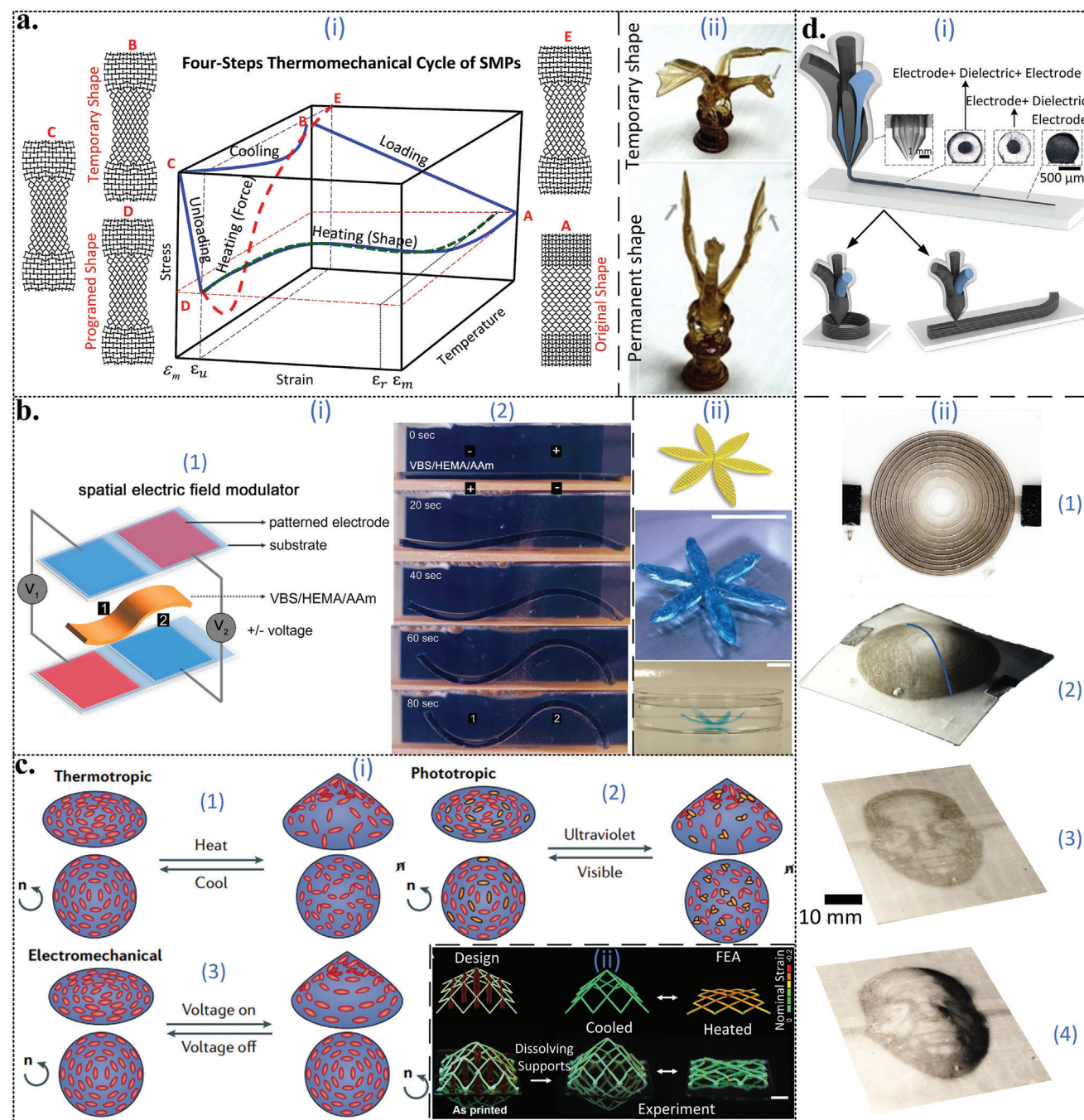
**ADVANCED
SCIENCE NEWS**

www.advancedsciencenews.com

**ADVANCED
MATERIALS**

www.advmat.de

Figure 1. Examples of different stimulus-responsive materials. a-i) A 3D schematic drawing of programming and recovery thermomechanical cycles in the 4D printing process is presented for typical temperature-responsive shape memory polymers (SMPs). It includes four steps, namely loading, cooling, unloading, and heating, with their corresponding shapes. a-ii) An illustration demonstrating the permanent and temporary shapes of a 4D printed structure made by liquid crystal display (LCD). Reproduced with permission.[67] Copyright 2022, Elsevier. b-i) Electroactive hydrogel actuation under a multipolar spatial electric field for inducing negative and positive mean radii of curvatures[87] (i1). This implementation creates a sequential actuation process within 80 s in an electroactive hydrogel-based actuator (i2). ii) A 4D bioprinted water-responsive hydrogel made through direct ink writing (DIW).[15] The top, middle, and bottom subfigures show the initial design, the initial shape of the 4D printed hydrogel, and the transformed shape. The scale bars represent 10 mm. c-i) The microconfigurations of liquid crystal polymers (LCPs), showing the disruption of orders in the presence of heat (1), light (2), and an electric field (3). Reproduced with permission.[94] Copyright 2022, Springer Nature. c-ii) A 4D printed LCP is depicted, exhibiting a shape-morphing behavior upon exposure to temperature changes. Reproduced with permission.[95] Copyright 2022, Wiley-VCH. The scale bar represents 10 mm. d-i) A schematic drawing illustrating inkjet-based multimaterial 4D printing of dielectric elastomers (DEs). Reproduced with permission.[157] Copyright 2021, Wiley-VCH. d-ii) 4D printing of multilayer DEs with different configurations and their topological shape-morphing to mimic a simple semispherical out-of-plane deformation (1 and 2) as well as a human face (3 and 4).[146]

**ADVANCED
SCIENCE NEWS**

www.advancedsciencenews.com

**ADVANCED
MATERIALS**

www.advmat.de

possibilities in soft robotics and actuators by allowing the formation of reversible shape-morphing structures.[82] However, achieving complex shape morphing with hydrogels for advanced applications requires rational mechanical design, including nonhomogeneous geometries, multimaterial constructs, and carefully engineered mechanisms for the application of external stimuli.[15,83,84]

Electroactive hydrogels add another layer of functionality by enabling both negative and positive curvatures within a single construct. Achieved through rational design of electrode patterns and the modulation of electric fields,[85–87] (Figure 1bi[87]), this capability allows for complex shape morphing in hydrogels. Such capability and their printability have opened up new avenues for applications, such as tissue engineering (e.g., 4D bioprinting of engineered cartilage with tailored shape-morphing behavior,[15] Figure 1bii).

Furthermore, hydrogels have demonstrated significant potential in the domain of controlled drug delivery. They provide an optimized platform for controlled drug release and ensure biocompatibility with both the encapsulated drugs and the surrounding biological tissues. This encapsulation also affords a protective mechanism against environmental contaminants, thereby enhancing the stability and efficacy of the carried drugs.[88–90]

Liquid Crystal Materials: LCPs and liquid crystalline elastomers (LCEs) are distinct classes of liquid crystalline materials[91,92] that offer unique mechanical and functional characteristics, owing to their specialized molecular structures. LCPs are thermoplastic polymers renowned for their superior mechanical strength, excellent chemical resistance, high-temperature stability, and biocompatibility.[93] These properties make them suitable candidates for a range of biomedical applications, such as surgical instruments, dental devices, orthopedic implants, and controlled drug delivery systems.[94]

Conversely, LCEs fall under the category of soft smart polymers and are capable of large, reversible, and rapid actuations. They consist of liquid crystals (or mesogens) integrated within an elastomeric matrix, demonstrating molecular anisotropy and entropic elasticity.[95] The actuation behavior in LCEs depends on the alignment of the mesogens, which can be triggered through mechanical stretching, shearing, or external stimuli, such as temperature changes. Mesogens can be incorporated into an elastomeric matrix either as a side chain or a main chain.[96] The exposure to external stimuli causes a nematic–isotropic phase transition, leading to SME in LCPs.[95,97,98] Figure 1ci illustrates the micromechanism of three different LCEs in the presence of heat, light, and electric field.[94] LCEs find applications in areas, such as soft robotics (e.g., robotic surgical tools), artificial muscles, actuators, and controlled drug delivery systems.[99]

Advanced AM techniques have been employed to fabricate structures from both LCPs and LCEs, with each method presenting specific advantages and limitations.[100] For example, DIW is a technique that permits mesogen alignment along the printing direction.[96] Although it lacks precision and complex shape-morphing capabilities, DIW enables the creation of functionally graded LCE-based structures by modulating the printing parameters. In contrast, DLP offers high-precision fabrication but faces challenges in mesogen alignments, resulting in simpler structures.[101] Hybrid AM techniques combine the advantages

of DIW with those of DLP to facilitate the fabrication of complex LCE-based constructs (Figure 1cii).[95]

While the potential of LCPs and LCEs in the realm of 4D printing and soft robotic is undeniable, significant challenges remain. For instance, in electroactive LCP-based actuators, there is a risk of undesirable increases in electrical conductivity. Furthermore, the high-temperature sintering process involved in 4D printing can lead to unintended deformations. Additionally, the curing times for LCP actuators, which can span from a few minutes to several hours, limit rapid fabrication capabilities.[102–104]

To address these challenges, innovative approaches are being investigated. One such approach involves the use of UV-assisted printing to produce LCE-based soft actuators with biphasic liquid metal conductors.[105] This technique enables the realization of multifaceted shape-changing patterns through the employment of different LCE double-layer cross-structures. By modulating the sequence and path of the printing process for these double layers, diverse deformation modes can be achieved.[105]

SMAs: SMAs are metal-based smart materials that exhibit remarkable shape recovery capabilities in response to certain types of stimuli, such as temperature changes or magnetic fields. Generally composed of two main phases (i.e., martensite (at lower temperatures) and austenite phase (at higher temperatures)), SMAs can undergo transformations between various shapes.[26] Depending on the cyclic behavior of SMAs, they can be categorized into three groups: one-way, two-way, and pseudoelastic SMAs.[106] The first two categories exhibit SMEs and thus can be programmed. However, pseudoelastic SMAs can completely recover their shapes without any additional recovery processes (without SME). Therefore, pseudoelastic SMAs behave similarly to elastic materials and are, thus, less desirable for 4D printing applications.[106]

The behavior of SMAs is dependent on their chemical compositions and microstructures. An archetypal example is the Nickel-Titanium (NiTi) alloy. At temperatures below the martensite finish temperature, the alloy can be deformed and adopts a different shape. However, upon heating above the austenite start temperature, it reverts to its original form, thereby demonstrating one-way SME. This behavior is closely related to the nickel content and the microstructure of the alloy. Conversely, two-way SME, where the alloy "remembers" distinct shapes at varying temperatures, is facilitated through mechanical training of the material. Moreover, an increment in the nickel content usually correlates with elevated transformation temperatures in SMAs.

The fabrication of SMA structures typically employs NiTi and Ni-Mn-Ga alloys. These structures can be manufactured using various AM techniques, such as powder bed-based methods (e.g., SLM[26,107–109] directed energy deposition, electron beam melting,[110] powder bed binder jetting[108,111]), or extrusion-based techniques (e.g., inject 3D printing).[112] However, the 4D printing of SMAs remains relatively less studied as compared to smart polymers, such as SMPs and hydrogels. This can be attributed to several factors, including their low stretchability, challenges in their 3D printing processes, prolonged manufacturing timelines, and higher costs.[26] Each of the AM techniques used for the fabrication of SMA specimens has certain advantages and disadvantages. The SLM technique offers high resolution and the ability to create complex geometries from SMA. However, these benefits come at the cost of high energy consumption and

**ADVANCED
SCIENCE NEWS**

www.advancedsciencenews.com

**ADVANCED
MATERIALS**

www.advmat.de

the necessity for specialized equipment and extensive parameter optimization. The high-temperature gradients involved in SLM processes can also affect the phase transitions in SMAs, impacting their SME properties.[113,114] Directed energy deposition is well known for its ability to manufacture large-scale components. However, the deposition process may induce internal stresses that affect the mechanical properties of the SMA.[115] Electron beam melting offers high precision but is generally more expensive and requires a high-vacuum environment, which can be restrictive.[116] Powder bed binder jetting provides an option with lower thermal impact. However, the binder materials can interfere with the properties of SMAs.[108,117] Finally, extrusion-based techniques, such as inkjet 3D printing, have the advantage of low material waste but often face limitations in resolution and speed, making them less suitable for complex SMA components.[118]

As an alternative to nickel-based alloys, copper (Cu) alloys have recently been used as other types of SMAs, next to high-temperature β-Ti alloys. Cu alloys present distinctive advantages, such as significantly lower costs as compared to nickel-based SMAs. Cu alloys (e.g., Cu-Al-Ni[26]), also offer versatility in tailoring thermal and mechanical properties through alloying.[26] These alloys are also capable of demonstrating both one-way and two-way SMEs. The use of Cu alloys allows for a broader range of activation temperatures and may enhance electrical conductivity, offering new avenues for stimulus-responsiveness in 4D printing applications.[26] However, the transition to Cu-based SMAs requires extensive evaluation for biomedical applications, particularly focusing on issues, such as biocompatibility and corrosion resistance.[26] Furthermore, β-Ti SMAs (e.g., Ti–Nb) exhibit high transition temperature, large theoretical shape morphing and low costs.[119]

Despite these challenges, 4D printed SMAs have distinct advantages over other smart materials, such as SMPs and hydrogels, in terms of their superior mechanical strength. This characteristic makes them increasingly attractive for specialized applications that require robust mechanical performance.

Ceramic-Based Materials: The utilization of shape memory ceramics (SMCs) in biomedical and 4D printing applications is an emerging domain that necessitates further investigation to better understand their potential applications. Zirconia ceramics,[120] notably, have demonstrated SME and superelastic properties. This can be attributed to their ability to undergo a martensitic phase transformation, a mechanism that effectively converts thermal energy (i.e., heat) into mechanical strain or the other way around.[121] The brittle nature of these ceramics, which typically results in failure at low strains after a few cycles, can be mitigated by providing a fine-scale structure with few crystal grains. These oligocrystalline structures reduce internal mismatch stresses during the martensitic transformation, leading to robust SMCs that can endure many superelastic cycles up to large strains.[122]

Moreover, zirconia ceramics can exhibit superior SMEs when deformed at a temperature between their martensite and austenite transition temperatures. This can be accomplished through a stress-induced transformation from austenite to martensite, which, when the load is removed, retains the new shape. Subsequent heating above the austenite transition temperature causes the martensite to revert to austenite, returning the material to its original shape.[120]

Advancements in 4D printing technologies have enabled the fabrication of complex ceramic structures through the use of zirconia (ZrO_2) inks with varying solid contents.[123,124] This method allows for the sintering of 3D printed lattices and bilayer ceramic architectures that can undergo preprogrammed shape transformations.[125] The development of this technology holds promise for generating complex ceramic structures with specific functionalities.

An alternative approach for shaping ceramics draws inspiration from nature, specifically, the self-folding behavior seen in plant seed dispersal units that occur due to differential swelling behaviors.[126] This technique involves manipulating the microstructure of the material to undergo local anisotropic shrinkage during heat treatments. The methodology involves magnetically aligning functionalized ceramic platelets in a liquid ceramic suspension, which is then consolidated through an enzyme-catalyzed reaction. This process can be used to create alumina compacts with bioinspired bilayer architectures, allowing for controlled shape change during the sintering step. Different complex shapes, such as bending, twisting, or combinations of these deformations, could be programmed.[126]

Furthermore, recent research has synthesized a reconfigurable and shape memory preceramic suitable for 4D printing, composed of liquid silicone (polydimethylsiloxane, PDMS), shape memory epoxy, and ceramic nanoparticles (ZrB2 NPs).[127] For this purpose, the structure with an initial shape is printed through DIW and is then reshaped into the desired complex geometry through a two-step curing process at different temperatures. The SME of the precursor allows it to be programmed into temporary shapes and revert to the original state under heat stimulus.

Another innovative strategy merges 4D printing and origami techniques to fabricate ceramic structures.[128] This entails the use of specialized inks made from elastomers and ceramic precursors. After printing, these structures are subjected to pyrolysis, transforming them into ceramics. The ability to program these structures for specific deformations during pyrolysis expands the design space for ceramics, offering a new paradigm for constructing lightweight and strong ceramic components.[128]

2.1.2. Properties of Types of 4D-Printable Materials

Temperature-Responsive Materials: Temperature-responsive materials, commonly referred to as thermoresponsive polymers, are recognized by their intrinsic capacity to undergo changes in physical or chemical properties in response to external temperature stimuli. The ability to exhibit such changes, coupled with inherent biocompatibility and adjustable phase transition characteristics, makes these materials particularly advantageous for advanced biomedical and 4D printing applications.[129]

Poly(*N*-isopropylacrylamide) (PNIPAM), serves as an example in this category and has gained considerable attention in the biomedical field. The important feature of this polymer is its lower critical solution temperature, which is close to the human body temperature. This unique characteristic enables its use in a plethora of biomedical applications, such as controlled drug

**ADVANCED
SCIENCE NEWS**

www.advancedsciencenews.com

**ADVANCED
MATERIALS**

www.advmat.de

delivery, tissue engineering, and bioseparation.[130] Specifically, hydrogels synthesized from PNIPAM can encapsulate pharmaceutical agents and modulate their release kinetics in a temperature-dependent manner.[131] Such materials offer the potential for targeted and timed drug delivery systems that can be manipulated via external temperature stimuli.[132]

In addition to PNIPAM, Pluronic F-127 and polyethylene glycol (PEG) based polymers are also notable examples of temperature-responsive materials. Pluronic F-127 has been successfully employed in thermal-ablation therapies targeting malignant cells, thereby displaying its potential for use in oncological applications.[133] Similarly, PEG-based polymers have found applications in wound healing, where temperature-responsive behavior can facilitate the timely release of a healing agent or cytokines to accelerate tissue repair.[134]

Electroactive Materials: Electroactive materials represent another class of smart materials that manifest a change in dimensional or functional properties upon exposure to an electric field. Such materials are composites, comprising a base substrate and an electrically responsive conductive filler. While metals can serve as the base material, polymers have gained greater importance in the context of 4D printing.[135,136]

Electroactive materials find their primary applications in sensors, actuators, and energy-harvesting devices due to their intrinsic stimuli-responsive properties.[137] The most frequently used electroactive materials used in 4D printing include piezoelectric materials and DEs.

Piezoelectric Materials: Piezoelectric materials offer a unique suite of characteristics that are tailored for smart structures. These materials, comprising either metal-based ceramics or polymers, exhibit the capacity to generate electrical charges when subjected to mechanical deformation, such as pressure, strain, vibrations, and sound.[138] Metal-based ceramics (e.g., lead zirconate titanate and barium titanate[138]) are prevalently used in transducer applications. Polymeric examples include polyvinylidene difluoride (PVDF), known for its high flexibility.

Innovative fabrication methods have emerged in the domain of piezoelectric materials, enabled by advanced 4D printing techniques. FDM, for instance, facilitates the fabrication of thermoplastic-based piezoelectric materials, such as polypropylene, acrylonitrile butadiene styrene (ABS), and polytetrafluoroethylene (PTFE), overcoming the limitations inherent to traditional ceramic processing techniques.[138–140] These materials are selected due to their relatively low dielectric and elastic properties.[140–142]

Furthermore, piezoelectric materials offer new horizons in biomedical engineering. The fabrication of smart (porous) biomedical implants utilizing these materials brings forth a host of advantages, including but not limited to mechanical strength, high mass transport properties, and tunable biodegradation rates.[143–145]

Dielectrics Elastomers (DEs): DEs constitute another category of electroactive materials that are predominantly utilized in soft robotics.[146] Dielectric elastomer actuators (DEAs), functioning as deformable capacitors, exhibit large strains under electric fields. These materials are structured with an elastomer sheet sandwiched between two compliant electrodes, resulting in deformation upon electric stimulation.

Two common types of DEs are based on acrylic and silicone elastomers. The fabrication methods for DEAs generally employ pre-stretching of the elastomer material, which is subsequently framed to enhance its electric field-induced deformation and breakdown strength.[147] Conventional (and planar) manufacturing techniques, such as spin coating[147–149] and sequential mechanical assembly,[150] have been used to fabricate DEAs. While these methods yield primarily planar shape morphing, additional processes can transform such in-plane deformations into out-of-plane deformations (e.g., bending, rolling).[149,151]

Recent innovations have presented multilayer techniques, which allow DEAs to deform without the necessity for pre-stretching.[152] Examples include bioinspired mechanisms, such as the jumping features observed in click beetle.[147]

From an AM viewpoint, 4D printing of most of the current silicone-based DEs is still in its infancy due to the low viscosity and long curing time of silicone.[153] However, some AM techniques, such as FDM,[154] SLA,[155] and DOD inkjet 3D printing,[156] have been successfully used for DE fabrication. In particular, multimaterial inkjet 3D printing can be appealing to print multimaterial DEs to achieve more complex shape-morphing[157] (Figure 1di). Furthermore, FDM and SLA require long curing times and cannot achieve the same level of consistency in the layer thickness found in prefabricated elastomeric films.[158] In some cases, it is also possible to combine AM techniques with conventional techniques, such as spin coating, to fabricate certain sophisticated multilayer DEs (Figure 1dii).[149] 4D printing of DEs aiming at complex shape morphing remains an active area of research and extensive research is being conducted currently.[137,159–161]

Magnetoactive Materials: Magnetoactive polymers (MAPs) form a specialized category of smart materials whose properties (e.g., elastoplastic properties and stiffness) change upon the application of an external magnetic field. The interaction between magnetic fields and these polymers leads to a magnetic field-dependent torque until the magnetic domain within the material aligns with the applied field.[162,163] These materials are mainly composed of a soft base polymer, typically silicone-based, infused with magnetoactive fillers. These fillers exhibit ferromagnetic or paramagnetic properties, and encompass a range of materials, including carbon black, carbon nanotubes (CNTs), carbon nanofibers, and metallic particles (e.g., gold NPs, neodymium–iron–boron (NdFeB), or Fe_3O_4).[6] Iron oxide particles are often used as magnetoactive fillers due to their unique combination of chemical stability, high heating efficiency, and biocompatibility.[164]

MAPs can be classified into "soft" and "hard" categories based on the magnetic saturation levels of the fillers used. Soft magnetic MAPs incorporate low-saturation materials, such as iron oxides, whereas hard magnetic MAPs utilize fillers with high magnetic saturation, such as NdFeB.[163,165] The implication of this classification on the functional characteristics of MAPs requires more comprehensive investigation.

A further classification of MAPs can be done based on the types of base polymer used, resulting in magnetorheological elastomers (MREs) and magnetorheological plastomers

**ADVANCED
SCIENCE NEWS**

www.advancedsciencenews.com

**ADVANCED
MATERIALS**

www.advmat.de

(MRPs).[166] MREs are distinguished by their high sensitivity to applied magnetic fields and their capability for reversible deformation.[167,168] In contrast, MRPs demonstrate a more plastic nature, maintaining their deformed state even after the removal of stress. The inherent difference in properties makes MREs more suitable for dynamic systems requiring quick and reversible changes in mechanical characteristics. On the other hand, MRPs are tailored for applications requiring permanent deformations, thus offering strong plasticity and damping characteristics. Most MRP matrices are thermosets (i.e., cross-linked polymers, such as polyurethanes (PU) and poly(vinyl alcohol) (PVA). The versatility of these materials is exemplified by multifunctional MRPs, particularly 3D printed structures using PCL/thermoplastic PU (TPU) polymers that showcase SME and self-healing capacities.[166]

The topology of the magnetoactive fillers within the polymer matrix can be engineered to create complex shape-morphing and anisotropic properties in both MREs and MRPs. However, the mechanisms through which varying the distributions of various fillers can impact the overall performance of the material, and the types of optimization strategies still need to be explored.

Manufacturing techniques for MAPs are broadly classified into two categories: conventional methods (e.g., molding or templating) and AM techniques.[6,168] Each category presents its own set of challenges and advantages. For instance, conventional methods are often constrained by limitations in the creation of complex geometries and less control over filler dispersion[169] FDM, SLA, inkjet (including electrohydrodynamic inkjet[170]), and DLW are common AM techniques to make MAPs structures.[6] Alternatively, 4D printing allows for more complex designs and the capability to create MAPs without the need for external magnetic fields.[169]

Interestingly, hybrid manufacturing techniques are emerging to circumvent the limitations of each method.[27] In these techniques, high concentrations of magnetic particles (≈20–70 wt%) prevent the use of advanced micro-AM techniques, such as 2PP.[27] Therefore, micromolds are fabricated using 2PP, and the final MAP structures are created through molding. Such hybrid methods may also involve the encapsulation of magnetorheological (MR) fluids within elastomers, allowing the 3D printing of soft structures with tunable elastic properties. After creating hybrid MREs, a laser-assisted technique can be used to magnetize them. In this approach, local magnetization profiles are created by locally heating the magnetoactive polymer with a laser, which enables complex shape-morphing[163] (**Figure 2a**). This process is similar to multimaterial 3D printing.[169] Examples of such MREs include acrylate-based polymers containing Fe_3O_4 particles, which can be used to tune the mechanical and magnetic properties of 3D printed composites.[21]

Biocompatibility remains a crucial consideration for MAPs, especially in biomedical applications. While iron oxide NPs are generally considered biocompatible, other ferromagnetic particles, such as iron and its alloys may introduce toxicity risks. Therefore, a comprehensive evaluation of not only the type of fillers and based polymers but also their concentration and the nature of the magnetic fields applied is necessary for assessing cellular viability.[163]

2.2. Stimulation

Stimulation stands as a pivotal element in the efficacy of 4D printed structures within the context of biomedical applications. The core of 4D printing in biomedicine lies not just in its ability to fabricate structures capable of functioning in vivo without cytotoxic effects, but also in its requirement for external stimuli to trigger specific actions or changes. Stimulation used in 4D printing can, in general, be divided into three main categories: physical, chemical, and biological. Specific 4D printed structures can respond to multiple stimuli based on the composition of the smart structure, which can be a smart composite or a smart material with different fillers.[171] We will only focus on physical and chemical stimulation, as little information is available regarding the 4D printing of biologically responsive materials.

2.2.1. Physical Stimulation

Physical stimuli, such as temperature and magnetic fields, are widely used to trigger 4D printed medical devices. Owing to their ease of manipulation and reliable outcomes, these stimuli induce changes at the molecular level, affecting the conformation of polymeric chains or the internal arrangement of the material. These changes result in shape morphing and the creation of dynamic behavior in the printed objects, enabling them to adapt to environmental conditions, such as fluctuating body temperatures. The integration of physical stimuli into 4D printing offers a pathway for evolving more complex, adaptive medical devices.

Temperature: Temperature stands as a subcategory of physical stimulation, pivotal for actuating 4D printed structures. SMPs emerge as the material of choice for temperature-induced responses, prominently for their SMEs. It is also worth mentioning that temperature-responsive 4D printed objects possess the capability for multifunctional recovery, including morphological changes and even changes in optical properties, such as color. For instance, Figure 2b shows a 4D printed temperature-responsive chameleon, which changes its color upon exposure to different temperatures.[172]

The mechanism for SME requires a designated transition temperature, either the glass transition temperature (T_g) or the crystal-melt transition temperature (T_m), depending on the structure of the polymer (i.e., amorphous or crystalline, respectively).[59] SME results from a thermally induced phase transition between two rubbery and glassy (i.e., active and frozen, respectively) states. The molecular architecture generally consists of two key components: i) chemical cross-links (i.e., hard phases) that dictate the permanent shape, and ii) temperature-sensitive segments (i.e., soft phases), that facilitate temporary shape changes when the temperature crosses the transition temperature, T_{trans}.[173,174]

For biomedical applications, the direct method of temperature stimulation (e.g., immersing the 4D printed object in hot water or heating with hot air) is often impractical due to the in vivo environment's inaccessibility. Hence, alternative strategies for internal heat generation have been proposed, exploiting external stimuli, such as focused ultrasound,[175] infrared (IR) light,[55] microwaves,[176] laser light,[177] and magnetic or electric fields.[178]
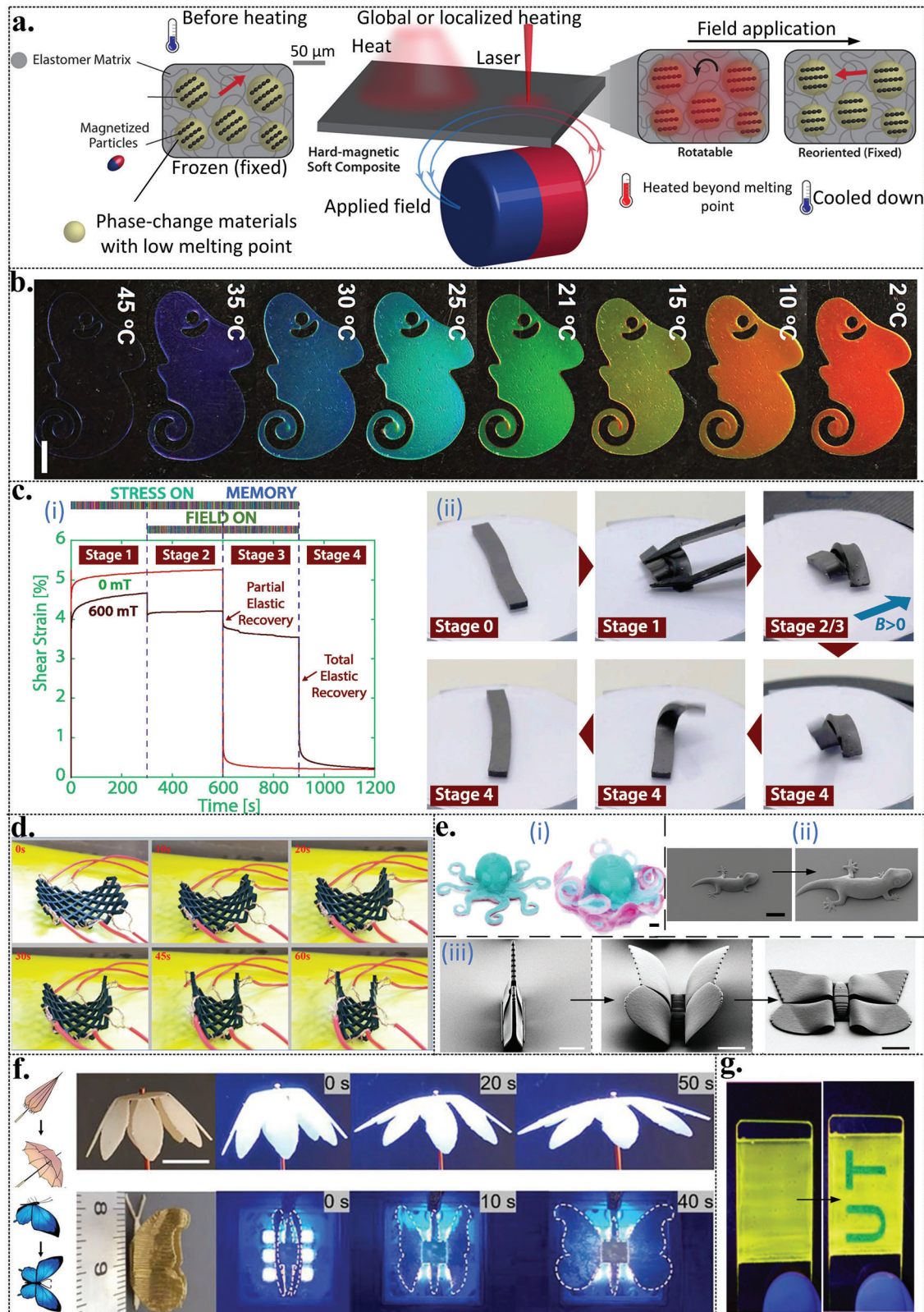
Figure 2. Examples of different stimuli for actuating the response of 4D printed materials. a) Laser-assisted magnetization profile in magnetoactive polymers.[163] b) Digital photographs of a temperature-responsive 4D printed chameleon. Reproduced with permission.[172] Copyright 2022, Elsevier. The scale bar represents 5 mm. c) A magnetoactive shape memory polymer (SMP) controlling the variation of applied/recovery strain in the absence of a magnetic field (red curve) and in the presence of a magnetic field of 600 mT (blue curve) (i). Reproduced with permission.[181] Copyright 2019,

**ADVANCED
SCIENCE NEWS**

www.advancedsciencenews.com

**ADVANCED
MATERIALS**

www.advmat.de

Magnetic Field: Magnetic fields stand as another prominent form of physical stimulation in the domain of 4D printing, particularly well-suited for untethered actuation in miniaturized soft robotics and biocompatible applications.[179,180] Similar to temperature-sensitive mechanisms, magnetic fields induce what is termed a "magnetic memory effect," allowing the material to revert to its predesigned form upon exposure to a magnetic field.

A typical example illustrating the magnetic memory effect is the fabrication of magnetoactive SMP composites. These composites consist of a stable elastomeric matrix and a MR fluid that serves as the programmable phase.[181] When subjected to a magnetic field, these composites exhibit specific stages of programming and recovery (Figure 2ci,ii). Initially, in the absence of a magnetic field, the elastomeric components of the composite bear the mechanical stress, while the MR fluid remains in a liquid state. Upon the application of a magnetic field, the MR fluid transitions to a more rigid phase, effectively bearing the stress and causing the elastomeric components to relax. Once the magnetic field is removed, the composite reverts to its original shape, illustrating its magnetic memory capabilities.

The mechanism of heat generation induced by magnetic fields is predicated on the principles of induction.[6] In such scenarios, the magnetic fillers within the magnetoactive materials undergo rearrangement when subjected to an alternating magnetic field. This rearrangement leads to energy dissipation and subsequent heat generation.[182] Such a mechanism is advantageous over other remote stimulation methods, such as light or electric fields, both in terms of speed of transition and the capacity for temperature control through a feedback mechanism based on magnetic hysteresis loss.[183,184] There is also no need for the connection of power transmission lines to the 4D printed devices, thus reducing the risk of failure. Furthermore, it is possible to induce selective heating by locally patterning the structure with magnetoactive particles.

In biological applications, stringent constraints must be considered so as not to adversely impact biological tissues. The safe frequency range for magnetic fields in biological contexts is generally considered to be between 50 and 100 kHz.[185] Another determinant factor is the size of the magnetoactive particles, which must be optimized to ensure cell compatibility while achieving the desired magnetic memory effect.[163]

Careful consideration is also required to achieve a balanced interplay among various parameters, such as the type of magnetic field (alternating vs. direct), the type of magnetoactive fillers, their particle sizes, concentration levels, and the base polymer. These factors collectively influence the versatility, safety, and efficacy of magnetic field-induced actuation in 4D printed structures.

Electric Field: Electric fields constitute another important modality for the activation of 4D printed structures. These structures incorporate electroactive fillers that become responsive when exposed to an electric field, resulting in shape-morphing behavior through various mechanisms, such as Joule heating.[135,136]

Joule heating serves as a prominent means to induce shape changes and presents several features, including rapid activation, uniformity, remote controllability, and convenience.[135,186] For instance, gold electrodes have been employed to initiate the shape recovery of nanocomposites at a relatively low voltage of 13.4 V.[135,186] This low voltage threshold enables simultaneous actuation and monitoring of 4D printed structures.

Electric fields have been widely used to activate SMEs in DEs, hydrogels, and SMPs. Various materials have been explored for these applications, including hydrogels made of acrylamide cross-linked with *N,N*'-ethylene bisacrylamide,[187] chitosan-based hydrogels,[85] and alginate-based hydrogel grafts.[188] For instance, a chitosan-based hydrogel was employed in an electric field and pH-responsive antibacterial drug delivery system.[85] Poly (D,L-lactide-co-trimethylene carbonate) (PLMCs) reinforced with CNTs have been 3D printed via DIW to function at high voltages up to 25 V.[189]

Various applications have originated from these advancements, including the creation of stent-like structures through the FDM of CNT-reinforced PLA.[190] These structures demonstrated shape recovery within 60 s at a voltage of 20 V (Figure 2d). Moreover, smart drug delivery systems employing methacrylate-based hydrogels have been designed to operate at voltages less than 2V.[191] On the microscale, 2PP has been utilized for the precision 3D printing of electroactive hydrogels, paving the way for biocompatible drug delivery systems.[192]

Water/Solvent: Water or moisture can serve as a physical stimulus to trigger hygroscopic materials, which tend to absorb moisture, to deform into a desired shape.[193,194] The Self-Assembly Lab at the Massachusetts Institute of Technology, a pioneer in 4D printing,[193] has developed a 3D printed hydrophilic polymer with up to 150% stretchability when exposed to moisture. This expansion is strategically guided by placing stiffer parts in the desirable direction to reach the final desired shapes. Utilizing a combination of rigid and hygroscopic materials to construct hinges, only the hygroscopic sections become active when exposed to water. By strategically placing these hinges on a 1D line or 2D plane, different shapes can be obtained upon stimulation. This technique can also be applied to 3D-to-3D or 3D-to-2D shape transformations. In this way, it is possible to 3D print multiple hydrophilic polymers that may react differently when immersed in water to create complex self-morphing behaviors.[195]

Wiley-VCH. A schematic drawing depicting the experimental steps involved in the programming and recovery cycles of a magnetically stimulated SMP (ii) Reproduced with permission.[181] Copyright 2019, Wiley-VCH. Stage 0 shows the permanent shape of the SMP. Within steps 1–3, the SMP is loaded in the presence of the magnetic field. Then, the SMP recovers its shape within a short time through step 4. d) Electroactive mechanical metamaterials based on SMP/carbon nanotubes (CNTs). Reproduced with permission.[190] Copyright 2022, Elsevier. The 4D printed metamaterial folds within 60 s under a 70 V electric field. e) Water- and solvent-responsive 4D printed structures depicted at the macro-scale (i). Reproduced with permission.[198] Copyright 2019, Wiley-VCH and microscale (ii,[23] and iii, Reproduced with permission.[9] Copyright 2021, Wiley-VCH). Scale bars in e-i, e-ii, and e-iii represent 1 cm, 20 μm, and 20 μm. f) Light-responsive 4D printed structures, which are shifted from temporary states to permanent shapes, mimicking the opening and closing of an umbrella and butterfly. Reproduced with permission.[217] Copyright 2022, Wiley-VCH. g) A schematic drawing of a mechanical loading stimulus (rubbing) and its effect on the changing luminescent color of a thin film substrate. Reproduced with permission.[225] Copyright 2009, Springer Nature.

**ADVANCED
SCIENCE NEWS**

www.advancedsciencenews.com

**ADVANCED
MATERIALS**

www.advmat.de

Hydrogels have emerged as the material of choice for water-responsive materials applications, especially given their high biomimetic potential.[196] Naturally driven hydrogels, such as gelatin, collagen, silk fibroin, and chitosan with hydrophilic natures, offer promising applications in 4D bioprinting.[197] Complex, dynamic shape-morphing can be achieved based on the concepts of multimaterials and rational design in a composite ink made of stiff cellulose fibrils and a soft acrylamide matrix.[83] For example, a water-responsive multimaterial structure was 4D printed via extrusion-based printing of hydrogels and elastomers. Different shape-morphing behaviors could be achieved that are inspired by the movement of the octopus's tentacles[198] (Figure 2ei). Water-responsive hydrogels also have the potential to be 4D printed at different length scales from the microscale[199] to the macroscale with programmed shape-morphing behaviors.

In tissue engineering applications, water-sensitive 4D printed scaffolds change their shapes in a spatiotemporally dependent manner at different levels of water absorption. An example is a two-layered construct made of photopatterned PEG layers with varying molecular weights, which demonstrates that differential swelling ratios could give rise to anatomically relevant shapes.[200] These biocompatible scaffolds have been observed to exhibit an impressive cell viability rate of 90% over an 8-week culture period.[200] In cartilage tissue engineering, water-responsive 4D printed constructs have been used to fabricate mesenchymal stem cells (MSCs) laden scaffolds featuring shape-morphing properties.[15] The bilayered hydrogel scaffold was made from hyaluronan and alginate with different swelling ratios via an extrusion-based 4D bioprinting technique.

Beyond water, solvents, such as ethyl acetate and isopropyl alcohol can also trigger reversible dynamic deformation in 4D printed structures.[9] These solvent-responsive materials, often referred to as capillary force-responsive materials, can undergo swelling or shrinkage as the solvent evaporates. The 4D printed constructs can even be manufactured at the microscale through 2PP.[9,23,201] As an example, Figure 2eii,iii shows two 4D printed self-assembly microstructures inspired by a butterfly[9] and a gecko,[23] respectively.

The use of solvent-responsive materials, such as chitosan, is further augmented by their irreversible dynamics. For instance, chitosan cross-linked with citric acid can undergo one-way shape morphing when immersed in a chemical solvent. This process creates a concentration gradient as the solvent diffuses through hydrophilic chitosan and hydrophobic materials. In contrast, immersing the material in ethanol can restore the original shape by minimizing this gradient.[202]

Light: Light offers a unique medium for the actuation of 4D printed structures due to its various advantageous properties: it is a clean-energy source, available ubiquitously, triggers a rapid response and can be controlled remotely without physical contact.[203,204] Consequently, light not only has the capability to heat 4D printed objects remotely but also serves as a vital stimulus for inducing shape-morphing behaviors, particularly in biomedical applications.[205,206]

Materials responsive to light can generally be classified into two categories: photochemical-responsive and photothermal-responsive.[204,207] Photochemical-responsive materials inherently convert light energy to mechanical energy through photochemical processes. For instance, UV-responsive SMPs, such

as densely branched polycoumarate derivatives have been developed to demonstrate multistimuli-responsive characteristics.[208] Conversely, photothermal-responsive materials contain additional photothermal reagents, such as gold nanoparticles or carbon-based nanoparticles to form a thermally responsive matrix.[204,209–211] These agents absorb light and convert it into internal heat, which in turn actuates the base material. For example, azobenzene-containing SMPs are widely used in photothermal-responsive 4D structures, owing to their trans–cis photoisomerization properties.[212]

To manufacture photoresponsive materials, photopolymerization 3D printing technologies are used for photochemical-responsive materials in the presence of specific wavelengths, typically UV (or IR light).[213] Alternatively, the FDM method can be used for photothermal-responsive materials without the need for UV light exposure.[214–216] In addition, photoresponsive fillers, such as carbon black, can be added to thermoplastic polymers, such as TPU for 3D printing applications.[215] Figure 2f shows a photoresponsive poly(ether ether ketone)-based SMP inspired by the opening of an umbrella and the flying of a butterfly, which exhibits shape-shifting behavior when exposed to UV light.[217]

However, the use of light as a stimulus is not without challenges.[218] Firstly, photoactivated reagents may induce cytotoxic effects, particularly detrimental in biomedical applications.[204] Secondly, the process of photothermal conversion can lead to overheating of the samples.[219] Lastly, the efficiency of light activation is highly dependent on specific wavelengths, which imposes a constraint on the materials and wavelengths used for the printing process to avoid undesired structural changes. The power and wavelength of the light should not only be sufficient for activating 4D printed structures but must also not damage the body.[218]

To mitigate some of these limitations, alternative light sources, such as sunlight have been considered for their natural, sustainable, and cost-effective characteristics.[204,215,220–222]

Acoustic Waves: Acoustic waves are another type of physical stimuli to activate 4D printed materials. These stimuli can manifest in various forms including vibrations, audible sound, ultrasound, and infrasound, each capable of being generated from distinct sources. For instance, vibration can be generated by exciting piezoelectric materials using an electric field.

Ultrasound refers to sound waves above the audible limit of human hearing and can be categorized into low-frequency, medium-frequency, and high-frequency domains. Each domain has unique penetration depths and focal points. Low-frequency ultrasound, for example, can penetrate deeper into the tissues, but lacks the capacity to concentrate its energy into a smaller area.[88] In contrast, high-frequency ultrasound is capable of localizing its energy, but its depth of penetration is comparatively shallow.

High-frequency ultrasound can induce local heating due to its elevated scattering properties. Utilizing this characteristic, therapeutic ultrasound-responsive hydrogels, such as one based on melamine-enhanced PVA have been developed.[223] However, ultrasound also exhibits nonthermal effects that may cause undesired consequences. One such effect is cavitation, wherein small gas bubbles are formed within the tissue due to acoustic vibrations generated by the ultrasound. These bubbles can expand to twice their original size within the tissue.[88] The subsequent

**ADVANCED
SCIENCE NEWS**

www.advancedsciencenews.com

**ADVANCED
MATERIALS**

www.advmat.de

collapse of these bubbles produces shock waves, which can act as microreactors within biological systems.[88]

Mechanical Loading: Mechanical is another form of physical stimulus that, although abundant in nature, has been relatively underexplored in the field 4D printing.[224,225] Various mechanically responsive materials exist, including organic molecules, polymers, and metal nanoparticles. These materials offer more than mere shape-morphing capabilities, they can also provide activation energy required for specific chemical responses in polymeric structures[224,226] (e.g., spiropyran polycarbonate).[227]

The applications of mechanical stimuli can lead to significant changes in the electronic configurations of chemical bonds within these materials. Such changes have the potential to modify a broad array of material properties, including chemical, optical, electrical, and magnetic characteristics.[224] Hence, integrating mechanically responsive materials with rational designs is crucial for achieving desired mechanically induced outcomes in 4D printed structures.

Mechanical stimuli can be synergistically integrated with other forms of stimuli, such as chemical stimuli, to create materials with dual responsiveness (i.e., mechano-chemo-responsive or mechano-chromic materials). These materials can undergo notable changes in properties, such as absorption and/or fluorescence upon the application of multiple stimuli, such as mechanochemical stimulation.[228]

One important example is the class of piezo-chromic luminescent materials, which change the color of their luminescence upon exposure to mechanical stimuli.[225] These materials are primarily constructed from dye-doped polymers and liquid-crystalline substances. A variety of mechanical loading types, including shearing, grinding, or elongation, can induce changes in their photoluminescent color.[225] For instance, the luminescent color of a thin film can be switched, manifesting the sign "UT," by applying an isothermal mechanical stimulus, such as rubbing with a glass rod at room temperature[225] (Figure 2g).

2.2.2. Chemical Stimulation

To better understand the operating mechanisms of 4D printed biomedical devices that respond to physiological conditions, it is crucial to evaluate their reactions to physiological variables, such as pH levels and ionic concentration. The analysis of these reactions can also aid in optimizing the performance and efficiency of such devices. Furthermore, understanding how 4D printed biomedical devices respond to changes in physiological conditions is essential for ensuring the safety and efficacy of these devices in real-world medical applications.

pH: pH, as the acidity level of an aqueous solution, can experience significant fluctuations under various pathological conditions, affecting the different organs of the human body (e.g., the gastrointestinal tract, vaginal tract, or blood vessels[229]). Accordingly, 4D printing technologies have been harnessed to develop pH-dependent systems for biomedical applications, including drug delivery and tissue engineering.[229] These systems are designed to be responsive across the entire pH spectrum (acidic, alkaline, and neutral). For instance, a 3D printed flow actuating valve constructed of poly (2-vinylpyridine, P2VP) has been developed that activates when exposed to a pH below 4.[230] The valve

features a globule-to-coil transition that controls its swelling, resulting in decreased water flow.[230]

In pH-responsive hydrogels composed of carboxyl groups, PVP, is usually added to tune the stiffness of hydrogels, thereby enabling their 3D printing. Altering the pH level influences the ionization of the carboxyl groups in the acrylic acid, allowing control over the stiffness and swelling ratio of the hydrogel.[74] Advances in 2PP have enabled 4D printing of such materials at the microscale.[231]

Ionic Concentration: Ionic concentration serves as a pivotal chemical stimulus in the manipulation of hydrogel-based 4D printed structures. It is particularly instrumental in influencing the mechanical properties and physiological responsiveness of hydrogels. This is manifested in scenarios where hydrogels can achieve a remarkable degree of swelling, up to 60%.[232]

A variation in ionic concentration dramatically changes the mechanical properties of hydrogels. An increase in ionic concentration, for example, can enhance rigidity owing to intensified cross-linking between ions and polymer chains.[232–236] Such cross-linking phenomena consequently affect the swelling behavior of hydrogels. For example, elevated ionic concentration can reduce swelling and contribute to a more rigid structure.[237] Furthermore, higher ion concentrations may create an osmotic pressure differential, inducing water influx and potentially increasing hydrogel volume.

Technological innovations have led to the 4D bioprinting of ion-sensitive hydrogel-based hollow tubular structures. Notably, structures sensitive to Ca^{2+} ions have been synthesized using methacrylate alginate and hyaluronic acid hydrogels.[43] Another application example is the fabrication of anatomically accurate and mechanically heterogeneous aortic valves using PEG-diacrylate (PEGDA).[238]

Ion-sensitive hydrogels have been employed effectively in drug delivery systems. They can be used for extended or regulated therapeutic release, responding dynamically to the surrounding ionic environment.[239–241] Such hydrogels offer the capability for site-specific drug delivery. For example, calcium-ion-sensitive hydrogels target areas of the body with elevated calcium concentrations, such as bone tissue.[236,242] The drug release kinetics can be rationally controlled through the hydrogel's swelling or shrinking in response to ionic concentration changes, thereby optimizing therapeutic effectiveness.

Beyond single responsiveness, hydrogels can be engineered to respond to multiple stimuli. For example, hydrogels comprised of poly γ-glutamic acid and ε-polylysine (γ-PGA/ϵ-PL) are designed to respond to temperature, pH, and ionic concentration simultaneously.[232] Such multiple stimuli-responsive hydrogels offer a wider range of applicability in biomedical applications, including but not limited to drug delivery and tissue engineering.

2.3. Design Strategies Toward Shape Morphing

In 4D printing, the shape transformation process is the result of a complex interplay between numerous factors, the most notable of which can be categorized into three fundamental motifs: the rational design of macro and microarchitectures, parameters associated with the AM process, and the configuration of the applied external stimuli. The complexity and level of detail of this

**ADVANCED
SCIENCE NEWS**

www.advancedsciencenews.com

**ADVANCED
MATERIALS**

www.advmat.de

multidimensional framework call for an in-depth analytical approach, bringing together materials science, engineering design, and computational modeling.

The motif concerning the rational design of architectures deserves particular attention because of its centrality to the way the shape-morphing process of 4D printed objects relates to the underlying design parameters. The relevant design parameters may include a complex layering of multiple materials as well as engineered nano and micropatterns. Notably, nature often serves as an inspirational source for these designs, with adaptations from floral morphologies,[83] the helical structure of DNA,[243] biomechanical characteristics of specific animals, such as geckos,[23] and even anthropomorphic features[146,244] used by many research groups to program complex shape transformations.

The second motif focuses on the variables inherent to the AM process. During fabrication, such factors as imperfections or temperature gradients can be introduced, which significantly impact the structural properties and subsequent shape-morphing capabilities of the printed constructs.[83,245,246] A multifaceted understanding of these variables and their interactions during the AM process is crucial for both optimization and quality control of 4D printing processes. For instance, the programmability and shape morphing of PLA-based 2D flat disks can be tuned through controlling the deposition of microdefects during the FDM 3D printing process.[247] This shows how phenomena that are generally considered to be undesirable can be harnessed to extend the programmability of 4D printed materials and their range of possible shape transformations.

The third motif relates to the external stimuli that are essential to induce the shape-morphing behavior. These stimuli can range from temperature and humidity fluctuations to magnetic fields, and their integration demands precise calibration with the (multiple) material and structural design for predictable and controlled shape transformations.[248]

Beyond these fundamental motifs, another layer of complexity is introduced when discussing multimaterial 4D printed objects, particularly smart composites. The unique properties of such objects can result from differences in the properties of various layers,[244,249] their orientations (e.g., anisotropic distribution of fibers[83,245,246]), or the use of multiple stimuli. For example, **Figure 3a** illustrates a 4D printed hydrogel inspired by the blossoming of flowers, which can achieve complex 3D shape morphing when in contact with water. The rational distribution of fibers in a soft matrix (hydrogel) leads to twisting and bending of the structure.[83] Concerning multimaterial 4D printing, Figure 3b shows a certain human face that is 3D printed with multiple hydrogels, exhibiting pattern transformation from a flat shape to an out-of-plane shape similar to a human face.[244] Pattern transformations can also be achieved using the differences in the thermal expansion coefficients of the different compartments of multi-material 4D printed objects (e.g.,[248]). Moreover, by integrating two distinct phases, such as an elastic element and a smart material (e.g., a SMP), a multifunctional object can be fabricated. The interaction between both phases can result in unusual phenomena, such as the stiffening/softening effect, SME, and debonding, leading to exciting shape transformation behaviors.[243,250–254] On the one hand, the softening effect is favorable for achieving complex shape-morphing and self-folding origami structures. On the other hand, it compromises the mechanical load-bearing func-

tion of such structures. Because of the competition between self-folding characteristics and final stiffness, there exists a theoretical limit to how high the stiffness of 4D printed (lattice) structures can be.[255] Such theoretical limits should be taken into account in the design of shape-morphing structures. Rational geometrical design can also achieve sequential self-folding, based on the definition of crease lines for origami-like structures.[29]

Proper structural design and the rational placement of a second material (e.g., magnetic particle patterns) into the design of 4D printed objects are very challenging, particularly at the microscale. These challenges involve complexities in predicting the pattern transformations resulting from these placements and the fabrication of microstructures and the engineering of the distribution of the second phase. From the perspective of the distribution of a second phase, for example, the rational control of the pattern of magnetic iron oxide nanoparticles embedded in a single-layer hydrogel-based sheet results in various 3D shapes with out-of-plane deformations[256] (Figure 3c). Similarly, it is possible to pattern anisotropic gradients in hydrogels using iron oxide nanoparticles and excite them using a magnetic field, inspired by sea jelly organisms.[257] Instead of magnetic particles, (macro) permanent magnets can be embedded into a temperature-responsive SMP to create 4D printed mechanical metamaterials with untethered and reversible programming and locking mechanisms.[258] NdFeB magnets, for example, were rationally designed and embedded into PLA during the FDM printing process and included the programming of PLA struts, the displacement between the magnets, the orientation of the magnets (N-S), and temperature changes[258] (Figure 3d).

From an AM process perspective, the pre-strain or residual stress stored in 4D printed structures and imperfections induced during the AM process are the main reasons for the shape-morphing properties of 4D printed structures.[245,259–263] The residual stresses can even be generated during simple and inexpensive 3D printing processes, such as FDM-based printing of PLA. Such SMPs can be automatically programmed during the printing process. For example, Figure 3e demonstrates the sequential shape-morphing behavior resulting from the introduction of porosity into the geometry as well as the adjustment of the printing parameters, such as printing patterns.[262] Such phenomena also exist in 4D printing at the micro- and nanoscales. Changing the dose in 2PP (depending on the scanning speed and laser power) allows for the control of the mechanical properties and thermal expansions of the polymerized resin. Various 4D printed structures, such as microscale mechanical meta-materials, have been fabricated using this approach (Figures 3f,g).[17,24,264,265] For example, the Poisson's ratio of mechanical metamaterials can be controlled through temperature gradients at the microscale (Figure 3g).[264]

The shape-morphing mechanism along with a locking capability can be also obtained by properly adjusting the base materials and designing an advanced stimulation setup. In this case, fast shape-morphing behavior is achieved, and the structure is locked at its temporary state in the absence of an external field (energy-sufficient).[164] The composite reported in that study was made of an acrylate-based amorphous SMP consisting of Fe_3O_4 and NdFeB particles. While Fe_3O_4 particles are responsive to inductive heating via a high-frequency magnetic field, NdFeB particles enable the programming of the structure
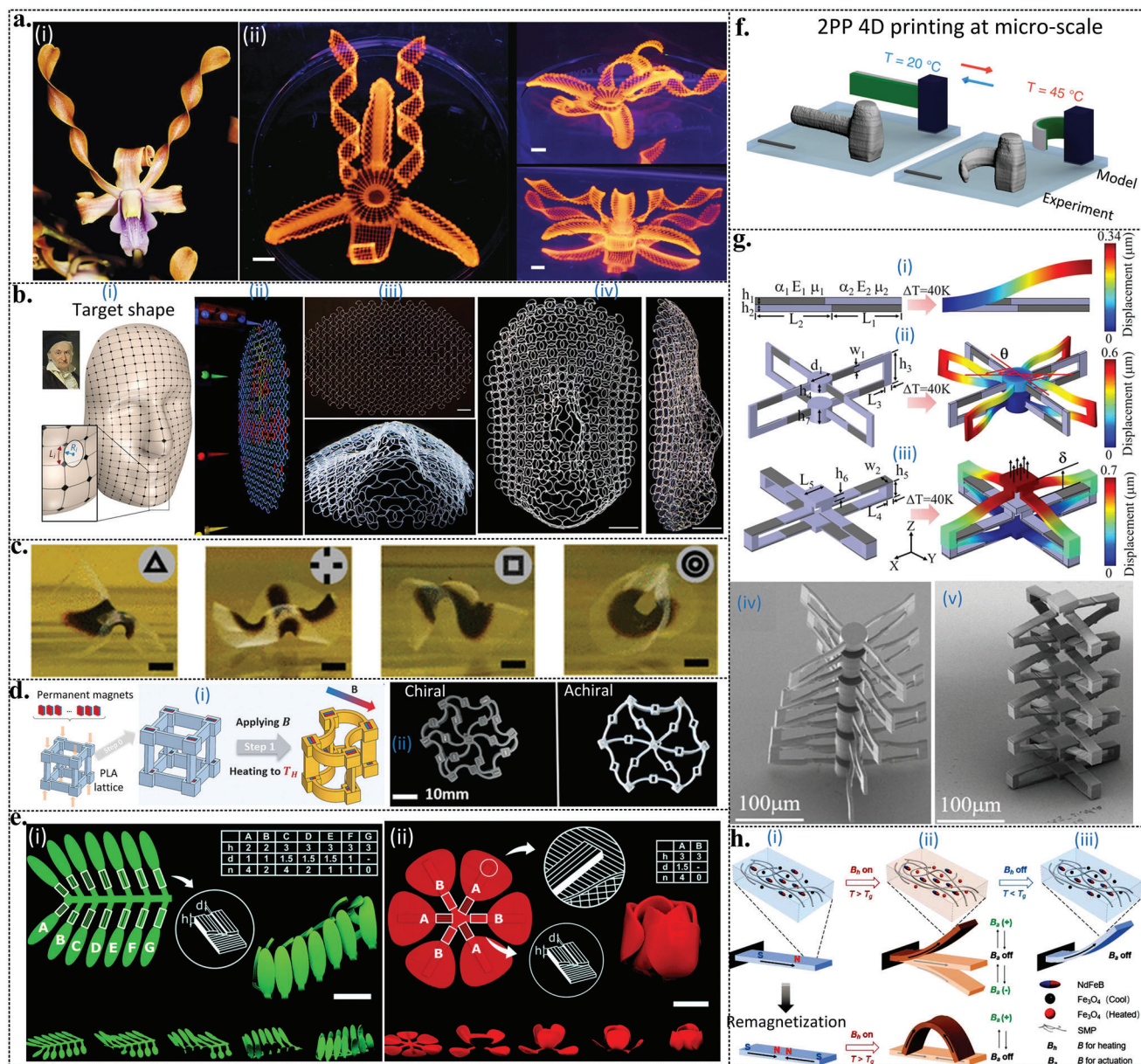
Figure 3. Examples of complex shape morphing behaviors achieved using 4D printing. a) 4D printing and shape-morphing of a flower inspired by a native orchid immersed in water. Reproduced with permission.[83] Copyright 2016, Springer Nature. Scale bars represent 5 mm. b) A schematic of a 3D lattice face of Carl Friedrich Gauss's likeness (i) and the corresponding lattice structure during (ii) and after printing (iii, top). iii) Bottom and iv show a 3D scan of the temporary shape of the 4D printed structures triggered by an external stimulus.[244] c) The pattern transformation of a composite hydrogel-based sheet made through different ferromagnetic particle distributions while exposed to light. Reprinted with permission.[256] Copyright 2019 American Chemical Society. d) A magneto-thermo-mechanically setup based on polylactic acid (PLA) and embedded NdFeB magnets (i) to morph lattice structures into chiral and achiral deformations (ii). Reproduced with permission.[258] Copyright 2022, Wiley-VCH. The scale bar represents 10 mm. e) The shape-shifting and pattern transformation of different architectures. The gradual closure of the leaves of a shy plant-inspired structure (i) and sequential shape-shifting from initially flat petals to a tulip in 20 s (ii).[262] f) A micro-4D printed beam featuring reversible shape-morphing behavior at low temperatures close to those of the human body.[24] The scale bar corresponds to 20 μm. g) A 4D printed metamaterial featuring a dynamic Poisson's ratio at the microscale made via two-photon polymerization (2PP).[264] i–iii) A FEM-based prediction of the shape morphing behavior of 4D printed structures, working based on the differences in thermal coefficients. iv–v) SEM images of the initial and stimulated configurations of the metamaterial at the microscale. h) An illustration showing the mechanism of pattern transformation in magnetoactive shape memory polymers (SMPs) at low temperatures (i), heating up the sample via an alternating magnetic field (ii), and heating and cooling the samples via alternating and constant magnetic fields (iii). Reproduced with permission.[381] Copyright 2020, Wiley-VCH.

**ADVANCED
SCIENCE NEWS**

www.advancedsciencenews.com

**ADVANCED
MATERIALS**

www.advmat.de

under an actuating magnetic field. The integration of both functionalities results in a locking mechanism, reversibility, and energy-efficient stimulation (Figure 3h).[164]

3. Biomedical Applications

The advent of 3D printing has undoubtedly announced a new era in the fabrication of complex structures, particularly for biomedical applications, such as tissue engineering. However, its limitation primarily lies in the inability to emulate the dynamic and evolving characteristics of native biological tissues. For example, vascularization within large 3D printed constructs remains an elusive goal, posing a significant impediment to the delivery of essential nutrients and oxygen to engineered tissues.

4D (bio)printing emerges as a transformative solution to these limitations. Unlike its 3D counterpart, 4D bioprinting facilitates the development of artificial tissues endowed with dynamic characteristics. These structures can encapsulate vascular or stem cells, thereby promoting rapid maturation and functional behavior over time.[15,34] The capacity to undergo dynamic changes makes 4D bioprinted structures highly applicable in the treatment of organ-specific diseases, such as cardiac conditions.

Specifically, in the domain of cardiovascular medicine, the dysfunction of the aortic valve, manifesting either as stenosis or regurgitation, poses serious health risks. The aortic valve is a complex, tri-leaflet structure responsible for regulating the unidirectional flow of blood from the heart to the aorta. Aortic valve stenosis refers to the thickening or stiffening of these cusps, while aortic valve regurgitation is characterized by improper closure, leading to retrograde blood flow. 4D printing technology shows promise in fabricating reversible aortic valves or stents that can adapt to these pathological changes[39] (**Figure 4a**).

The applications of 4D printing in the biomedical field extend beyond tissue engineering and cardiovascular treatments. The technology holds the potential for developing a myriad of smart medical devices, including but not limited to, occlusion devices, microneedles for minimally invasive procedures, specialized drug delivery systems, wound closure mechanisms, and various types of implants and scaffolds. Each of these applications leverages the dynamic, adaptive capabilities of 4D printed structures to offer enhanced therapeutic outcomes.

3.1. Biomedical Devices

4D printing is indeed emerging as a transformative technology in the field of biomedical engineering, significantly contributing to the evolution of minimally invasive medical devices and procedures. One of the most important applications lies in the domain of cardiovascular engineering. For example, self-expanding stents fabricated through 4D printing technologies show considerable promise for the treatment of vascular diseases, as corroborated by multiple studies.[266–268] Similarly, the technique allows for the production of sutureless anastomosis devices, thereby streamlining surgical procedures.[269] In addition, self-fitting scaffolds produced through 4D printing offer enhanced adaptability to diverse tissue topographies.[270]

Furthermore, in the area of bone tissue engineering, 4D printing is increasingly being employed for the fabrication of complex structures, such as bone repair tools and orthopedic biomaterials.[172,271] The technology also holds the potential for generating scaffolds that facilitate tissue regeneration. Moving beyond the musculoskeletal system, 4D printing technologies are also being applied in the development of peripheral nerve interfaces for treating ailments, such as hypertension and diabetes.[272] Researchers have recently advanced the field by creating a 4D printed nerve cuff electrode that features self-folding mechanisms, thereby facilitating the treatment of smaller peripheral nerves[272] (Figure 4b).

In the following sub-sections, we will discuss these innovative medical devices, elucidating the principles underlying their operation, and assessing the future potential of 4D printing in enhancing their effectiveness and broadening their applicability.

3.1.1. Stents

A stent is a medical device implanted into vascular structures to prevent them from collapsing and to reduce thrombotic risk. 4D printing can minimize the invasiveness of such medical devices by producing self-expanding stents that can be triggered by an external stimulus.[273] This emergent technology has already found applications in the creation of dynamic stents for a diverse array of medical conditions, including vascular, tracheal, and orbital anomalies.[274]

Vascular Stents: The exploration into 4D printing of vascular stents represents a pivotal transformation in the biomedical field, combining advances in material science, computational design, and advanced manufacturing technologies. These stents are employed for a range of medical applications, such as treating cardiovascular diseases (e.g., atherosclerosis), and ureteral-associated diseases (e.g., hydronephrosis).[275] While traditional stents serve as passive implants, 4D printed stents introduce dynamic functionalities, such as temperature responsiveness, which allows them to expand upon local heating.[275]

The operational mechanism of these 4D printed stents is governed by the types of SMPs used and the stimuli that activate them. For instance, stents printed with PLA/Fe_3O_4 composites through DIW are capable of magnetically activated shape recovery.[275] Such multifunctional stents can regain their original form when triggered by a magnetic field. Numerous numerical models and empirical proof-of-concept studies have been conducted to validate self-expanding or self-shrinking stents, further substantiating the potential of this technology.[276–281]

Drug-eluting functionalities are another field of application, particularly in the context of ureteral diseases.[266,282] Water-responsive stents fabricated from zein, a plant-based protein, have been successfully tested in porcine models, demonstrating both biodegradability and functional efficacy.[282] Another noteworthy innovation was the dual-responsive stent fabricated from acrylamide-acrylic acid/cellulose nanocrystal (AAm-AAc/CNC) that could respond to deionized water and Fe^{+3} ions. This design revealed a potential for closure in enter-atmospheric fistulas[266] (Figure 4c).

A promising area of research focuses on enhancing the reliability and longevity of stents through self-healing materials.[283] These include semi-interpenetrating polymer networks of PCL and urethane diacrylate, which offer exceptional stretchability

**ADVANCED
SCIENCE NEWS**

www.advancedsciencenews.com

**ADVANCED
MATERIALS**

www.advmat.de
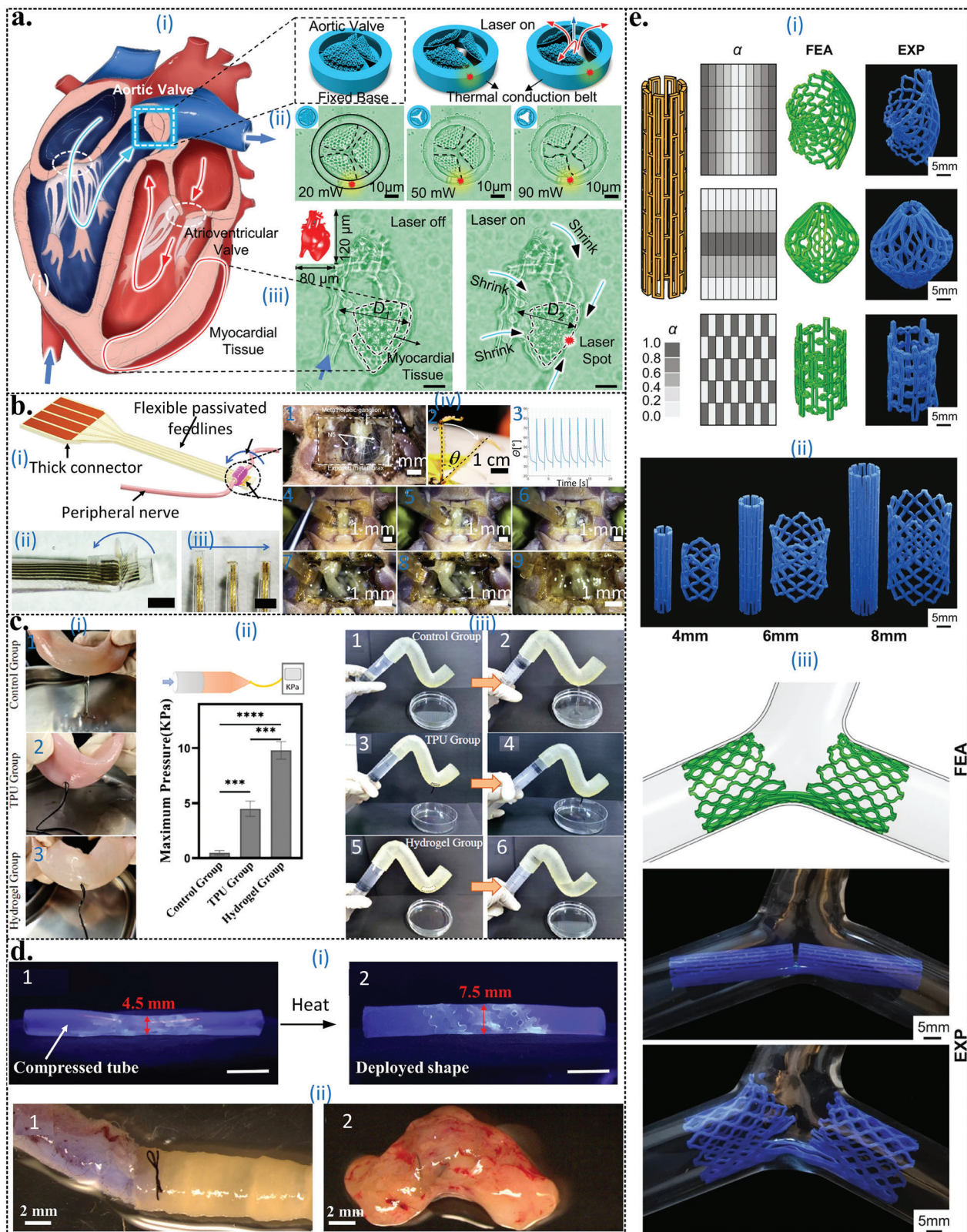
Figure 4. The applications of 4D printing in biomedical devices and medicine. a-i) A schematic drawing showing a temperature-responsive aortic valve. Reproduced with permission.[39] Copyright 2023, Wiley-VCH. a-ii) The opening and closing of the microaortic valve under different laser powers. a-iii) Optical micrographs of an artificial 4D printed heart in the presence and absence of light. The scale bar represents 20 μm. b) A 4D printed self-folding nerve cuff electrode.[272] i–iii) A schematic of the cuff electrode design and the 4D printed ones, respectively. The scale bar represents 1 mm. iv) The in

**ADVANCED
SCIENCE NEWS**

www.advancedsciencenews.com

**ADVANCED
MATERIALS**

www.advmat.de

and self-healing properties.[283] Longitudinal studies have started to evaluate the degradation patterns of these stents over extended periods under physiological conditions.[284]

A major challenge that some temperature-responsive stents face is the high glass transition temperature, which makes them challenging for implantation into the human body. Nevertheless, the operational activation temperatures of stents can also be modulated. In a proof-of-concept study, a vascular stent was 4D printed via DIW from PLMC, featuring a relatively low activation temperature (i.e., 40–45 °C) and a recovery within 30 s.[285] However, this activation temperature is still not low enough for either their implantation into the body or even in vitro mechanobiological studies as cells may not survive. For instance, a poly(glycerol dodecanoate) acrylate (PGDA) based vascular stent was engineered to recover at the body temperature (20–37 °C) and demonstrated a rapid recovery time (0.4 s) in both in vitro and in vivo settings (Figure 4d).[68] One common material to make temperature-responsive stents with a low transition temperature is PNIPAM. That is not only because of the low transition temperature of PNIPAM, but also because of its versatility in tuning the stiffness and inducing complex shape transformations. For example, stent-inspired tubular structures have been 4D printed via DIW from PNIPAM as the active part and from polyacrylamide as the passive one.[286] The integration of such active and passive components, as a design strategy, induces complex deformations, such as bending, clamping, elongation, and radial expansion, which expands the envelope of achievable shape transformations and can be instrumental in eventually making such types of medical devices available to surgeons.

The design space can further be expanded by the incorporation of mechanical metamaterials, offering unique characteristics, such as negative Poisson's ratios (i.e., auxeticity) and simultaneously high stiffness and toughness.[287,288] Several proof-of-concept tabular structures, predominantly exhibiting auxeticity, have been 4D printed using FDM for potential in vitro studies, notably in vascular applications.[289,290] Stent-like metamaterial tubes featuring SMEs can be simply designed by changing the printing parameters. For instance, a stent-like tube was 4D printed from PLA via FDM[20] (Figure 4e). Through the adjustment of printing speed and patterns, the radial expansion was achieved in an aquatic environment. Similarly, stents can be also designed based on the concepts of kirigami (e.g., bifurcated vascular stents from PU-SMPs[291]) and origami (e.g., a vascular stent from a thermoset SMP composite, epoxidized soybean oil,[292] and a 4D printed temperature-responsive stent via FDM from PLA[293]) featuring shape morphing and adaptability.

Finally, the capabilities of DLW techniques have been harnessed to create microscale stents that exhibit promising mechanical and functional characteristics.[294] These stents, composed of SMPs, can expand in aqueous environments, opening new opportunities for minimally invasive procedures.

As the horizon of the 4D printing technology continues to expand, future research works may benefit from focusing on the integration of advanced sensing mechanisms, improving biocompatibility, and optimizing the activation parameters for these complex, multifunctional stents. Specific technologies, such as real-time monitoring sensors and nanoscale actuators, could significantly augment the capabilities of these advanced biomedical devices, providing an integrated approach to patient-specific healthcare.

Tracheal Stents: Tracheal stents, instrumental in treating conditions, such as tracheal stenosis and tracheomalacia, represent another frontier of biomedical application for 4D printing technologies.[295,296] The incorporation of smart biomaterials into tracheal stents has been particularly promising, allowing for precise control over stent opening and thereby potentially mitigating the need for invasive surgical interventions.[297]

Among the examples in this emerging field is a bioinspired tracheal stent fabricated from a PLA (and PCL)/Fe_3O_4 composite. This 4D printed construct possesses magnetic activation capabilities.[295,298,299] However, it must be noted that comprehensive studies are still needed to determine the cell viability and long-term effects of these magnetoactive materials. Moreover, the in vitro and in vivo feasibility of such 4D printed tracheal stents in the presence of magnetic fields and magnetic fillers remains an area of active investigation.

In pediatric applications, a tracheobronchial splint device made from PCL has been successfully 4D printed to address tracheobronchomalacia[300] (**Figure 5a**). The design of this 4D printed splint is such that it can adapt to tissue growth, a feature achieved by careful mechanical design and regulated degradation behaviors.[300] To assess the long-term performance and shape-morphing capabilities of the device, in vivo tests were conducted on two infants, thereby substantiating its potential utility.

Orbital Stents: The application of 4D printing technologies in ophthalmic medicine introduces a paradigm shift, particularly in the treatment of enophthalmos, a condition characterized by the posterior displacement of the eyeball within the orbital cavity.[301] Conventional treatments often employ static implants and stents, which encounter various limitations including, but not limited to, inaccurate contour matching of the orbital coloboma, complications in CT imaging, and suboptimal volumetric filling capabilities.[302]

---

vivo implantation of the 4D printed cuff electrode in a locust. (1) The metathoracic cavity of the locust, (2) the movement of the hindleg triggered by the nerve, (3) the variation of the angle between legs. (4–9) The folding and unfolding of the 4D printed cuff electrodes. c) In vitro experiments with a 4D printed hydrogel-based sealing tool in an intestine. Reproduced with permission.[266] Copyright 2022, Elsevier. i) The sealing effect of the tool in a hydrogel porcine intestine featuring a hole. ii) Maximum pressure that the intestine can tolerate. iii) Another sealing test in a 4D printed bilayer hydrogel. d) The in vivo testing of a 4D printed vascular stent based on poly(glycerol dodecanoate) acrylate (PGDA). Reproduced with permission.[68] Copyright 2021, Elsevier. The implementation of the stent in a silicone-based blood vessel (temporary shape, i1) and the temperature-based deployment of the vessel (i2). The scale bar is 1 cm. The in vivo implementation of the 4D printed stent in a mouse aorta on days 0 (ii1) and 14 (ii2). e) A proof-of-concept study of a 4D printed stent-like structure made from polylactic acid (PLA) via fused deposition modeling (FDM).[20] i) The experimental and FEM results of different designs with different printing parameters to achieve sophisticated shapes and deformations. ii) The effects of dimensional scaling on the performance of 4D printed stents. iii) The implementation of the stents in a vein-like glass and its stimulation via temperature.

**ADVANCED
SCIENCE NEWS**

www.advancedsciencenews.com

**ADVANCED
MATERIALS**

www.advmat.de
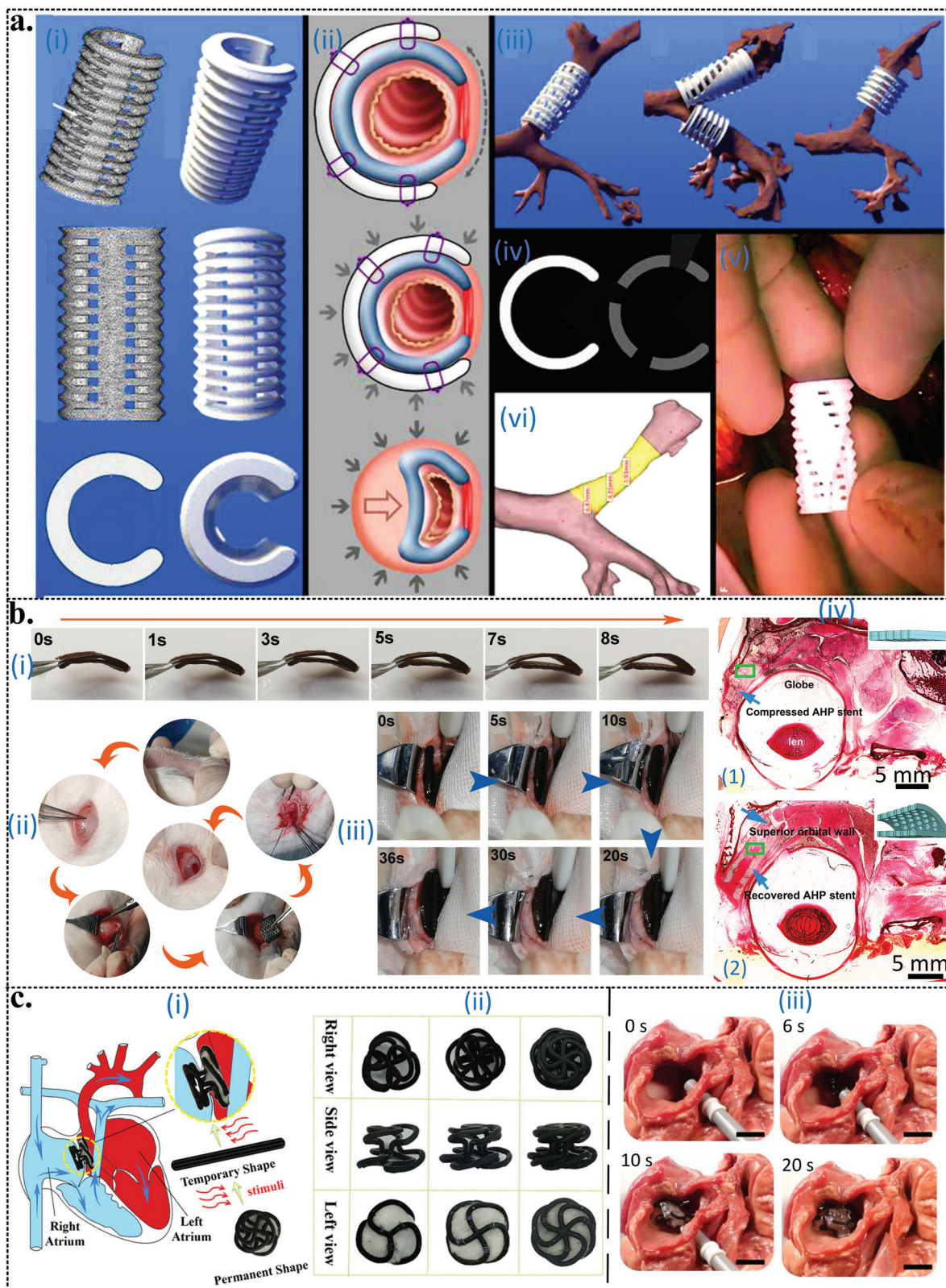
Figure 5. In vivo testing of 4D printed biomedical devices. a) A 4D printed tracheobronchial splint device made of polycaprolactone (PCL) through stereolithography (SLA) (i). Reproduced with permission.[300] Copyright 2015, The American Association for the Advancement of Science. The tracheobronchial splint mechanism in treating tracheobronchial collapse in tracheobronchomalacia (ii) and its splint over the segmented primary model fits three patients (iii). A 2D image of the airway and split wall (iv) and the final 4D printed device (v) with the 3D model of the patient's airway (vi).[300] b)

**ADVANCED
SCIENCE NEWS**

www.advancedsciencenews.com

**ADVANCED
MATERIALS**

www.advmat.de

To mitigate these shortcomings, recent innovations in 4D printing have enabled the fabrication of smart orbital stents with features, such as controllable shape-morphing and CT-developable capabilities.[302] These advanced stents are typically composed of PU, gold nanoparticles, and nano-hydroxyapatite, thereby integrating mechanical robustness, radiopacity for CT imaging, and bioactivity, respectively. The stent's performance and shape recovery were evaluated both in vitro and in vivo using a rabbit orbit model. Interestingly, the stent demonstrated promising shape-recovery characteristics when stimulated by a saline solution at 44 °C[302] (Figure 5b). The analytical evaluation of this 4D printed stent[302] not only confirms its theoretical viability but also underlines its empirical effectiveness in a controlled animal model.

Such advancements pave the way for further clinical trials and can help shape the future of personalized ophthalmic treatments. However, for a comprehensive understanding and eventual clinical implementation, several aspects need further investigation. These include the long-term biocompatibility of such medical devices, the potential for the biointegration of the material, and the stent's performance under various physiological conditions. Furthermore, the scalability of this technology to human models and its economic viability are questions that remain to be answered.

3.1.2. Occlusion Devices

Interventional therapy, a percutaneous nonsurgical procedure, has established itself as a methodology for the treatment of congenital heart diseases.[303] Yet, the field has persistently faced issues related to the precision, biodegradability, and remote controllability of the occlusion devices used. 4D printing technology provides a groundbreaking avenue to address these challenges by enabling the fabrication of personalized, high-precision occlusion devices.[52]

Specifically, 4D printed occlusion devices have proven their efficacy in closing atrial septal defects with enhanced treatment accuracy[52,304] (Figure 5ci,ii[52] and Figure 5ciii[53]). These devices often incorporate SMPs, as evidenced in a study where a 4D printed device consisting of a supporting frame made from a PLA/Fe_3O_4 composite was demonstrated.[53] The SMP allows for remote controllability, whereby the device can change its shape in situ in response to external stimuli, such as temperature or magnetic fields. Covered with thin occluding membranes, these devices further demonstrate biodegradability, durability, and biocompatibility, as suggested by a 48-week in vivo study on mice.[53]

In another proof-of-concept study, a custom-made occluder constructed from porous, radiopaque PU was 4D printed using FDM for interventional radiology applications.[305] An analytical evaluation of the device focused on its mechanical properties, specifically shape recovery ratio and stiffness, thus indicating its potential applicability in real-world clinical scenarios.

The research into 4D printed occlusion devices is ongoing and needs to make further progress before clinical adoptions are feasible. While in vivo studies and prototype evaluations are promising, the path to clinical translation demands an exhaustive assessment of various aspects of the performance of such devices. In particular, long-term stability, the potential for immune responses, and real-world mechanical stresses under diverse physiological conditions are yet to be comprehensively understood. Moreover, the economic feasibility and scalability of these 4D printed devices for large-scale clinical use require additional feasibility research.

3.1.3. Microneedles

MNs represent a paradigm shift in transdermal drug delivery and biosensing technologies, transcending traditional limitations associated with pain and tissue damage. Employed for a plethora of applications, including long-term drug delivery (e.g., vaccines and insulin) and biosensing (e.g., glucose and DNA biomarkers), MNs can penetrate the epidermal layer without triggering nerve endings, thus permitting efficient uptake of macromolecules into the capillaries and lymphatic networks sans pain.[306–310] Furthermore, MNs are being explored for precision drug delivery in oncology.[309]

While the physiological advantages of MNs are substantial, their fabrication process plays an important role in their efficacy. Traditional manufacturing techniques for MNs, such as micromolding, laser cutting, and lithography, have numerous disadvantages including low precision, high costs, and extended processing times.[311,312] In contrast, micro-4D printing emerges as a revolutionary technology that improves many of these drawbacks. It confers superior mechanical properties, enhances intracellular drug delivery, offers high printing accuracy, is cost-effective, and simplifies the fabrication workflow.[311,313,314]

A groundbreaking development in this area is the use of micro-4D printing techniques that synergistically combine micro-DLP and projection micro-SLA. This innovation has led to the creation of bioinspired MNs featuring backward-facing curved barbs, designed to enhance tissue adhesion[311] (**Figure 6a**). Such intricate design features, previously difficult to achieve through conventional methods, become feasible through micro-4D printing. It allows for geometries that can significantly improve the MN's efficiency in drug delivery and biosensing applications.

Considering the pivotal role of MNs in precision medicine and remote monitoring, the evolution of micro-4D printing technologies is likely to have profound impact. Future research may focus on the exploration of biocompatible and biodegradable materials, the development of MNs with real-time biosensing capabilities, and the application of machine learning algorithms to the optimization of MN design parameters for specific clinical applications.

A 4D printed orbital stent to treat enophthalmic invagination. Reproduced with permission.[302] Copyright 2022, Elsevier. i) The shape memory recovery of a stent immersed in 44 °C water. ii) The implantation steps of a 4D printed stent in the eyeballs of a rabbit. iii) The in vivo shape recovery of the stent in a rabbit. The images of the implanted stent when it is compressed (iv) and after recovery (v). c) 4D printed occluders. A schematic drawing of an atrial septal defect before and after an interventional therapy with an occlude (i). Reproduced with permission.[52] Copyright 2019, Wiley-VCH. The final shapes of the 4D printed occlude (ii) are shown.[52] In vivo illustration of the magnetoactive 4D printed left atrial appendage occlude (iii). Reprinted with permission.[53] Copyright 2021, American Chemical Society. The scale bar is 10 mm.
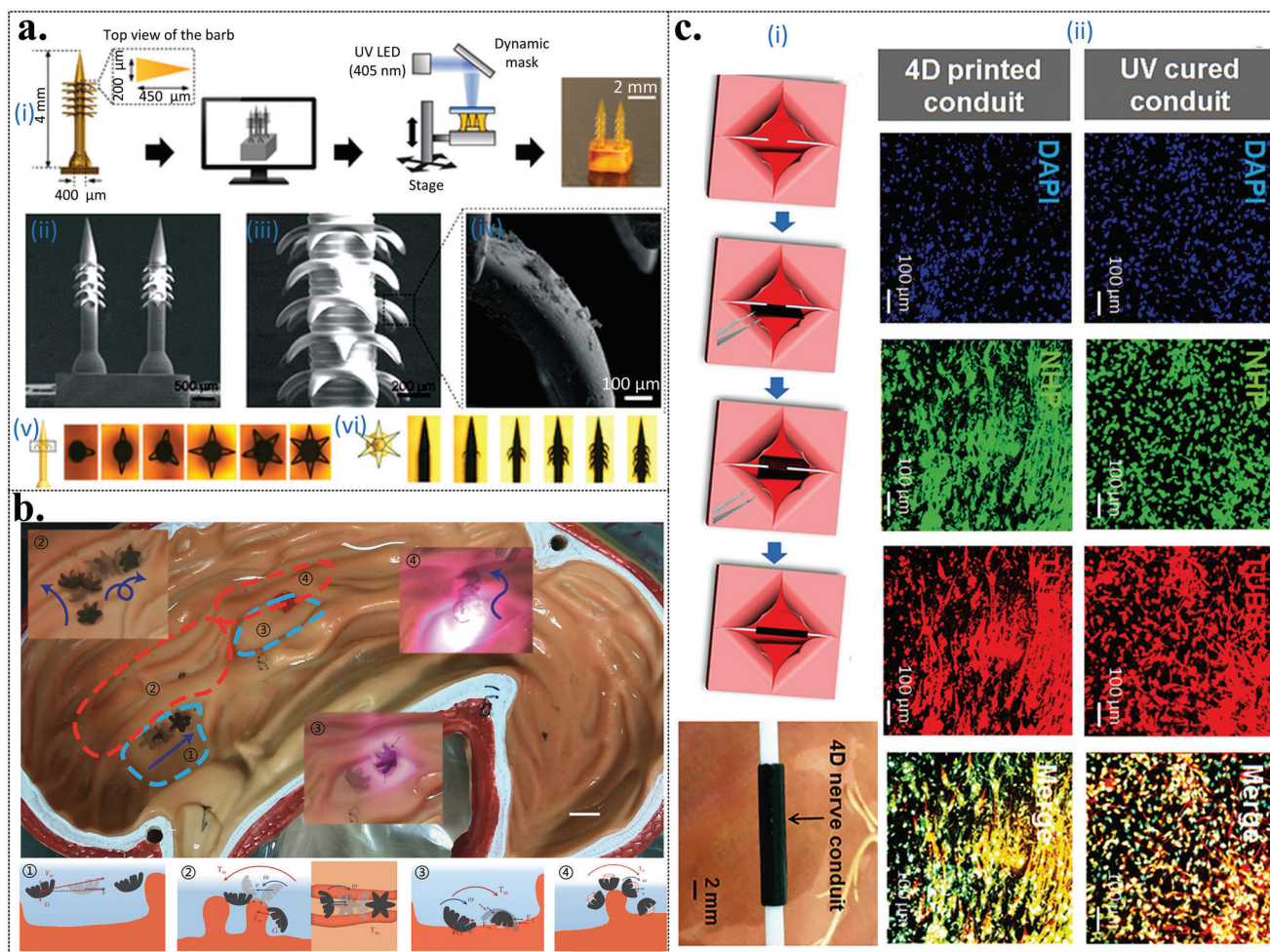
Figure 6. In vitro testing of 4D printed biomedical devices. a) The 4D printing of a bioinspired microneedle (MN) with triangular backward-facing curved barbs. The schematic drawing depicts the fabrication steps via a light-assisted additive manufacturing (AM) technique (i). Reproduced with permission.[311] Copyright 2020, Wiley-VCH. The SEM images of the backward-faced curved barbs are presented in (ii–iv). The various configurations of the MN with different barbs can result in different pattern transformations (v–vi).[311] b) The movement and delivery of a 4D printed leptasteria-like microrobot based on NIPAM/NdFeB for drug delivery systems in a stomach model. Reproduced with permission.[321] Copyright 2022, Elsevier. The scale bar corresponds to 6 mm. c-i) An illustration showing thermomechanical cycles of the full entubulation of a 4D nerve guidance conduit. Reproduced with permission.[353] Copyright 2018, Wiley-VCH. c-ii) The immunofluorescence images corresponding to the neurogenic differentiation of human mesenchymal stem cells (hMSCs) on the 4D printed nerve guidance conduit and their UV-cured counterpart. Reproduced with permission.[353] Copyright 2018, Wiley-VCH.

3.2. Drug Delivery Systems

4D printing technologies offer unparalleled opportunities in controlled drug delivery systems, a topic of substantial importance in the pharmaceutical and biomedical sectors.[315] Employing stimuli-responsive materials, 4D printing facilitates the temporal and spatial control of drug release in a programmable manner, triggered by specific biological signals or environmental stimuli (e.g., pathological anomalies in vivo).[196]

One example of such applications is the ingestible tablets designed for ulcer treatment, which employ a pH-responsive shell. As the gastric environment turns acidic, the tablet releases a predetermined dose of medication.[316] This innovative approach was later extended in a proof-of-concept study, where an SMP-based capsule was developed to modulate drug release via crack propagation mechanisms within the capsule.[51]

Another remarkable advancement is the conceptualization and fabrication of "multisomes," complex droplet networks comprising small aqueous droplets encased in a larger oil droplet and suspended in an aqueous medium.[317] Utilizing 3D printing technologies, these droplets can encapsulate aqueous-based drugs and release them responsively based on environmental pH or temperature.[317] These multisomes are also osmoreactive and can be fabricated in very complex shapes, offering a number of possibilities in drug delivery.[318]

ADVANCED
SCIENCE NEWS

www.advancedsciencenews.com

**ADVANCED
MATERIALS**

www.advmat.de

Drawing inspiration from the SMEs of 4D printing, researchers have also been experimenting with gastric retention devices aimed at regulating drug release and preventing premature gastric emptying.[50,319,320] A key focus of these devices is to maintain retention within the stomach by manipulating the transition from a collapsed configuration to a preprogrammed shape under physiological conditions. For example, an SMP-based device fabricated from PVA was developed that could transform from a compressed to an expanded state upon exposure to aqueous fluids at body temperature, thus prolonging its retention in the stomach.[50]

Finally, there is an emergent demand for remote controllability in microscale drug delivery systems. To address this requirement, recent advances have been made in the 4D printing of microrobots capable of ferrying and releasing drugs upon stimulation by magnetic fields and temperature changes (Figure 6b).[321]

4D printing has started a new era in drug delivery, offering unprecedented control over the pharmacokinetics and pharmacodynamics of medications. However, the field is still developing, and extensive in vitro and in vivo studies are required to better realize the technology's transformative potential. Future investigations could consider employing advanced imaging techniques and multiphysics computational models to better understand the mechanics and kinetics involved in these complex drug delivery systems.

3.3. Implants and Scaffolds

The application of 4D printing technologies in tissue engineering and regenerative medicine holds significant promise for overcoming the limitations of traditional 3D printed scaffolds and implants. One primary advantage of 4D printed structures is their ability to dynamically adapt to physiological conditions, thereby offering a more robust solution for tissue growth and function restoration.[322,323]

Scaffolds function as 3D matrices that support cellular adhesion, proliferation, and differentiation, leading to tissue regeneration. Implants, on the other hand, serve to replace or augment physiological functions. In the field of regenerative medicine, 4D printing technologies offer a specific advantage by allowing for the fabrication of scaffolds and implants with stimuli-responsive features. For instance, a scaffold printed from PU-based SMP demonstrated tunable cellular adhesion properties. This allowed for regulated cell growth when mechanical deformations were applied to the structure, thereby making it more physiologically adaptive.[322]

Further studies have elucidated the potential for multiresponsiveness in 4D printed scaffolds. For example, a 3D porous scaffold manufactured via SLA-based 4D printing, which utilized a biocompatible soybean oil epoxidized acrylate (SOEA) resin, has been shown to facilitate the maturation of multipotent human mesenchymal stem cells (hMSCs).[324,325] In another innovative application, a dual-responsive scaffold comprising PU and acrylate was fabricated using inkjet-based 3D bioprinting. The resultant structure exhibited responsiveness to both temperature and light stimuli.[326]

Another avenue for innovation resides in the ability of 4D printing technologies to fabricate geometrically complex implants with complex surface nanopatterns, which is generally not possible with traditional manufacturing techniques.[30] The incorporation of surface nanopatterns on scaffolds and implants can be highly advantageous for inducing specific cellular responses, such as osteogenic differentiation,[327] antibacterial activity,[328] and immunomodulation.[329] Pioneering approaches suggest initiating the fabrication process with a flat structure that can be programmed to self-fold into complex 3D architectures upon exposure to external stimuli both for strut-based unit cells[30] and sheet-based hyperbolic surfaces, such as triply periodic minimal surfaces.[330]

The significance of geometric features, particularly curvature, has been highlighted in recent research, demonstrating its influential role in modulating cellular behavior and, thus, the progression of tissue regeneration.[331] Given these capabilities, 4D printed structures offer an exceptional platform for advancing the development of scaffolds and implants tailored for the regeneration of various tissue types, including bone, cartilage, and muscle. Thus, this section discuss different potentials and innovative applications of 4D printed scaffolds and implants, specifically focusing on their roles in regenerating bone, cartilage, muscle, and other tissues.

3.3.1. Bone and Cartilage Tissues

The emerging field of 4D printing for bone tissue applications holds transformative potential for orthopedic surgery, presenting areas for reduced infection risks, minimized surgical invasiveness, and enhanced osseointegration. With particular emphasis on the challenge of mimicking the native bone's biomechanical properties,[34] current advancements are largely categorized into four groups: i) injectable stimuli-responsive hydrogels, ii) shape memory scaffolds, iii) functional transformation mechanisms, and iv) neovascularization and neurogenesis to foster bone growth and mineralization.[236]

Firstly, injectable temperature-responsive hydrogels, such as hydroxypropyl methylcellulose and hydroxybutyl chitosan, offer the advantage of in situ gelation at the body temperature. These hydrogels serve as biocompatible matrices for the encapsulation and delivery of cellular components, growth factors, or bone-stimulating inorganic composites, such as hydroxyapatite.[236]

Secondly, SMPs serve as a substrate for 3D/4D printed scaffolds, facilitating their deployment through minimally invasive procedures.[305] These SMP-based scaffolds have been shown to enhance osteoblast adhesion, proliferation, and osteogenic gene expression, thereby fulfilling crucial criteria for successful bone repair.[332,333]

In the third approach, functional transformation mechanisms are utilized to design mechanical strategies that increase bone regeneration. An example in this category is mechanically deployable meta-implants[271] (**Figure 7a**). This novel application demonstrates how mechanical pattern transformation can contribute to the success of minimally invasive and effective bone regeneration strategies.

The fourth approach addresses the unmet need for vascularization and regeneration of neural networks in bone tissue engineering.[34,236,334–336] While 4D printing is yet to be fully
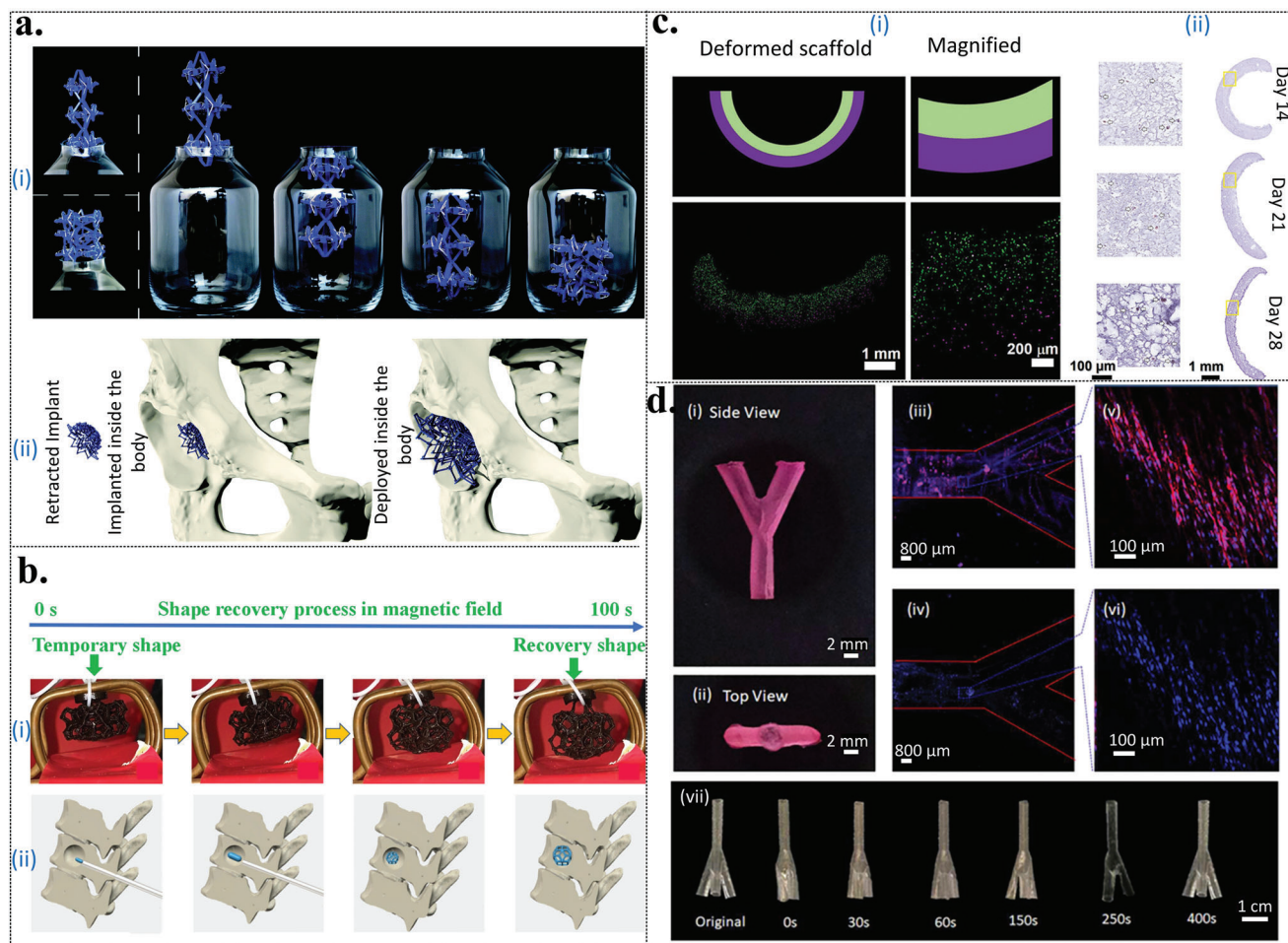
**ADVANCED
SCIENCE NEWS**

www.advancedsciencenews.com

**ADVANCED
MATERIALS**

www.advmat.de

Figure 7. 4D printed scaffolds and implants. a-i) An example of deployable structures that expand inside confined environments. ii) A proof-of-concept study of a deployable implant to fill damaged bone.[271] b) A 4D printed bone scaffold made from polylactic acid (PLA)/Fe$_3$O$_4$, which expands upon exposure to a magnetic field (i) and can be used to fill bone defects (ii). Reproduced with permission.[172] Copyright 2019, Elsevier. c) 4D bioprinted artificial cartilage (scaffold).[15] i) A schematic drawing depicting bilayer cell-free scaffolds with their corresponding optical images, confirming the presence of cells in both top and bottom layers in green and red, respectively. ii) The histological images of hematoxyline-eosin (H&E staining) on days 14, 21, and 28 with two different magnifications. d) The illustration of 4D anisotropic scaffolds by integrating the staircase effect of fused deposition modeling (FDM) printing with a coating technique. Reproduced with permission.[349] Copyright 2019, IOP Publishing. i,ii) The 4D printed anisotropic scaffolds before cell seeding. iii–vi) The confocal images of the seeded scaffolds.

exploited for this purpose, it undoubtedly represents a frontier for further research and development.

SMP-based constructs have been tailored for specialized applications in bone repair. Magnetoactive SMP-based scaffolds were fabricated for personalized bone defect treatment, wherein these structures could be actuated by an external magnetic field to achieve the desired shape[49,172] (Figure 7b[172]). Moreover, temperature-responsive SMP scaffolds have been 3D printed to investigate their biomechanical compatibility.[324,337–341] The piezoelectric properties of certain smart materials have also been investigated for their potential to stimulate osteoblast growth.[342]

Advancements in 4D bioprinting have allowed for the incorporation of living cells into the fabrication process, creating dynamic and biocompatible structures. A hydrogel-based scaffold 4D printed from PEG, alginate, gelatin, and MSCs showed reversible shape morphing behavior and biocompatibility, demonstrating promise for enhanced osteointegration.[343]

Regarding cartilage tissue engineering, several polymers, including nanocellulose, alginate, and PU have been employed in various AM techniques, such as SLS and ink-jet bioprinting.[344–347] A case study involving the 4D bioprinting of a cartilage scaffold demonstrated promising chondrogenesis responses, facilitated by the scaffold's high degree of shape morphing[15] (Figure 7c). To induce a shape-morphing behavior in the scaffolds, they were fabricated based on dual-layer hydrogels, in which one layer had a lower swelling ratio than the other.

3.3.2. Muscle Tissues

The intricate nature of skeletal muscle tissues, characterized by their unique anisotropic structures known as myofibers, necessitates advanced techniques for successful tissue engineering.[348,349] This anisotropy is vital for muscle
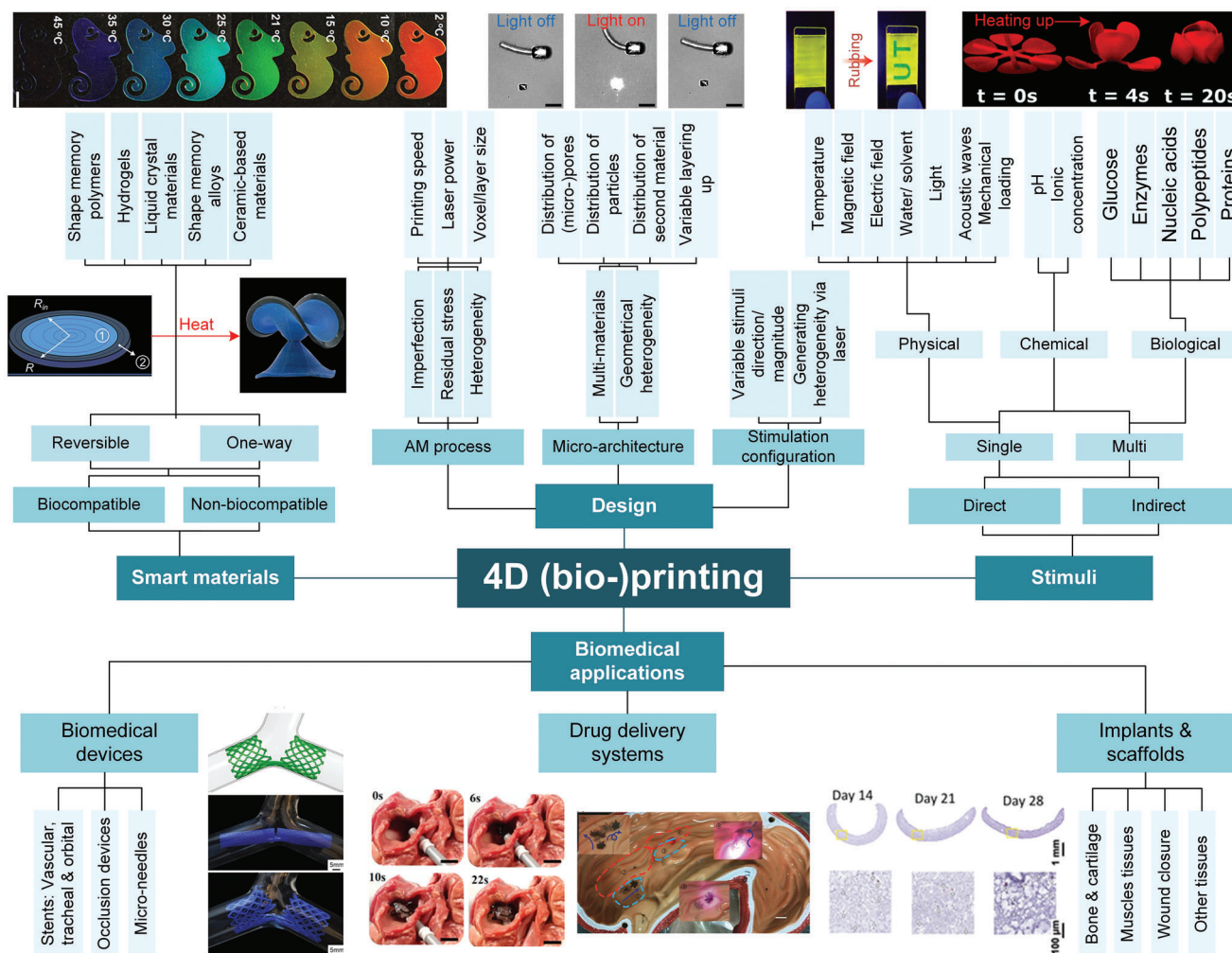
**ADVANCED
SCIENCE NEWS**

www.advancedsciencenews.com

**ADVANCED
MATERIALS**

www.advmat.de

Figure 8. An overview of the 4D bioprinting of tissue-engineered constructs. The sub-figures are derived from the following references, from top to bottom and left to right: Reproduced with permission.[172] Copyright 2022, Elsevier,[24] Reproduced with permission.[225] Copyright 2009, Springer Nature,[20,247,262] Reprinted with permission.[53] Copyright 2021, American Chemical Society, Reproduced with permission.[321] Copyright 2022, Elsevier.[15]

functionality as it modulates force transmission and regulates muscle contraction.[348] A primary aim in skeletal muscle tissue engineering is the fabrication of scaffolds that not only mimic the anisotropic properties of native tissue but also guide cellular processes, such as proliferation, differentiation, and maturation.[349]

Magnetic-based 4D bioprinting has emerged as a sophisticated technique to achieve the desired anisotropic cellular orientation. The strategy may involve the utilization of magnetic fields to align collagen fibers at the nanoscale within an agarose-collagen-based hydrogel.[40] In this approach, iron nanoparticles are incorporated into the printable hydrogel. When exposed to a magnetic field, these nanoparticles move unidirectionally, forcing the collagen fibers to orient themselves in parallel arrangements. This magnetic field-assisted alignment is a cruicial step toward achieving anisotropic scaffolds that closely mimic native skeletal muscle tissue.

Moreover, the layer-by-layer nature of AM processes has been exploited to contribute to the anisotropic orientation of scaf-

folds. Termed the "staircase effect," this phenomenon can be observed in FDM 3D printing.[349] By combining the staircase effect with subsequent coating techniques, one can achieve shape-specific 4D printed scaffolds featuring anisotropic properties[349] (Figure 7d).

3.3.3. Wound Closure

Trauma-induced organ damage necessitates rapid and effective intervention, with challenges extending to fractures, nerve damage, and other forms of skeletal and soft tissue injuries.[350] In this context, 4D printing has emerged as an important technology with significant therapeutic implications. For instance, wound closure—a relatively emergent application of 4D printing—has demonstrated multifaceted functionalities, including SME, self-responsiveness, and reversibility.[196,351–353] Specific cases include the fabrication of multiresponsive SMP-based materials using SLA for nerve repair (Figure 6c).[353] Comprising a unique blend

ADVANCED
SCIENCE NEWS

www.advancedsciencenews.com

ADVANCED
MATERIALS

www.advmat.de

of graphene-mixed SOEA, these materials have displayed outstanding physical and chemical signaling properties, further supplemented by electrical conductivity, thereby promoting enhanced nerve regeneration.[302]

The use of 3D/4D printing in the preparation of wound dressings marks a significant stride in medical technology. Customized dressings can be produced to fit wounds of diverse shapes, which contribute to accelerated wound healing.[354] Furthermore, these technologies eliminate the need for additional manufacturing resources, thereby generating cost-effective solutions with improved efficacy. In this regard, 3D/4D printed dressings have showcased versatility, incorporating innovative designs, such as porous structures embedded with bacteriophage for sustained release[355] or scaffolds that facilitate continuous exosome release,[356] thereby stimulating cellular repair mechanisms.

One of the important features of 4D printing is its ability to create complex 3D structures using spatially distributed materials. However, high-fidelity bioprinting cannot yet achieve the functional characteristics of natural tissues. As such, there is a growing emphasis on the integration of bioactive compounds into biologically functional inks.[196,351–353] This seeks to ensure the biofunctional relevance of the printed structures in addition to their morphological accuracy.

Another paradigm-shifting innovation is the use of hydrogel-based smart bioadhesives for sutureless wound closure.[350,357,358] These materials possess the capability to adhere to damaged tissues and facilitate wound closure with significantly reduced pain and scarring as compared to conventional methods, such as sutures and staples. However, a key parameter requiring attention is the temporal span between wound closure and complete healing. To address this, recent studies have introduced hydrogel-based bioadhesives[350] and hydrogel-forming double-layered adhesive MN patches.[359] These innovations not only demonstrate the capability for efficient wound closure but also present an avenue for post-wound closure care, thereby enhancing the healing process.

3.3.4. Other Tissues

The domain of nerve tissue engineering has been significantly enriched by the advent of 4D bioprinting technologies. These methods offer the capacity to precisely control the anisotropic orientation of nerve fibers, which is a crucial determinant of functional nerve tissue. Various AM techniques, including SLA, FDM, and inkjet printing, have been harnessed for this purpose.[345]

Polymeric substrates, such as collagen, fibrin, PLA, gellan, carboxymethyl chitosan, gelatin methacryloyl (GelMA), PU, and PEGDA, serve as base materials for fabricating various nerve constructs.[345,360] For instance, a bilayer scaffold was engineered with a combination of aligned PCL and poly(glycerol sebacate), along with randomly aligned hyaluronic acid methacrylate fibers.[361] This construct underwent biological assays involving the culture of PC-12 neuron cells, substantiating its potential for nerve regeneration.[361] A similar milestone was achieved through SLA-based 4D printing of a soft scaffold, characterized by its capacity to integrate seamlessly into void or damaged zones without imposing deformative stress on surrounding tissues. In

vivo evaluation indicated neovascularization over a 2-month cell culture period.[362]

Among the recent innovations, the incorporation of electroactive biomaterials (e.g., multiresponsive graphene hybrid structures) has opened new avenues in nerve tissue regeneration.[353] These structures offer many benefits: physical guidance, chemical cues, and seamless integration. Given the inherent anisotropic behavior of nerve cells, the orientation of cellular components during the bioprinting process is a focal point of consideration.[353] 3D bioprinting has emerged as a robust strategy to mitigate this constraint, enabling the deposition of cells in diverse orientations.[345,363]

Combining 3D/4D printing with other fabrication methods, such as electrospinning can further enhance the quality of nerve tissue constructs. For instance, PEGDA scaffolds have been printed on electrospun PCL or PCL/gelatin fibers to enhance nerve tissue properties.[364] An overview of the 4D bioprinting of tissue-engineered constructs is represented in **Figure 8** and **Table 1**.

4. Discussion and Future Perspectives

The controllability, repeatability, and reproducibility of 3D printing techniques have been extensively studied. There is, however, a lack of concrete evidence on how 4D bioprinting can contribute to the treatment of various conditions particularly considering the potential mechanobiological implications. Furthermore, the available studies on 4D printed biomedical devices are mostly limited to conceptual designs or proof-of-concept studies and need to be further analyzed in vitro and in vivo. We, therefore, believe that future studies should focus on the following avenues to advance the state-of-the-art in this exciting area of research.

Fabricating complex structures, such as irregular doubly curved and inflatable surfaces using custom-built four-axis 3D printers[365,366] or five-axis 3D printers[367–369] is an area that may further improve the available 4D (bio-) printing technologies. That is because curved-layer manufacturing techniques allow for nonplanar lattice shells to be 3D printed, even using three-axis 3D printers. In this method, different nonplanar structures can be 3D printed on Bézier surfaces (i.e., a set of control points in space that create smooth curves and surfaces) by using a reusable mandrel.[370,371] We, therefore, believe that the concept of 4D printing using four- or five-axis AM may lead to the production of smart biomedical devices with complex shapes. For example, orthopedic braces with complex geometries can be 4D printed from smart materials so as to allow for remote control of their shape upon application of various stimuli. As a related example, a customized silicone aortic heart valve has been recently fabricated using a custom-built nonplanar 3D printer with a flexible degree of freedom.[372]

Most studies related to 4D printing have investigated the irreversible behavior of 4D printed structures, particularly the temperature-responsive ones. However, the reversibility and reliability under cyclic loading are highly important factors that need to be considered. For example, a transcatheter 4D printed aortic valve needs to be reversible and operate cyclically. In soft robotics for biomedical applications, multiple opening and closing cycles

**ADVANCED
SCIENCE NEWS**

www.advancedsciencenews.com

**ADVANCED
MATERIALS**

www.advmat.de

Table 1. An overview of the 4D (bio)printing for biomedical applications.

Perspective	Applications	Stimuli	3D printing technique	Materials	Refs.
Smart materials	Stent	Heat	SLS	PCL	[300]
			FDM	PLA	[20,281,284,290,293,376]
				PU-based SMP	[294,291,305]
				FlexiFil	[377]
				TangoBlackPlus and VeroWhitePlus	[280]
			SLA	α,ω-polytetrahydrofuranether-diacrylate (PTHF-DA) resins	[378]
				Methacrylate based polymer	[279,297]
				Gelatin	[294]
			DIW	Polyurethane diacrylate	[283]
				PLMC	[285]
				Epoxidized soybean oil	[292]
				Alginate and hyaluronic acid	[43]
				PLA-based nanocomposite	[275]
				PNIPAM	[286]
				PGDA	[68]
				PU/hydroxyapatite/gold nanoparticles	[302]
		Magnetic	FDM	PLA/Fe$_3$O$_4$	[295]
			DIW	PLA-based nanocomposite	[275]
		Water	DIW	Zein	[282]
		Ion		AAm-AAc/CNC	[266]
	Occluder	Heat	FDM	PU composite	[305]
		Magnetic		PLA/Fe$_3$O$_4$	[52,53]
	Microneedle	–	Custom SLA	PEGDA	[314]
	Wound closure	Heat	SLA	SOEA	[353]
	Drug delivery systems	Heat and magnetic	Custom SLA	PNIPAM/NdFeB	[321]
	Scaffold	Heat	–	SMP	[341]
			SLA	SOEA	[324]
			FDM	PLA	[337,338,379]
				PU	[322]
			DLP and SLA	Acrylate PEG	[380]
				SOEA	[325,353]
			Extrusion	PU	[326]
		Magnetic	FDM	PLA/Fe$_3$O$_4$	[54,295]
		Light	DIW	PU	[326]
		Water	DIW	Hyaluronan and alginate	[15]
Design strategies for shape morphing	Implant	Mechanical	FDM	PLA	[271]

of a soft gripper are required to manipulate an object. 4D printed structures with two-way behavior may be a solution to these challenges.

So far, the 4D printing of biomedical devices has been mainly limited to conceptual and proof-of-concept studies. For example, a magnetoactive 4D printed implant was fabricated as a bone repair tool,[172] which can be tested in vivo (or in vitro) in the future. Moreover, AM techniques can be an alternative to conventional techniques for making biomedical devices featuring dynamic behavior (e.g., an SMP-based ureteral stent).[373]

Cell mechanobiology and cell responses in 4D bioprinted medical devices have not been thoroughly studied yet. Therefore, the response of cells to external stimuli and the recovery of 4D printed biomedical devices are areas that can benefit from further exploration. Moreover, the interaction between external stimuli (e.g., heat or magnetic fields) and the body's immune systems is crucial. For instance, when a 4D printed stent is implemented in the body, it should be possible to activate it at temperatures close to those of the human body.

In the context of wound healing applications, 4D printing technology has the potential to create smart wound healing patches

**ADVANCED
SCIENCE NEWS**

www.advancedsciencenews.com

**ADVANCED
MATERIALS**

www.advmat.de

and bandages that can dynamically adjust their shape to conform to the wound.[315] This system also has the potential to function as a drug delivery mechanism, releasing medications directly into the wound in addition to adapting its shape. The same concept can be extended to internal sutures within the body. A promising future direction in 4D printing involves the development of self-folding protein-based structures and capsules with self-adjusting drug release profiles.

Multimaterial 3D printing has the potential to enhance 4D printing technologies. By using multimaterial 3D printing, the deposition of different material phases in the 3D space can be controlled to induce nonaffine deformations[374] while also enabling advanced functionalities (e.g., complex shape-morphing) and unique properties (e.g., those found in functionally graded composites).[375]

To create biomedical devices at the microscale, further studies are required to explore advanced AM techniques and stimulation mechanisms. For example, to produce wireless microrobots for use in drug delivery systems, the manufacturing process, remote actuation mechanism, response time (fast or slow), and energy efficiency need to be further optimized.

The design strategy of 4D (bio)printed devices may require a combination of machine learning techniques and multiphysics in silico models. The effects of geometrical designs, external stimuli, and mechanical loading in conjunction with cell interaction and tissue growth, while considering the body environment, must be analyzed first. Such models could predict and, thus, improve the interactions of 4D printed medical devices with the human body. Specifically, there is a growing demand for the development of an inverse design approach capable of forecasting the optimal input parameters (i.e., material, geometrical properties, AM parameters, and stimulation factors) to achieve any desired function or shape transformations. Furthermore, most existing computational models in 4D printing are static in nature (only predicting the final shape or state). Therefore, there is ample opportunity for enhancement by introducing more dynamic models that can predict both the function and shape morphing at any given moment. This holds particular significance in drug delivery systems, where precise control of drug-release rates is of particular importance.

To gain a deeper comprehension of the process–structure–property relationships (e.g., the effects of external stimuli parameters and rheological properties) and to develop a robust computational platform, more experiments focused on the characterization of 4D printed materials are required under coupled mechanical loading, such as torsion-extension loading or coupled multiphysics conditions, such as magnetomechanical loading. In this context, measurement monitoring systems of 4D printable materials (e.g., LCEs)[100] are highly recommended. Moreover, mechanical properites, such as fatigue life and longevity of 4D printable biomaterials, need to be further investigated particularly within the context of implantable medical devices.

Finally, the environmental impact of 4D (bio-)printing technologies has not been adequately assessed and, thus, represents an underexplored domain that requires further exploration and attention. As 4D (bio-)printing proliferates within the medical sector, considerations of sustainability, biodegradability, and ecological footprint become indispensable. Investigations into utilizing biocompatible and biodegradable materials could serve as

a next step toward achieving environmental sustainability while maintaining medical efficacy.

Moreover, the ethical and regulatory considerations governing 4D (bio-)printing are yet to be fully articulated. As this technology transitions from a developing stage to widespread clinical applications, a comprehensive framework that addresses ethical considerations, quality assurance, and safety protocols becomes critical. Instituting such a framework would not only assure ethical integrity but would also optimize the translational potential of 4D (bio-)printing technologies.

5. Conclusion

4D (bio)printing transforms time-independent 3D printed structures into dynamic and time-dependent ones and offers the ability to program various shape morphing behaviors into biomaterials, bioprinted tissues/organs, and (implantable) medical devices. This enables precise control over shape, function, cell response, and the formation of new tissue over time. Triggered by external stimuli and shape memory effect, 4D bioprinting offers unique and promising features in regenerative medicine and organ transplantation research. These unique behaviors stem from the intrinsic properties of stimuli-responsive materials used in 4D printing. To integrate 4D bioprinting into clinical applications, four vital criteria must be met: i) the use of a suitable stimuli-responsive biomaterial, ii) the application of an effective and safe external stimulus, iii) the adaptation of a rational design strategy to achieve a desired shape morphing, and iv) the employment of an effective AM technique. These criteria empower 4D printing as a groundbreaking technology for creating next-generation biomedical devices with a unique combination of characteristics, including minimal invasiveness, remote control, and adaptability to the changing dynamics of the body's environment. However, it is essential to acknowledge that 4D printing in biomedicine is still in its early stages. Indeed, further proof-of-concept (ex vivo and in vitro) and preclinical studies (in vivo) are required in the future to elucidate the interrelationships of the shape morphing behavior and biological functions, for example, within the context of mechanobiology. In the context of drug delivery systems, which require small-scale 4D printed systems, more studies are required at the microscale to demonstrate high-precision remote control. Moreover, for biomedical devices capable of reversibly switching between permanent and temporary shapes without energy loss, the sustainability of 4D printed structures needs to be further improved. We hope that this critical and comprehensive review article serves as a guide for biomedical engineers and scientists engaged in the development of smart biomedical devices.

Conflict of Interest

The authors declare no conflict of interest.

**ADVANCED
SCIENCE NEWS**

www.advancedsciencenews.com

**ADVANCED
MATERIALS**

www.advmat.de

[1] J. S. Cuellar, G. Smit, D. Plettenburg, A. Zadpoor, *Addit. Manuf.* **2018**, *21*, 150.

[2] A. Azarniya, X. G. Colera, M. J. Mirzaali, S. Sovizi, F. Bartolomeu, M. k. S. Weglowski, W. W. Wits, C. Y. Yap, J. Ahn, G. Miranda, F. S. Silva, H. R. Madaah Hosseini, S. Ramakrishna, A. A. Zadpoor, *J. Alloys Compd.* **2019**, *804*, 163.

[3] M. J. Mirzaali, A. Azarniya, S. Sovizi, J. Zhou, A. A. Zadpoor, in *Fundamentals of Laser Powder Bed Fusion of Metals*, (Eds: I. Yadroitsev, I. Yadroitsava, A. du Plessis, E. MacDonald), Elsevier, Oxford **2021**, pp. 423–465.

[4] M. J. Mirzaali, V. Moosabeiki, S. M. Rajaai, J. Zhou, A. A. Zadpoor, *Materials* **2022**, *15*, 5457.

[5] M. J. Mirzaali, N. Shahriari, J. Zhou, A. A. Zadpoor, in *Quality Analysis of Additively Manufactured Metals*, (Eds: J. Kadkhodapour, S. Schmauder, F. Sajadi), Elsevier, Oxford **2023**, pp. 689–743.

[6] E. Yarali, M. Baniasadi, A. Zolfagharian, M. Chavoshi, F. Arefi, M. Hossain, A. Bastola, M. Ansari, A. Foyouzat, A. Dabbagh, *Appl. Mater. Today* **2022**, *26*, 101306.

[7] P. Fu, H. Li, J. Gong, Z. Fan, A. T. Smith, K. Shen, T. O. Khalfalla, H. Huang, X. Qian, J. McCutcheon, *Prog. Polym. Sci.* **2022**, *126*, 101506.

[8] D.-G. Shin, T.-H. Kim, D.-E. Kim, *Int. J. Precision Eng. Manuf.-Green Technol.* **2017**, *4*, 349.

[9] X. Liu, M. Wei, Q. Wang, Y. Tian, J. Han, H. Gu, H. Ding, Q. Chen, K. Zhou, Z. Gu, *Adv. Mater.* **2021**, *33*, 2100332.

[10] B. Peng, Y. Yang, T. Ju, *ACS Appl. Mater. Interfaces* **2020**, *13*, 12777.

[11] S.-D. Wu, S. Hsu, *Biofabrication* **2021**, *13*, 045029.

[12] C. Yuan, F. Wang, Q. Ge, *Extreme Mech. Lett.* **2021**, *42*, 101122.

[13] C. Xin, D. Jin, R. Li, D. Wang, Z. Ren, B. Liu, C. Chen, L. Li, S. Liu, B. Xu, Y. Zhang, Y. Hu, J. Li, L. Zhang, D. Wu, J. Chu, *Small* **2022**, *18*, 2202272.

[14] X. Wan, Y. He, Y. Liu, J. Leng, *Addit. Manuf.* **2022**, *53*, 102689.

[15] P. J. Díaz-Payno, M. Kalogeropoulou, I. Muntz, E. Kingma, N. Kops, M. D'Este, G. H. Koenderink, L. E. Fratila-Apachitei, G. J. van Osch, A. Zadpoor, *Adv. Healthcare Mater.* **2022**, *12*, 2201891.

[16] E. Pei, G. H. Loh, *Prog. Addit. Manuf.* **2018**, *3*, 95.

[17] C. A. Spiegel, M. Hippler, A. Münchinger, M. Bastmeyer, C. Barner-Kowollik, M. Wegener, E. Blasco, *Adv. Funct. Mater.* **2019**, *30*, 1907615.

[18] M. Hippler, K. Weißenbruch, K. Richler, E. D. Lemma, M. Nakahata, B. Richter, C. Barner-Kowollik, Y. Takashima, A. Harada, E. Blasco, *Sci. Adv.* **2020**, *6*, eabc2648.

[19] C. A. Spiegel, M. Hackner, V. P. Bothe, J. P. Spatz, E. Blasco, *Adv. Funct. Mater.* **2022**, *32*, 2110580.

[20] T. van Manen, S. Janbaz, K. M. Jansen, A. Zadpoor, *Commun. Mater.* **2021**, *2*, 56.

[21] S. Lantean, G. Barrera, C. F. Pirri, P. Tiberto, M. Sangermano, I. Roppolo, G. Rizza, *Adv. Mater. Technol.* **2019**, *4*, 1900505.

[22] B. Zhang, H. Li, J. Cheng, H. Ye, A. H. Sakhaei, C. Yuan, P. Rao, Y. F. Zhang, Z. Chen, R. Wang, *Adv. Mater.* **2021**, *33*, 2101298.

[23] Y. Jia, C. A. Spiegel, A. Welle, S. Heißler, E. Sedghamiz, M. Liu, W. Wenzel, M. Hackner, J. P. Spatz, M. Tsotsalas, E. Blasco, *Adv. Funct. Mater.* **2023**, *33*, 2207826.

[24] M. Hippler, E. Blasco, J. Qu, M. Tanaka, C. Barner-Kowollik, M. Wegener, M. Bastmeyer, *Nat. Commun.* **2019**, *10*, 232.

[25] H. Ouyang, X. Li, X. Lu, H. Xia, *ACS Appl. Polym. Mater.* **2022**, *4*, 4035.

[26] D. Abolhasani, S. W. Han, C. J. VanTyne, N. Kang, Y. H. Moon, *J. Alloys Compd.* **2022**, *922*, 166228.

[27] Z. Liu, M. Li, X. Dong, Z. Ren, W. Hu, M. Sitti, *Nat. Commun.* **2022**, *13*, 2016.

[28] B. Q. Y. Chan, Y. T. Chong, S. Wang, C. J. J. Lee, C. Owh, F. Wang, F. Wang, *Chem. Eng. J.* **2022**, *430*, 132513.

[29] T. van Manen, S. Janbaz, M. Ganjian, A. A. Zadpoor, *Mater. Today* **2020**, *32*, 59.

[30] S. Janbaz, N. Noordzij, D. S. Widyaratih, C. W. Hagen, L. E. Fratila-Apachitei, A. A. Zadpoor, *Sci. Adv.* **2017**, *3*, eaao1595.

[31] J. Li, X. Zhang, S. An, Z. Zhu, Z. Deng, Z. You, *Int. J. Solids Struct.* **2022**, *244*, 111587.

[32] C. M. Wintersinger, D. Minev, A. Ershova, H. M. Sasaki, G. Gowri, J. F. Berengut, F. E. Corea-Dilbert, P. Yin, W. M. Shih, *Nat. Nanotechnol.* **2023**, *18*, 281.

[33] Y. Wang, H. Cui, T. Esworthy, D. Mei, Y. Wang, L. G. J. Zhang, *Adv. Mater.* **2022**, *34*, 2109198.

[34] B. Gao, Q. Yang, X. Zhao, G. Jin, Y. Ma, F. Xu, *Trends Biotechnol.* **2016**, *34*, 746.

[35] W. Zhu, T. J. Webster, L. G. Zhang, *Nanomedicine* **2019**, *14*, 1643.

[36] A. Subash, B. Kandasubramanian, *Eur. Polym. J.* **2020**, *134*, 109771.

[37] M. Y. Khalid, Z. U. Arif, R. Noroozi, A. Zolfagharian, M. Bodaghi, *J. Manuf. Processes* **2022**, *81*, 759.

[38] J. M. Zelis, E. Meiburg, J. J. Roijen, K. L. Janssens, M. van't Veer, N. H. Pijls, N. P. Johnson, F. N. van de Vosse, P. A. Tonino, M. C. Rutten, *Int. J. Cardiol.* **2020**, *313*, 32.

[39] C. Deng, Y. Liu, X. Fan, B. Jiao, Z. Zhang, M. Zhang, F. Chen, H. Gao, L. Deng, W. Xiong, *Adv. Funct. Mater.* **2023**, *33*, 2211473.

[40] M. Betsch, C. Cristian, Y. Y. Lin, A. Blaeser, J. Schöneberg, M. Vogt, E. M. Buhl, H. Fischer, D. F. Duarte Campos, *Adv. Healthcare Mater.* **2018**, *7*, 1800894.

[41] Y. Xia, Y. He, F. Zhang, Y. Liu, J. Leng, *Adv. Mater.* **2021**, *33*, 2000713.

[42] Y. Tang, M. Li, T. Wang, X. Dong, W. Hu, M. Sitti, *Adv. Mater.* **2022**, *34*, 2204185.

[43] A. Kirillova, R. Maxson, G. Stoychev, C. T. Gomillion, L. Ionov, *Adv. Mater.* **2017**, *29*, 1703443.

[44] T. Uchida, H. Onoe, *Micromachines* **2019**, *10*, 433.

[45] Y. Dong, S. Wang, Y. Ke, L. Ding, X. Zeng, S. Magdassi, Y. Long, *Adv. Mater. Technol.* **2020**, *5*, 2000034.

[46] M. Behl, M. Y. Razzaq, A. Lendlein, *Adv. Mater.* **2010**, *22*, 3388.

[47] S. Nam, E. Pei, *Prog. Addit. Manuf.* **2019**, *4*, 167.

[48] J. Delaey, P. Dubruel, S. Van Vlierberghe, *Adv. Funct. Mater.* **2020**, *30*, 1909047.

[49] W. Zhou, X. Dong, Y. He, W. Zheng, J. Leng, *Smart Mater. Struct.* **2022**, *31*, 105002.

[50] A. Melocchi, M. Uboldi, N. Inverardi, F. Briatico-Vangosa, F. Baldi, S. Pandini, G. Scalet, F. Auricchio, M. Cerea, A. Foppoli, A. Maroni, L. Zema, A. Gazzaniga, *Int. J. Pharm.* **2019**, *571*, 118700.

[51] M. Baniasadi, E. Yarali, A. Foyouzat, M. S. Baghani, *Eur. J. Mech., A* **2021**, *85*, 104093.

[52] C. Lin, J. Lv, Y. Li, F. Zhang, J. Li, Y. Liu, L. Liu, J. Leng, *Adv. Funct. Mater.* **2019**, *29*, 1906569.

[53] C. Lin, L. Liu, Y. Liu, J. Leng, *ACS Appl. Mater. Interfaces* **2021**, *13*, 12668.

[54] W. Zhao, Z. Huang, L. Liu, W. Wang, J. Leng, Y. J. C. S. Liu, *Compos. Sci. Technol.* **2021**, *203*, 108563.

[55] Q. Li, M. Yang, X. Sun, Q. Wang, B. Yu, A. Gong, F. Du, *Materials Today Bio* **2023**, *19*, 100566.

[56] Z. Li, Z. Chen, Y. Gao, Y. Xing, Y. Zhou, Y. Luo, W. Xu, Z. Chen, X. Gao, K. J. B. Gupta, *Biomaterials* **2022**, *283*, 121426.

[57] N. Roudbarian, M. Baniasadi, P. Nayyeri, M. Ansari, R. Hedayati, M. Baghani, *Smart Mater. Struct.* **2021**, *30*, 105006.

**ADVANCED
SCIENCE NEWS**

www.advancedsciencenews.com

**ADVANCED
MATERIALS**

www.advmat.de

[58] J. Hu, Y. Zhu, H. Huang, J. Lu, *Prog. Polym. Sci.* **2012**, *37*, 1720.

[59] J. Wu, C. Yuan, Z. Ding, M. Isakov, Y. Mao, T. Wang, M. L. Dunn, H. Qi, *Sci. Rep.* **2016**, *6*, 24224.

[60] A. Lendlein, S. Kelch, *Angew. Chem., Int. Ed.* **2002**, *41*, 2034.

[61] S. Y. Leo, W. Zhang, Y. Zhang, Y. Ni, H. Jiang, C. Jones, P. Jiang, V. Basile, C. Taylor, *Small* **2018**, *14*, 1703515.

[62] M. Martina, D. W. Hutmacher, *Polym. Int.* **2007**, *56*, 145.

[63] M. J.-L. Tschan, E. Brulé, P. Haquette, C. M. Thomas, *Polym. Chem.* **2012**, *3*, 836.

[64] D. Moura, R. F. Pereira, I. C. Gonçalves, *Mater. Today Chem.* **2022**, *23*, 100617.

[65] H. Ramaraju, R. E. Akman, D. L. Safranski, S. J. Hollister, *Adv. Funct. Mater.* **2020**, *30*, 2002014.

[66] S. Erkeçoğlu, A. D. Sezer, S. Bucak, *Smart Drug Delivery System*, In-Tech, TX, USA **2016**.

[67] B. C. Kholkhoev, K. N. Bardakova, E. O. Epifanov, Z. A. Matveev, T. A. Shalygina, E. B. Atutov, S. Y. Voronina, P. S. Timashev, V. F. Burdukovskii, *Chem. Eng. J.* **2022**, *454*, 140423.

[68] C. Zhang, D. Cai, P. Liao, J.-W. Su, H. Deng, B. Vardhanabhuti, B. D. Ulery, S.-Y. Chen, J. Lin, *Acta Biomater.* **2021**, *122*, 101.

[69] H. Wu, P. Chen, C. Yan, C. Cai, Y. Shi, *Mater. Des.* **2019**, *171*, 107704.

[70] C.-Y. Cheng, H. Xie, Z.-y. Xu, L. Li, M.-N. Jiang, L. Tang, K.-K. Yang, Y.-Z. Wang, *Chem. Eng. J.* **2020**, *396*, 125242.

[71] A. Cortés, A. Cosola, M. Sangermano, M. Campo, S. González Prolongo, C. F. Pirri, A. Jiménez-Suárez, A. Chiappone, *Adv. Funct. Mater.* **2021**, *31*, 2106774.

[72] D. Fan, U. Staufer, A. Accardo, *Bioengineering* **2019**, *6*, 113.

[73] K. Varaprasad, C. Karthikeyan, M. M. Yallapu, R. Sadiku, *Int. J. Biol. Macromol.* **2022**, *212*, 561.

[74] Y. Hu, Z. Wang, D. Jin, C. Zhang, R. Sun, Z. Li, K. Hu, J. Ni, Z. Cai, D. Pan, *Adv. Funct. Mater.* **2020**, *30*, 1907377.

[75] J. Li, C. Wu, P. K. Chu, M. Gelinsky, *Mater. Sci. Eng., R* **2020**, *140*, 100543.

[76] Z. Ataie, S. Kheirabadi, J. W. Zhang, A. Kedzierski, C. Petrosky, R. Jiang, C. Vollberg, A. Sheikhi, *Small* **2022**, *18*, 2202390.

[77] J. R. Dias, N. Ribeiro, S. Baptista-Silva, A. R. Costa-Pinto, N. Alves, A. L. Oliveira, *Front. Bioeng. Biotechnol.* **2020**, *8*, 85.

[78] B. Liu, B. Dong, C. Xin, C. Chen, L. Zhang, D. Wang, Y. Hu, J. Li, L. Zhang, D. Wu, *Small* **2023**, *19*, 2204630.

[79] R. Suntornnond, W. L. Ng, X. Huang, C. H. E. Yeow, W. Y. Yeong, *J. Mater. Chem. B* **2022**, *10*, 5989.

[80] C. Cheng, Y. J. Moon, S. H. Kim, Y.-C. Jeong, J. Y. Hwang, G. T.-C. Chiu, B. Han, *Int. J. Heat Mass Transfer* **2020**, *150*, 119327.

[81] Y. Wang, N. Alizadeh, M. Barde, M. L. Auad, B. S. Beckingham, *ACS Appl. Polym. Mater.* **2022**, *4*, 971.

[82] S. Naficy, R. Gately, R. Gorkin III, H. Xin, G. M. Spinks, *Macromol. Mater. Eng.* **2017**, *302*, 1600212.

[83] A. S. Gladman, E. A. Matsumoto, R. G. Nuzzo, L. Mahadevan, J. A. Lewis, *Nat. Mater.* **2016**, *15*, 413.

[84] J. Lai, X. Ye, J. Liu, C. Wang, J. Li, X. Wang, M. Ma, M. Wang, *Mater. Des.* **2021**, *205*, 109699.

[85] J. Qu, X. Zhao, P. X. Ma, B. Guo, *Acta Biomater.* **2018**, *72*, 55.

[86] Z. Shi, X. Gao, M. W. Ullah, S. Li, Q. Wang, G. Yang, *Biomaterials* **2016**, *111*, 40.

[87] M.-Y. Choi, Y. Shin, H. S. Lee, S. Y. Kim, J.-H. Na, *Sci. Rep.* **2020**, *10*, 2482.

[88] D. Qureshi, S. K. Nayak, S. Maji, A. Anis, D. Kim, K. Pal, *Eur. Polym. J.* **2019**, *120*, 109220.

[89] H. Banerjee, M. Suhail, H. Ren, *Biomimetics* **2018**, *3*, 15.

[90] Y. S. Zhang, A. Khademhosseini, *Science* **2017**, *356*, eaaf3627.

[91] S. J. Woltman, G. D. Jay, G. P. Crawford, *Nat. Mater.* **2007**, *6*, 929.

[92] S. Mayer, R. Zentel, *Mater. Sci.* **2002**, *6*, 545.

[93] A. Akram, T. G. Shahzady, S. Hussain, N. A. Saad, M. T. Islam, M. Ikram, *Russ. J. Appl. Chem.* **2021**, *94*, 1585.

[94] K. M. Herbert, H. E. Fowler, J. M. McCracken, K. R. Schlafmann, J. A. Koch, T. J. White, *Nat. Rev. Mater.* **2022**, *7*, 23.

[95] X. Peng, S. Wu, X. Sun, L. Yue, S. M. Montgomery, F. Demoly, K. Zhou, R. R. Zhao, H. J. Qi, *Adv. Mater.* **2022**, *34*, 2204890.

[96] A. Kotikian, R. L. Truby, J. W. Boley, T. J. White, J. A. Lewis, *Adv. Mater.* **2018**, *30*, 1706164.

[97] M. Del Pozo, J. A. Sol, A. P. Schenning, M. G. Debije, *Adv. Mater.* **2022**, *34*, 2104390.

[98] Q. Yang, H. Shahsavan, Z. Deng, H. Guo, H. Zhang, H. Liu, C. Zhang, A. Priimagi, X. Zhang, H. Zeng, *Adv. Funct. Mater.* **2022**, *32*, 2206939.

[99] D. Sun, J. Zhang, H. Li, Z. Shi, Q. Meng, S. Liu, J. Chen, X. Liu, *Polymers* **2021**, *13*, 1889.

[100] M. Chen, M. Gao, L. Bai, H. Zheng, H. J. Qi, K. Zhou, *Adv. Mater.* **2023**, *35*, 2209566.

[101] M. Tabrizi, T. H. Ware, M. R. Shankar, *ACS Appl. Mater. Interfaces* **2019**, *11*, 28236.

[102] J. Sgotti Veiga, M. Reis Carneiro, R. Molter, M. Vinciguerra, L. Yao, C. Majidi, M. Tavakoli, *Adv. Mater. Technol.* **2023**, *8*, 2300144.

[103] S. Li, Z. Song, Y. Fan, D. Wei, Y. Liu, *Biomimetics* **2023**, *8*, 196.

[104] M. R. Vinciguerra, D. K. Patel, W. Zu, M. Tavakoli, C. Majidi, L. Yao, *ACS Appl. Mater. Interfaces* **2023**, *15*, 24777.

[105] J. S. Veiga, M. R. Carneiro, R. Molter, M. Vinciguerra, L. Yao, C. Majidi, M. Tavakoli, *Adv. Mater. Technol.* **2023**, *8*, 2300144.

[106] A. Y. Lee, J. An, C. K. Chua, *Engineering* **2017**, *3*, 663.

[107] H. Lu, C. Yang, X. Luo, H. Ma, B. Song, Y. Li, L. Zhang, *Mater. Sci. Eng., A* **2019**, *763*, 138166.

[108] M. P. Caputo, A. E. Berkowitz, A. Armstrong, P. Müllner, C. V. Solomon, *Addit. Manuf.* **2018**, *21*, 579.

[109] I. Shishkovsky, V. Scherbakov, *Proc. SPIE* **2018**, *10523*, 1052311.

[110] C. Wang, X. Tan, Z. Du, S. Chandra, Z. Sun, C. Lim, S. B. Tor, C. S. Lim, C. H. Wong, *J. Mater. Process. Technol.* **2019**, *271*, 152.

[111] K. Lu, W. T. Reynolds, *Powder Technol.* **2008**, *187*, 11.

[112] S. Akbari, A. H. Sakhaei, S. Panjwani, K. Kowsari, A. Serjouei, Q. Ge, *Sens. Actuators, A* **2019**, *290*, 177.

[113] A. N. Alagha, S. Hussain, W. Zaki, *Mater. Des.* **2021**, *204*, 109654.

[114] S. Saedi, A. S. Turabi, M. Taheri Andani, C. Haberland, H. Karaca, M. Elahinia, *J. Alloys Compd.* **2016**, *677*, 204.

[115] S. Gao, S. Weng, F. Weng, O. P. Bodunde, M. Qin, W.-H. Liao, P. Guo, *J. Manuf. Processes* **2021**, *71*, 417.

[116] J. Otubo, O. D. Rigo, C. M. Neto, P. R. Mei, *Mater. Sci. Eng., A* **2006**, *438*, 679.

[117] A. Mostafaei, K. A. Kimes, E. L. Stevens, J. Toman, Y. L. Krimer, K. Ullakko, M. Chmielus, *Acta Mater.* **2017**, *131*, 482.

[118] M. Nachimuthu, R. P. K., *Rapid Prototyping J.* **2023**, *29*, 437.

[119] K. Sun, X. Meng, Z. Gao, W. Cai, *Shape Memory Superelasticity* **2023**, *9*, 252.

[120] F. Wang, C. Liu, H. Yang, H. Wang, H. Zhang, X. Zeng, C. Wang, W. Zhang, W. Lv, P. Zhu, *Addit. Manuf.* **2023**, *63*, 103411.

[121] A. Lai, C. A. Schuh, *Phys. Rev. Lett.* **2021**, *126*, 015701.

[122] A. Lai, Z. Du, C. L. Gan, C. A. Schuh, *Science* **2013**, *341*, 1505.

[123] M. Yarahmadi, P. Barcelona, G. Fargas, E. Xuriguera, J. J. Roa, *Ceram. Int.* **2022**, *48*, 4775.

[124] I. Buj-Corral, J. A. Padilla, J. Minguella-Canela, L. Rodero, L. Marco, E. Xuriguera, *Key Eng. Mater.* **2023**, *958*, 157.

[125] F. Wang, C. Liu, H. Yang, H. Wang, H. Zhang, X. Zeng, C. Wang, W. Zhang, W. Lv, P. Zhu, B. Li, *Addit. Manuf.* **2023**, *63*, 103411.

[126] F. L. Bargardi, H. Le Ferrand, R. Libanori, A. R. Studart, *Nat. Commun.* **2016**, *7*, 13912.

[127] S. Chen, J. Li, H. Shi, X. Chen, G. Liu, S. Meng, J. Lu, *Chem. Eng. J.* **2023**, *455*, 140655.

[128] G. Liu, Y. Zhao, G. Wu, J. Lu, *Sci. Adv.* **2018**, *4*, eaat0641.

**ADVANCED
SCIENCE NEWS**

www.advancedsciencenews.com

**ADVANCED
MATERIALS**

www.advmat.de

[129] Y.-J. Kim, Y. T. Matsunaga, *J. Mater. Chem. B* **2017**, *5*, 4307.

[130] P. Zarrintaj, M. Jouyandeh, M. R. Ganjali, B. S. Hadavand, M. Mozafari, S. S. Sheiko, M. Vatankhah-Varnoosfaderani, T. J. Gutiérrez, M. R. Saeb, *Eur. Polym. J.* **2019**, *117*, 402.

[131] M. Liu, X. Song, Y. Wen, J.-L. Zhu, J. Li, *ACS Appl. Mater. Interfaces* **2017**, *9*, 35673.

[132] M. Hippler, E. Blasco, J. Qu, M. Tanaka, C. Barner-Kowollik, M. Wegener, M. Bastmeyer, *Nat. Commun.* **2019**, *10*, 232.

[133] D. Zhang, J. Yang, C. Liu, S. Ye, Q. Zhang, R. Liu, *Int. J. Nanomed.* **2021**, 4901.

[134] A. T. Andrgie, H. F. Darge, T. W. Mekonnen, Y. S. Birhan, E. Y. Hanurry, H.-Y. Chou, C.-F. Wang, H.-C. Tsai, J. M. Yang, Y.-H. Chang, *Polymers* **2020**, *12*, 2619.

[135] H. Lu, M. Lei, C. Zhao, Y. Yao, J. Gou, D. Hui, Y. Q. Fu, *Composites, Part B* **2015**, *80*, 37.

[136] H. Luo, Z. Li, G. Yi, X. Zu, H. Wang, H. Huang, Y. Wang, Z. Liang, S. Zhang, *Mater. Lett.* **2014**, *137*, 385.

[137] A. Chortos, E. Hajiesmaili, J. Morales, D. R. Clarke, J. A. Lewis, *Adv. Funct. Mater.* **2020**, *30*, 1907375.

[138] H. Cui, R. Hensleigh, D. Yao, D. Maurya, P. Kumar, M. G. Kang, S. Priya, X. R. Zheng, *Nat. Mater.* **2019**, *18*, 234.

[139] D. Kuscer, O. Noshchenko, H. Uršič, B. Malič, *J. Am. Ceram. Soc.* **2013**, *96*, 2714.

[140] I. Kierzewski, S. S. Bedair, B. Hanrahan, H. Tsang, L. Hu, N. Lazarus, *Addit. Manuf.* **2020**, *31*, 100963.

[141] Y. A. O. Assagra, R. A. P. Altafim, R. A. C. Altafim, J. Carmo, *Electron. Lett.* **2015**, *51*, 2028.

[142] A. M. Peterson, *Addit. Manuf.* **2019**, *27*, 363.

[143] S. J. Callens, D. Fan, I. A. van Hengel, M. Minneboo, L. E. Fratila-Apachitei, A. A. Zadpoor, *Nat. Commun.* **2020**, *14*, 855.

[144] A. A. Zadpoor, *Mater. Horiz.* **2016**, *3*, 371.

[145] H. M. A. Kolken, K. Lietaert, T. van der Sloten, B. Pouran, A. Meynen, G. Van Loock, H. Weinans, L. Scheys, A. A. Zadpoor, *J. Mech. Behav. Biomed. Mater.* **2020**, *104*, 103658.

[146] E. Hajiesmaili, N. M. Larson, J. A. Lewis, D. R. J. S. A. Clarke, *Sci. Adv.* **2022**, *8*, eabn9198.

[147] M. Duduta, F. Berlinger, R. Nagpal, D. Clarke, R. Wood, F. Z. Temel, *Smart Mater. Struct.* **2019**, *28*, 09LT01.

[148] H. Zhao, A. M. Hussain, M. Duduta, D. M. Vogt, R. J. Wood, D. R. Clarke, *Adv. Funct. Mater.* **2018**, *28*, 1804328.

[149] E. Hajiesmaili, E. Khare, A. Chortos, J. Lewis, D. R. Clarke, *Extreme Mech. Lett.* **2019**, *30*, 100504.

[150] S. Rosset, O. A. Araromi, S. Schlatter, H. R. Shea, *J. Visualized Exp.* **2016**, 53423.

[151] Y. Chen, H. Zhao, J. Mao, P. Chirarattananon, E. F. Helbling, N. P. Hyun, D. R. Clarke, R. J. Wood, *Nature* **2019**, *575*, 324.

[152] M. Duduta, R. J. Wood, D. R. Clarke, *Adv. Mater.* **2016**, *28*, 8058.

[153] L. Zhou, Q. Gao, J. Fu, Q. Chen, J. Zhu, Y. Sun, Y. He, *ACS Appl. Mater. Interfaces* **2019**, *11*, 23573.

[154] J. Rossiter, P. Walters, B. Stoimenov, Electroactive Polymer Actuators and Devices (EAPAD) 2009, Proc. SPIE, Bellingham, WA **2009**, p. 72870H.

[155] A. Creegan, I. Anderson, *Proc. SPIE* **2014**, *9056*, 905629.

[156] D. McCoul, S. Rosset, S. Schlatter, H. Shea, *Smart Mater. Struct.* **2017**, *26*, 125022.

[157] A. Chortos, J. Mao, J. Mueller, E. Hajiesmaili, J. A. Lewis, D. R. Clarke, *Adv. Funct. Mater.* **2021**, *31*, 2010643.

[158] J. Maas, D. Tepel, T. Hoffstadt, *Meccanica* **2015**, *50*, 2839.

[159] R. L. Truby, M. Wehner, A. K. Grosskopf, D. M. Vogt, S. G. Uzel, R. J. Wood, J. A. Lewis, *Adv. Mater.* **2018**, *30*, 1706383.

[160] G. Haghiashtiani, E. Habtour, S.-H. Park, F. Gardea, M. C. McAlpine, *Extreme Mech. Lett.* **2018**, *21*, 1.

[161] A. H. Zamanian, D. A. Porter, P. Krueger, E. Richer, ASME 2018 Dynamic Systems and Control Conference, Atlanta, Georgia, USA, October **2018**.

[162] J. J. Abbott, E. Diller, A. J. Petruska, *Rob. Auton. Syst.* **2020**, *3*, 57.

[163] Y. Kim, X. Zhao, *Chem. Rev.* **2022**, *122*, 5317.

[164] Q. Ze, X. Kuang, S. Wu, J. Wong, S. M. Montgomery, R. Zhang, J. M. Kovitz, F. Yang, H. J. Qi, R. Zhao, *Adv. Mater.* **2020**, *32*, 1906657.

[165] Y. Kim, H. Yuk, R. Zhao, S. A. Chester, X. Zhao, *Nature* **2018**, *558*, 274.

[166] S. Qi, J. Fu, Y. Xie, Y. Li, R. Gan, M. Yu, *Compos. Sci. Technol.* **2019**, *183*, 107817.

[167] E. Yarali, M. A. Farajzadeh, R. Noroozi, A. Dabbagh, M. J. Khoshgoftar, M. Mirzaali, *Compos. Struct.* **2020**, *254*, 112881.

[168] J. Silva, C. Gouveia, G. Dinis, A. Pinto, A. Pereira, *Composites, Part B* **2022**, *243*, 110125.

[169] A. Bastola, M. Paudel, L. Li, *J. Magn. Magn. Mater.* **2020**, *494*, 165825.

[170] Z. Wang, Y. Wu, D. Wu, D. Sun, L. Lin, *Composites, Part B* **2022**, *231*, 109596.

[171] X. Ding, Y. Shi, S. Xu, Y. Zhang, J. Du, J. J. S. Qiu, *Small* **2023**, *19*, 2205797.

[172] J. Liao, C. Ye, J. Guo, C. E. Garciamendez-Mijares, P. Agrawal, X. Kuang, J. O. Japo, Z. Wang, X. Mu, W. Li, T. Ching, L. S. Mille, C. Zhu, X. Zhang, Z. Gu, Y. S. Zhang, *Mater. Today* **2022**, *56*, 29.

[173] A. Lendlein, O. E. Gould, *Nat. Rev. Mater.* **2019**, *4*, 116.

[174] E. Yarali, A. Taheri, M. Baghani, *J. Intell. Mater. Syst. Struct.* **2020**, *31*, 1243.

[175] A. Bhargava, K. Peng, J. Stieg, R. Mirzaeifar, S. Shahab, *RSC Adv.* **2017**, *7*, 45452.

[176] K. Yu, Y. Liu, J. Leng, *RSC Adv.* **2014**, *4*, 2961.

[177] H. Deng, K. Sattari, Y. Xie, P. Liao, Z. Yan, J. Lin, *Nat. Commun.* **2020**, *11*, 6325.

[178] F. Zhang, L. Wang, Z. Zheng, Y. Liu, J. Leng, *Composites, Part A* **2019**, *125*, 105571.

[179] S. R. Goudu, I. C. Yasa, X. Hu, H. Ceylan, W. Hu, M. Sitti, *Adv. Funct. Mater.* **2020**, *30*, 2004975.

[180] J. Zhang, R. H. Soon, Z. Wei, W. Hu, M. Sitti, *Adv. Sci.* **2022**, *9*, 2203730.

[181] P. Testa, R. W. Style, J. Z. Cui, C. Donnelly, E. Borisova, P. M. Derlet, E. R. Dufresne, L. J. Heyderman, *Adv. Mater.* **2019**, *31*, 6.

[182] C. Zhang, X. Li, L. Jiang, D. Tang, H. Xu, P. Zhao, J. Fu, Q. Zhou, Y. Chen, *Adv. Funct. Mater.* **2021**, *31*, 2102777.

[183] M. Mazurek-Budzyńska, M. Y. Razzaq, M. Behl, A. Lendlein, in *Functional Polymers*, (Eds: M. A. Jafar Mazumder, H. Sheardown, A. Al-Ahmed), Springer International Publishing, Cham **2019**, pp. 605–663.

[184] A. M. Schmidt, *Macromol. Rapid Commun.* **2006**, *27*, 1168.

[185] T. Pretsch, *Polymers* **2010**, *2*, 120.

[186] H. Lu, M. Lei, C. Zhao, B. Xu, J. Leng, Y. Q. Fu, *Smart Mater. Struct.* **2015**, *24*, 045015.

[187] M. Curcio, U. Spizzirri, G. Cirillo, O. Vittorio, N. Picci, F. Nicoletta, F. Iemma, S. Hampel, *RSC Adv.* **2015**, *5*, 44902.

[188] X. Shi, Y. Zheng, C. Wang, L. Yue, K. Qiao, G. Wang, L. Wang, H. Quan, *RSC Adv.* **2015**, *5*, 41820.

[189] X. Wan, F. Zhang, Y. Liu, J. Leng, *Carbon* **2019**, *155*, 77.

[190] X. Dong, F. Zhang, L. Wang, Y. Liu, J. S. Leng, *Composites, Part A* **2022**, *157*, 106925.

[191] D. Samanta, R. Mehrotra, K. Margulis, R. N. Zare, *Nanoscale* **2017**, *9*, 16429.

[192] K. M. Lichade, S. Shiravi, J. D. Finan, Y. Pan, *Addit. Manuf.* **2024**, 104123.

[193] S. Tibbits, *Archit. Des.* **2014**, *84*, 116.

[194] J. Yang, Y. Zheng, L. Sheng, H. Chen, L. Zhao, W. Yu, K.-Q. Zhao, P. Hu, *Ind. Eng. Chem. Res.* **2018**, *57*, 15046.

2402301 (29 of 34)

**ADVANCED
SCIENCE NEWS**

www.advancedsciencenews.com

**ADVANCED
MATERIALS**

www.advmat.de

[195] D. Raviv, W. Zhao, C. McKnelly, A. Papadopoulou, A. Kadambi, B. Shi, S. Hirsch, D. Dikovsky, M. Zyracki, C. Olguin, R. Raskar, S. Tibbits, *Sci. Rep.* **2014**, *4*, 7422.

[196] Q. Yang, B. Gao, F. Xu, *Biotechnol. J.* **2020**, *15*, 1900086.

[197] J. Huang, H. Fu, Z. Wang, Q. Meng, S. Liu, H. Wang, X. Zheng, J. Dai, Z. Zhang, *RSC Adv.* **2016**, *6*, 108423.

[198] H. Yang, C. Li, M. Yang, Y. Pan, Q. Yin, J. Tang, H. J. Qi, Z. Suo, *Adv. Funct. Mater.* **2019**, *29*, 1901721.

[199] C. Lv, X.-C. Sun, H. Xia, Y.-H. Yu, G. Wang, X.-W. Cao, S.-X. Li, Y.-S. Wang, Q.-D. Chen, Y.-D. Yu, H. B. Sun, *Sens. Actuators, B* **2018**, *259*, 736.

[200] M. Jamal, S. S. Kadam, R. Xiao, F. Jivan, T. M. Onn, R. Fernandes, T. D. Nguyen, D. H. Gracias, *Adv. Healthcare Mater.* **2013**, *2*, 1142.

[201] M. J. Mirzaali, A. Ghorbani, K. Nakatani, M. Nouri-Goushki, N. Tümer, S. J. Callens, S. Janbaz, A. Accardo, J. Bico, M. Habibi, *Adv. Mater.* **2021**, *33*, 2008082.

[202] S. Parimita, A. Kumar, H. Krishnaswamy, P. J. M. P. Ghosh, *J. Manuf. Processes* **2023**, *85*, 875.

[203] M. Herath, J. Epaarachchi, M. Islam, F. Zhang, J. Leng, L. Fang, C. Yan, G. D. Peng, W. Schade, *Smart Mater. Struct.* **2020**, *29*, 047001.

[204] X. Cui, J. Chen, Y. Zhu, W. Jiang, *Chem. Eng. J.* **2020**, *382*, 122823.

[205] Y. Lee, J. Moon, J. Choi, M. Cho, *Sci. Rep.* **2017**, *7*, 14277.

[206] F. Ercole, T. P. Davis, R. A. Evans, *Polym. Chem.* **2010**, *1*, 37.

[207] Y. Shi, Z. Chen, *J. Mater. Chem. C* **2018**, *6*, 11817.

[208] S. Q. Wang, D. Kaneko, M. Okajima, K. Yasaki, S. Tateyama, T. Kaneko, *Angew. Chem., Int. Ed.* **2013**, *52*, 11143.

[209] Q. Guo, C. J. Bishop, R. A. Meyer, D. R. Wilson, L. Olasov, D. E. Schlesinger, P. T. Mather, J. B. Spicer, J. H. Elisseeff, J. J. Green, *ACS Appl. Mater. Interfaces* **2018**, *10*, 13333.

[210] Z. Chen, R. Cao, S. Ye, Y. Ge, Y. Tu, X. Yang, *Sens. Actuators, B* **2018**, *255*, 2971.

[211] J. Huang, L. Zhao, T. Wang, W. Sun, Z. Tong, *ACS Appl. Mater. Interfaces* **2016**, *8*, 12384.

[212] J. Ban, L. Mu, J. Yang, S. Chen, H. Zhuo, *J. Mater. Chem. A* **2017**, *5*, 14514.

[213] C. Greant, B. Van Durme, J. Van Hoorick, S. Van Vlierberghe, *Adv. Funct. Mater.* **2023**, *33*, 2212641.

[214] R. Matsuzaki, M. Ueda, M. Namiki, T.-K. Jeong, H. Asahara, K. Horiguchi, T. Nakamura, A. Todoroki, Y. Hirano, *Sci. Rep.* **2016**, *6*, 23058.

[215] H. Yang, W. R. Leow, T. Wang, J. Wang, J. Yu, K. He, D. Qi, C. Wan, X. Chen, *Adv. Mater.* **2017**, *29*, 1701627.

[216] P. J. Kitson, S. Glatzel, W. Chen, C.-G. Lin, Y.-F. Song, L. Cronin, *Nat. Protoc.* **2016**, *11*, 920.

[217] X. Yang, W. Chen, H. Liu, B. Yang, Y. Xie, Y. Wang, Y. Lei, L. Xue, *Adv. Mater. Technol.* **2022**, *7*, 2200266.

[218] Y. S. Lui, W. T. Sow, L. P. Tan, Y. Wu, Y. Lai, H. Li, *Acta Biomater.* **2019**, *92*, 19.

[219] Z.-x. Zhang, J.-x. Dou, J.-h. He, C.-x. Xiao, L.-y. Shen, J.-h. Yang, Y. Wang, Z. Zhou, *J. Mater. Chem. C* **2017**, *5*, 4145.

[220] F. Li, L. Liu, X. Lan, C. Pan, Y. Liu, J. Leng, Q. Xie, *Smart Mater. Struct.* **2019**, *28*, 075023.

[221] R. Bayan, N. Karak, *New J. Chem.* **2017**, *41*, 8781.

[222] W. M. Xu, M. Z. Rong, M. Q. Zhang, *J. Mater. Chem. A* **2016**, *4*, 10683.

[223] G. Li, Q. Yan, H. Xia, Y. Zhao, *ACS Appl. Mater. Interfaces* **2015**, *7*, 12067.

[224] C. Weder, *J. Mater. Chem.* **2011**, *21*, 8235.

[225] Y. Sagara, T. Kato, *Nat. Chem.* **2009**, *1*, 605.

[226] T. J. Kucharski, R. Boulatov, *J. Mater. Chem.* **2011**, *21*, 8237.

[227] Y. Vidavsky, S. J. Yang, B. A. Abel, I. Agami, C. E. Diesendruck, G. W. Coates, M. N. Silberstein, *J. Am. Chem. Soc.* **2019**, *141*, 10060.

[228] J. Han, K.-M. Tang, S.-C. Cheng, C.-O. Ng, Y.-K. Chun, S.-L. Chan, S.-M. Yiu, M.-K. Tse, V. A. Roy, C.-C. Ko, *Inorg. Chem. Front.* **2020**, *7*, 786.

[229] H. Chen, Y. Li, Y. Liu, T. Gong, L. Wang, S. Zhou, *Polym. Chem.* **2014**, *5*, 5168.

[230] M. Nadgorny, Z. Xiao, C. Chen, L. A. Connal, *ACS Appl. Mater. Interfaces* **2016**, *8*, 28946.

[231] J. Y. Wang, F. Jin, X. Z. Dong, J. Liu, M. X. Zhou, T. Li, M. L. Zheng, *Small* **2023**, *19*, 2303166.

[232] Y. Wang, G. He, Z. Li, J. Hua, M. Wu, J. Gong, J. Zhang, L.-t. Ban, L. Huang, *Polymers* **2018**, *10*, 112.

[233] A. G. Tabriz, M. A. Hermida, N. R. Leslie, W. Shu, *Biofabrication* **2015**, *7*, 045012.

[234] W. Nan, W. Wang, H. Gao, W. Liu, *Soft Matter* **2013**, *9*, 132.

[235] A. Skardal, A. Atala, *Ann. Biomed. Eng.* **2015**, *43*, 730.

[236] Z. Wan, P. Zhang, Y. Liu, L. Lv, Y. Zhou, *Acta Biomater.* **2020**, *101*, 26.

[237] M. Champeau, D. A. Heinze, T. N. Viana, E. R. de Souza, A. C. Chinellato, S. Titotto, *Adv. Funct. Mater.* **2020**, *30*, 1910606.

[238] L. Hockaday, K. Kang, N. Colangelo, P. Cheung, B. Duan, E. Malone, J. Wu, L. Girardi, L. Bonassar, H. Lipson, *Biofabrication* **2012**, *4*, 035005.

[239] Y. M. Abul-Haija, G. G. Scott, J. K. Sahoo, T. Tuttle, R. V. Ulijn, *Chem. Commun.* **2017**, *53*, 9562.

[240] E. Fleige, M. A. Quadir, R. Haag, *Adv. Drug Delivery Rev.* **2012**, *64*, 866.

[241] R. A. Siegel, *J. Controlled Release* **2014**, *190*, 337.

[242] J. Bai, R. Wang, X. Wang, S. Liu, X. Wang, J. Ma, Z. Qin, T. Jiao, *Cell Rep. Phys. Sci.* **2021**, *2*, 100623.

[243] S. Janbaz, R. Hedayati, A. Zadpoor, *Mater. Horiz.* **2016**, *3*, 536.

[244] J. W. Boley, W. M. van Rees, C. Lissandrello, M. N. Horenstein, R. L. Truby, A. Kotikian, J. A. Lewis, L. Mahadevan, *Proc. Natl. Acad. Sci. U. S. A.* **2019**, *116*, 20856.

[245] B. Goo, C.-H. Hong, K. Park, *Mater. Des.* **2020**, *188*, 108485.

[246] S. Weng, X. Kuang, Q. Zhang, C. M. Hamel, D. J. Roach, N. Hu, H. Jerry Qi, *ACS Appl. Mater. Interfaces* **2021**, *13*, 12797.

[247] V. Moosabeiki, E. Yarali, A. Ghalayaniesfahani, S. J. Callens, T. van Manen, A. Accardo, S. Ghodrat, J. Bico, M. Habibi, M. J. Mirzaali, *Commun. Mater.* **2024**, *5*, 10.

[248] X. Ni, X. Guo, J. Li, Y. Huang, Y. Zhang, J. A. Rogers, *Adv. Mater.* **2019**, *31*, 1905405.

[249] H. Arslan, A. Nojoomi, J. Jeon, K. Yum, *Adv. Sci.* **2019**, *6*, 1800703.

[250] A. B. Baker, S. R. Bates, T. M. Llewellyn-Jones, L. P. Valori, M. P. Dicker, R. S. Trask, *Mater. Des.* **2019**, *163*, 107544.

[251] C. Song, J. Ju, *Extreme Mech. Lett.* **2020**, 100625.

[252] G. Sossou, F. Demoly, H. Belkebir, H. J. Qi, S. Gomes, G. Montavon, *Mater. Des.* **2019**, *175*, 107798.

[253] T. van Manen, S. Janbaz, A. A. Zadpoor, *Mater. Today* **2018**, *21*, 144.

[254] X. P. Hao, Z. Xu, C. Y. Li, W. Hong, Q. Zheng, Z. L. Wu, *Adv. Mater.* **2020**, *32*, 2000781.

[255] T. van Manen, V. M. Dehabadi, M. C. Saldívar, M. J. Mirzaali, A. A. Zadpoor, *Commun. Mater.* **2022**, *3*, 43.

[256] H. Guo, J. Cheng, K. Yang, K. Demella, T. Li, S. R. Raghavan, Z. Nie, *ACS Appl. Mater. Interfaces* **2019**, *11*, 42654.

[257] J. M. McCracken, B. M. Rauzan, J. C. Kjellman, H. Su, S. A. Rogers, R. G. Nuzzo, *Adv. Funct. Mater.* **2019**, *29*, 1806723.

[258] B. Zou, Z. Liang, Z. Cui, K. Xiao, S. Shao, J. J. Ju, *Adv. Mater.* **2023**, *35*, 2207349.

[259] Y. Wang, X. Li, *Mech. Mater.* **2020**, *151*, 103628.

[260] Y. Feng, J. Xu, S. Zeng, Y. Gao, J. Tan, *Smart Mater. Struct.* **2020**, *29*, 085042.

[261] M. Bodaghi, A. Damanpack, W. Liao, *Mater. Des.* **2017**, *135*, 26.

[262] T. van Manen, S. Janbaz, A. A. Zadpoor, *Mater. Horiz.* **2017**, *4*, 1064.

[263] H. Deng, C. Zhang, K. Sattari, Y. Ling, J.-W. Su, Z. Yan, J. Lin, *ACS Appl. Mater. Interfaces* **2021**, *13*, 12719.

[264] Q. Ji, J. Moughames, X. Chen, G. Fang, J. J. Huaroto, V. Laude, J. A. I. Martínez, G. Ulliac, C. Clévy, P. Lutz, K. Rabenorosoa, V. Guelpa, A.

Spangenberg, J. Liang, A. Mosset, M. Kadic, *Commun. Mater.* **2021**, *2*, 1.

[265] J. Qu, M. Kadic, A. Naber, M. J. S. Wegener, *Sci. Rep.* **2017**, *7*, 1.

[266] G. Qu, J. Huang, Z. Li, Y. Jiang, Y. Liu, K. Chen, Z. Xu, Y. Zhao, G. Gu, X. Wu, *Mater Today Bio* **2022**, *16*, 100363.

[267] M. Azaouzi, A. Makradi, S. Belouettar, *Mater. Des.* **2012**, *41*, 410.

[268] D. Stoeckel, A. Pelton, T. Duerig, *Eur. Radiol.* **2004**, *14*, 292.

[269] W. M. Huang, C. Song, Y. Q. Fu, C. C. Wang, Y. Zhao, H. Purnawali, H. Lu, C. Tang, Z. Ding, J. Zhang, *Adv. Drug Delivery Rev.* **2013**, *65*, 515.

[270] L. Wang, Y. Qiu, H. Lv, Y. Si, L. Liu, Q. Zhang, J. Cao, X. Yu, X. Li, B. Ding, *Adv. Funct. Mater.* **2019**, *29*, 1901407.

[271] F. Bobbert, S. Janbaz, A. Zadpoor, *J. Mater. Chem. B* **2018**, *6*, 3449.

[272] L. Hiendlmeier, F. Zurita, J. Vogel, F. D. Duca, G. A. Boustani, H. Peng, I. Kopic, M. Nikić, T. Teshima, B. Wolfrum, *Adv. Mater.* **2023**, *35*, 2210206.

[273] W. Zhou, Z. Qiao, E. Nazarzadeh Zare, J. Huang, X. Zheng, X. Sun, M. Shao, H. Wang, X. Wang, D. Chen, *J. Med. Chem.* **2020**, *63*, 8003.

[274] Y. Li, F. Zhang, Y. Liu, J. Leng, *Sci. China Technol. Sci.* **2020**, *63*, 545.

[275] H. Wei, Q. Zhang, Y. Yao, L. Liu, Y. Liu, J. Leng, *ACS Appl. Mater. Interfaces* **2017**, *9*, 876.

[276] P. Cao, J. Yang, J. Gong, L. Tao, T. Wang, J. Ju, Y. Zhou, Q. Wang, Y. Zhang, *J. Appl. Polym. Sci.* **2023**, *140*, 53241.

[277] Y. Zhou, D. Zhou, P. Cao, X. Zhang, Q. Wang, T. Wang, Z. Li, W. He, J. Ju, Y. Zhang, *Macromol. Rapid Commun.* **2021**, *42*, 2100176.

[278] L. Zhang, M. Hanif, J. Li, A. H. Shah, W. Hussain, G. Zhang, *Polymers* **2023**, *15*, 390.

[279] Q. Ge, A. H. Sakhaei, H. Lee, C. K. Dunn, N. X. Fang, M. L. Dunn, *Sci. Rep.* **2016**, *6*, 31110.

[280] M. Bodaghi, A. Damanpack, W. Liao, *Smart Mater. Struct.* **2016**, *25*, 105034.

[281] H. Jia, S. Y. Gu, K. Chang, *Adv. Polym. Technol.* **2018**, *37*, 3222.

[282] Y. Zhang, A. Raza, Y.-Q. Xue, G. Yang, U. Hayat, J. Yu, C. Liu, H.-J. Wang, J.-Y. Wang, *Bioact. Mater* **2023**, *23*, 343.

[283] X. Kuang, K. Chen, C. K. Dunn, J. Wu, V. C. Li, H. J. Qi, *ACS Appl. Mater. Interfaces* **2018**, *10*, 7381.

[284] X. Wang, Y. Zhang, P. Shen, Z. Cheng, C. Chu, F. Xue, J. Bai, *Biomater. Sci.* **2022**, *10*, 2302.

[285] X. Wan, H. Wei, F. Zhang, Y. Liu, J. Leng, *J. Appl. Polym. Sci.* **2019**, *136*, 48177.

[286] J. Liu, O. Erol, A. Pantula, W. Liu, Z. Jiang, K. Kobayashi, D. Chatterjee, N. Hibino, L. H. Romer, S. H. Kang, *ACS Appl. Mater. Interfaces* **2019**, *11*, 8492.

[287] M. Mirzaali, A. Caracciolo, H. Pahlavani, S. Janbaz, L. Vergani, A. Zadpoor, *Appl. Phys. Lett.* **2018**, *113*, 241903.

[288] A. A. Zadpoor, *Biomater. Sci.* **2020**, *8*, 18.

[289] Z. Wu, J. Zhao, W. Wu, P. Wang, B. Wang, G. Li, S. Zhang, *Materials* **2018**, *11*, 1357.

[290] C. Lin, L. Zhang, Y. Liu, L. Liu, J. Leng, *Sci. China Technol. Sci.* **2020**, *63*, 578.

[291] T. Kim, Y.-G. Lee, *Sci. Rep.* **2018**, *8*, 13911.

[292] J. N. Rodriguez, C. Zhu, E. B. Duoss, T. S. Wilson, C. M. Spadaccini, J. P. Lewicki, *Sci. Rep.* **2016**, *6*, 27933.

[293] W. Zhao, N. Li, L. Liu, J. Leng, Y. Liu, *Compos. Struct.* **2022**, *293*, 115669.

[294] C. de Marco, C. C. J. Alcântara, S. Kim, F. Briatico, A. Kadioglu, G. de Bernardis, X. Chen, C. Marano, B. J. Nelson, S. Pané, *Adv. Mater. Technol.* **2019**, *4*, 1900332.

[295] W. Zhao, F. Zhang, J. Leng, Y. Liu, *Compos. Sci. Technol.* **2019**, *184*, 107866.

[296] L. Huang, L. Wang, J. He, J. Zhao, D. Zhong, G. Yang, T. Guo, X. Yan, L. Zhang, D. Li, *J. Thorac. Dis.* **2016**, *8*, 3323.

[297] M. Zarek, N. Mansour, S. Shapira, D. Cohn, *Macromol. Rapid Commun.* **2017**, *38*, 1600628.

[298] F. Zhang, N. Wen, L. Wang, Y. Bai, J. Leng, *Int. J. Smart Nano Mater.* **2021**, *12*, 375.

[299] W. Zhao, Z. Huang, L. Liu, W. Wang, J. Leng, Y. J. C. S. Liu, *Compos. Sci. Technol.* **2022**, *229*, 109671.

[300] R. J. Morrison, S. J. Hollister, M. F. Niedner, M. G. Mahani, A. H. Park, D. K. Mehta, R. G. Ohye, G. E. Green, *Sci. Transl. Med.* **2015**, *7*, 285ra64.

[301] H.-H. Chen, C.-H. Pan, A.-M. Leow, P.-K. Tsay, C.-T. Chen, *Formosan J. Surg.* **2016**, *49*, 1.

[302] Y. Deng, B. Yang, F. Zhang, Y. Liu, J. Sun, S. Zhang, Y. Zhao, H. Yuan, *Biomaterials* **2022**, *291*, 121886.

[303] F. Godart, A. Houeijeh, M. Recher, C. Francart, A.-S. Polge, M. Richardson, M.-A. Cajot, A. Duhamel, *Arch. Cardiovasc. Dis.* **2015**, *108*, 57.

[304] C. Lin, Z. Huang, Q. Wang, Z. Zou, W. Wang, L. Liu, Y. Liu, J. Leng, *Adv. Healthcare Mater.* **2023**, *12*, 2201999.

[305] D. Kashyap, P. Kishore Kumar, S. Kanagaraj, *Addit. Manuf.* **2018**, *24*, 687.

[306] K. J. Krieger, N. Bertollo, M. Dangol, J. T. Sheridan, M. M. Lowery, E. D. O'Cearbhaill, *Microsyst. Nanoeng.* **2019**, *5*, 42.

[307] K.-Y. Seong, M.-S. Seo, D. Y. Hwang, E. D. O'Cearbhaill, S. Sreenan, J. M. Karp, S. Y. Yang, *J. Controlled Release* **2017**, *265*, 48.

[308] R. Jamaledin, C. Di Natale, V. Onesto, Z. B. Taraghdari, E. N. Zare, P. Makvandi, R. Vecchione, P. A. Netti, *J. Clin. Med.* **2020**, *9*, 542.

[309] J. Yang, X. Liu, Y. Fu, Y. Song, *Acta Pharm. Sin. B* **2019**, *9*, 469.

[310] R. Ye, J. Yang, Y. Li, Y. Zheng, J. Yang, Y. Li, B. Liu, L. Jiang, *ACS Biomater. Sci. Eng.* **2020**, *6*, 2487.

[311] D. Han, R. S. Morde, S. Mariani, A. A. La Mattina, E. Vignali, C. Yang, G. Barillaro, H. Lee, *Adv. Funct. Mater.* **2020**, *30*, 1909197.

[312] X. Li, W. Shan, Y. Yang, D. Joralmon, Y. Zhu, Y. Chen, Y. Yuan, H. Xu, J. Rong, R. Dai, *Adv. Funct. Mater.* **2021**, *31*, 2003725.

[313] L. Lin, Y. Wang, M. Cai, X. Jiang, Y. Hu, Z. Dong, D. Yin, Y. Liu, S. Yang, Z. Liu, *Adv. Funct. Mater.* **2022**, *32*, 2109187.

[314] J. Kevin, F. Xu, S. Toufanian, K. J. Chan, S. Said, T. C. Stimpson, E. González-Martínez, J. M. Moran-Mirabal, E. D. Cranston, T. Hoare, *Acta Biomater.* **2021**, *128*, 250.

[315] T. S. Tran, R. Balu, S. Mettu, N. R Choudhury, N. K. Dutta, *Pharmaceuticals* **2022**, *15*, 1282.

[316] Y. Lu, A. A. Aimetti, R. Langer, Z. Gu, *Nat. Rev. Mater.* **2017**, *2*, 16075.

[317] G. H. Yang, M. Yeo, Y. W. Koo, G. H. Kim, *Macromol. Biosci.* **2019**, *19*, 1800441.

[318] G. Villar, A. D. Graham, H. Bayley, *Science* **2013**, *340*, 48.

[319] D. B. Mahmoud, M. Schulz-Sigmund, *Adv. Healthcare Mater.* **2023**, *12*, 2202631.

[320] S. Zu, Z. Zhang, Q. Liu, Z. Wang, Z. Song, Y. Guo, Y. Xin, S. Zhang, *Bio-Des. Manuf.* **2022**, *5*, 294.

[321] X. Hu, Z. Ge, X. Wang, N. Jiao, S. Tung, L. E. Liu, *Composites, Part B* **2022**, *228*, 109451.

[322] W. J. Hendrikson, J. Rouwkema, F. Clementi, C. A. Van Blitterswijk, S. Farè, L. Moroni, *Biofabrication* **2017**, *9*, 031001.

[323] C. Zhang, D. Cai, P. Liao, J.-W. Su, H. Deng, B. Vardhanabhuti, B. D. Ulery, S.-Y. Chen, J. Lin, *Acta Biomater.* **2021**, *122*, 101.

[324] S. Miao, W. Zhu, N. J. Castro, M. Nowicki, X. Zhou, H. Cui, J. P. Fisher, L. G. Zhang, *Sci. Rep.* **2016**, *6*, 27226.

[325] S. Miao, H. Cui, M. Nowicki, S.-j. Lee, J. Almeida, X. Zhou, W. Zhu, X. Yao, F. Masood, M. W. Plesniak, *Biofabrication* **2018**, *10*, 035007.

[326] S.-H. Hsiao, S. Hsu, *ACS Appl. Mater. Interfaces* **2018**, *10*, 29273.

[327] K. Modaresifar, M. Ganjian, L. Angeloni, M. Minneboo, M. K. Ghatkesar, P. L. Hagedoorn, L. E. Fratila-Apachitei, A. A. Zadpoor, *Small* **2021**, *17*, 2100706.

[328] M. Ganjian, K. Modaresifar, M. R. Ligeon, L. B. Kunkels, N. Tümer, L. Angeloni, C. W. Hagen, L. G. Otten, P. L. Hagedoorn, I. Apachitei, *Adv. Mater. Interfaces* **2019**, *6*, 1900640.

[329] M. Nouri-Goushki, A. Isaakidou, B. Eijkel, M. Minneboo, Q. Liu, P. Boukany, M. Mirzaali, L. Fratila-Apachitei, A. Zadpoor, *Nanoscale* **2021**, *13*, 14304.

[330] S. J. Callens, N. Tümer, A. A. Zadpoor, *Appl. Mater. Today* **2019**, *15*, 453.

[331] S. J. Callens, R. J. Uyttendaele, L. E. Fratila-Apachitei, A. A. Zadpoor, *Biomaterials* **2020**, *232*, 119739.

[332] D. Zhang, O. J. George, K. M. Petersen, A. C. Jimenez-Vergara, M. S. Hahn, M. A. Grunlan, *Acta Biomater.* **2014**, *10*, 4597.

[333] M. Bao, X. Lou, Q. Zhou, W. Dong, H. Yuan, Y. Zhang, *ACS Appl. Mater. Interfaces* **2014**, *6*, 2611.

[334] A. S. Neto, J. M. Ferreira, *Materials* **2018**, *11*, 1702.

[335] G. D. Barabaschi, V. Manoharan, Q. Li, L. E. Bertassoni, *Engineering Mineralized and Load Bearing Tissues*, Springer, Berlin **2015**, pp. 79–94.

[336] B. P. dos Santos, B. Garbay, M. Fenelon, M. Rosselin, E. Garanger, S. Lecommandoux, H. Oliveira, J. Amédée, *Acta Biomater.* **2019**, *99*, 154.

[337] F. S. Senatov, K. V. Niaza, M. Y. Zadorozhnyy, A. V. Maksimkin, S. D. Kaloshkin, Y. Z. Estrin, *J. Mech. Behav. Biomed. Mater.* **2016**, *57*, 139.

[338] F. Senatov, M. Y. Zadorozhnyy, K. Niaza, V. Medvedev, S. Kaloshkin, N. Y. Anisimova, M. Kiselevskiy, K.-C. Yang, *Eur. Polym. J.* **2017**, *93*, 222.

[339] L. Zhang, G. Yang, B. N. Johnson, X. Jia, *Acta Biomater.* **2019**, *84*, 16.

[340] S. Miao, P. Wang, Z. Su, S. Zhang, *Acta Biomater.* **2014**, *10*, 1692.

[341] S. Miao, W. Zhu, N. J. Castro, J. Leng, L. G. Zhang, *Tissue Eng., Part C* **2016**, *22*, 952.

[342] B. Tandon, J. J. Blaker, S. H. Cartmell, *Acta Biomater.* **2018**, *73*, 1.

[343] A. Ding, S. J. Lee, S. Ayyagari, R. Tang, C. T. Huynh, E. Alsberg, *Bioactive Mater.* **2022**, *7*, 324.

[344] X. Yang, Z. Lu, H. Wu, W. Li, L. Zheng, J. Zhao, *Mater. Sci. Eng., C* **2018**, *83*, 195.

[345] D. G. Tamay, T. Dursun Usal, A. S. Alagoz, D. Yucel, N. Hasirci, V. Hasirci, *Front. Bioeng. Biotechnol.* **2019**, *7*, 164.

[346] S. Camarero-Espinosa, C. Tomasina, A. Calore, L. Moroni, *Mater. Today Bio* **2020**, *6*, 100051.

[347] Y. Deng, F. Zhang, Y. Liu, S. Zhang, H. Yuan, J. Leng, *ACS Appl. Polym. Mater.* **2023**, *5*, 1283.

[348] S. Jana, S. K. L. Levengood, M. Zhang, *Adv. Mater.* **2016**, *28*, 10588.

[349] S. Miao, M. Nowicki, H. Cui, S.-J. Lee, X. Zhou, D. K. Mills, L. G. Zhang, *Biofabrication* **2019**, *11*, 035030.

[350] S. Li, N. Chen, X. Li, Y. Li, Z. Xie, Z. Ma, J. Zhao, X. Hou, X. Yuan, *Adv. Funct. Mater.* **2020**, *30*, 2000130.

[351] B. Mirani, E. Pagan, B. Currie, M. A. Siddiqui, R. Hosseinzadeh, P. Mostafalu, Y. S. Zhang, A. Ghahary, M. Akbari, *Adv. Healthcare Mater.* **2017**, *6*, 1700718.

[352] P. Mostafalu, A. Tamayol, R. Rahimi, M. Ochoa, A. Khalilpour, G. Kiaee, I. K. Yazdi, S. Bagherifard, M. R. Dokmeci, B. Ziaie, *Small* **2018**, *14*, 1703509.

[353] S. Miao, H. Cui, M. Nowicki, L. Xia, X. Zhou, S. J. Lee, W. Zhu, K. Sarkar, Z. Zhang, L. G. Zhang, *Adv. Biosyst.* **2018**, *2*, 1800101.

[354] L. Zhou, T. Min, X. Bian, Y. Dong, P. Zhang, Y. Wen, *ACS Appl. Bio Mater.* **2022**, *5*, 4055.

[355] H.-Y. Shen, Z.-H. Liu, J.-S. Hong, M.-S. Wu, S.-J. Shiue, H.-Y. Lin, *J. Controlled Release* **2021**, *331*, 154.

[356] M. Wang, C. Wang, M. Chen, Y. Xi, W. Cheng, C. Mao, T. Xu, X. Zhang, C. Lin, W. Gao, *ACS Nano* **2019**, *13*, 10279.

[357] J. Deng, Y. Tang, Q. Zhang, C. Wang, M. Liao, P. Ji, J. Song, G. Luo, L. Chen, X. Ran, Z. Wei, L. Zheng, R. Dang, X. Liu, H. Zhang, Y. S. Zhang, X. Zhang, H. Tan, *Adv. Funct. Mater.* **2019**, *29*, 1809110.

[358] R. Jain, S. Wairkar, *Int. J. Biol. Macromol.* **2019**, *137*, 95.

[359] E. Y. Jeon, J. Lee, B. J. Kim, K. I. Joo, K. H. Kim, G. Lim, H. J. Cha, *Biomaterials* **2019**, *222*, 119439.

[360] W. Zhu, J. K. George, V. J. Sorger, L. G. Zhang, *Biofabrication* **2017**, *9*, 025002.

[361] I. Apsite, G. Constante, M. Dulle, L. Vogt, A. Caspari, A. R. Boccaccini, A. Synytska, S. Salehi, L. Ionov, *Biofabrication* **2020**, *12*, 035027.

[362] A. C. Weems, M. C. Arno, W. Yu, R. T. Huckstepp, A. P. Dove, *Nat. Commun.* **2021**, *12*, 3771.

[363] F.-Y. Hsieh, H.-H. Lin, S. Hsu, *Biomaterials* **2015**, *71*, 48.

[364] S.-J. Lee, M. Nowicki, B. Harris, L. G. Zhang, *Tissue Eng., Part A* **2017**, *23*, 491.

[365] F. B. Coulter, B. S. Coulter, E. Papastavrou, A. Ianakiev, *3D Print. Addit. Manuf.* **2018**, *5*, 17.

[366] F. B. Coulter, B. S. Coulter, J. R. Marks, A. Ianakiev, *3D Print. Addit. Manuf.* **2018**, *5*, 5.

[367] H. Shen, H. Diao, S. Yue, J. Fu, *Rapid Prototyping J.* **2018**, *24*, 548.

[368] M. A. Isa, I. Lazoglu, *J. Manuf. Syst.* **2019**, *50*, 69.

[369] A. Haleem, M. Javaid, R. Vaishya, *J. Clin. Orthop. Trauma* **2019**, *10*, 809.

[370] J. C. S. McCaw, E. Cuan-Urquizo, *Mater. Des.* **2018**, *160*, 949.

[371] D. Zhao, T. Li, B. Shen, Y. Jiang, W. Guo, F. Gao, *Rapid Prototyping J.* **2020**, *26*, 1079.

[372] F. B. Coulter, M. Schaffner, J. A. Faber, A. Rafsanjani, R. Smith, H. Appa, P. Zilla, D. Bezuidenhout, A. R. Studart, *Matter* **2019**, *1*, 266.

[373] A. T. Neffe, B. D. Hanh, S. Steuer, A. Lendlein, *Adv. Mater.* **2009**, *21*, 3394.

[374] M. J. Mirzaali, H. Pahlavani, E. Yarali, A. A. Zadpoor, *Sci. Rep.* **2020**, *10*, 11488.

[375] M. Mirzaali, A. H. de la Nava, D. Gunashekar, M. Nouri-Goushki, R. Veeger, Q. Grossman, L. Angeloni, M. Ghatkesar, L. Fratila-Apachitei, D. Ruffoni, *Compos. Struct.* **2020**, *237*, 111867.

[376] W. Zhang, F. Zhang, X. Lan, J. Leng, A. S. Wu, T. M. Bryson, C. Cotton, B. Gu, B. Sun, T.-W. Chou, *Compos. Sci. Technol.* **2018**, *160*, 224.

[377] M. S. Cabrera, B. Sanders, O. J. Goor, A. Driessen-Mol, C. W. Oomens, F. P. Baaijens, *3D Print. Addit. Manuf.* **2017**, *4*, 19.

[378] W. Meyer, S. Engelhardt, E. Novosel, B. Elling, M. Wegener, H. Krüger, *J. Funct. Biomater.* **2012**, *3*, 257.

[379] A. Pandey, G. Singh, S. Singh, K. Jha, C. Prakash, *J. Mech. Behav. Biomed. Mater.* **2020**, *108*, 103781.

[380] C. D. Devillard, C. A. Mandon, S. A. Lambert, L. J. Blum, C. A. Marquette, *Biotechnol. J.* **2018**, *13*, 1800098.

[381] Q. Ze, X. Kuang, S. Wu, J. Wong, S. M. Montgomery, R. Zhang, J. M. Kovitz, F. Yang, H. J. Qi, R. Zhao, *Adv. Mater.* **2020**, *32*, 1906657.

**ADVANCED
SCIENCE NEWS**

www.advancedsciencenews.com

**ADVANCED
MATERIALS**

www.advmat.de

Ebrahim Yarali is currently a Ph.D. candidate in the Departments of Biomechanical Engineering and Precision and Microsystems Engineering, at Delft University of Technology (TU Delft). He holds an M.Sc. and a B.Sc. in Mechanical Engineering. His research focuses on the mechanobiology of meta-biomaterials, including the rational design of architected materials with tailored mechanical and morphometric properties, advanced microadditive manufacturing for their fabrication, and their biological assessments. He is also interested in clinical applications of 4D printing of stimuli-responsive biomaterials, such as temperature- and magneto-responsive hydrogels, for drug delivery systems and tissue engineering at the microscale.

Mohammad J. Mirzaali obtained his Ph.D. (cum laude) in Mechanical Engineering from the Department of Mechanical Engineering at Politecnico di Milano in 2018. Currently, he is as an assistant professor at the Department of Biomedical Engineering at Delft University of Technology and a board member of the Netherlands Society for Biomaterials and Tissue Engineering (NBTE). Dr. Mirzaali's primary interests are centered on biomechanics, biomaterials and biomimicry, with a particular focus on the biomechanics of natural hard-soft interfaces and their emulation in synthetic interfaces with tailored and unprecedented properties. He has received several national and international awards and grants.

Ava Ghalayaniesfahani is a Ph.D. candidate in the Department of Design Production and Management (DPM) at the University of Twente. Her research interests lie in additive manufacturing, specifically 3D/4D printing of smart materials. She received her B.Sc. in Chemical Engineering from Shiraz University and her M.Sc. in Materials Engineering and Nanotechnology from Politecnico di Milano. She carried out her master's thesis at TU Delft with a focus on programming single and multimaterial 4D printed structures.

Angelo Accardo is Associate Professor at the Department of Precision and Microsystems Engineering of Delft University of Technology, board member of the Delft Young Academy, and Steering Committee Member of the International Micro and Nanoengineeriing (MNE) Conference. By exploiting high-resolution light-assisted 3D additive manufacturing techniques, he creates engineered polymeric/hydrogel microenvironments for fundamental mechanobiology, in vitro disease/treatment modeling and tissue engineering applications involving brain (e.g. microglia, iPSCs-derived/primary neurons), cancer (e.g. glioblastoma), or bone (e.g. preosteoblasts) cells. He is author of 55+ publications in peer-reviewed journals and he was awarded several prizes and grants by the Dutch Research Council (NWO).

**ADVANCED
SCIENCE NEWS**

www.advancedsciencenews.com

**ADVANCED
MATERIALS**

www.advmat.de

Pedro J. Díaz-Payno is a MSCA Fellow, currently working in Dr. Patterson lab at IMDEA Materials (Spain). Originally from Madrid, Dr. Díaz-Payno got his B.Sc. Biotechnology (2013) from UFV (Spain) and AIT (Ireland) and MSc (2015) from TCD (Ireland). Dr. Díaz-Payno joined Prof. Kelly lab (TCD) and was awarded an IRC Ph.D. Fellowship. After his Ph.D. defense (2019), he worked on the REGMED4D Medical Delta project with Prof. Zadpoor (TUDelft) and Prof. van Osch (ErasmusMC). From 2020 to 2023, he was Secretary of the TERMIS-EU SYIS. In 2022 he moved back to work as Scientific Advisor at ROVI before joining IMDEA.

Amir A. Zadpoor is Antoni van Leeuwenhoek Professor and Chaired Professor of Biomaterials and Tissue Biomechanics at Delft University of Technology as well as Professor of Orthopedics at Leiden University Medical Center. He develops machine learning and 3D/4D (bio)printing techniques for the design and fabrication of metamaterials and tissues with unprecedented properties. Moreover, he is a world recognized expert in origami/kirigami-based (bio-)materials combining shape shifting with additive manufacturing. Prof. Zadpoor has received many awards including an ERC grant, a Vidi grant, a Veni grant, the Jean Leray award of the European Society of Biomaterials, and the Early Career Award of JMBBM.